

Interstitially Insulated Coaxial Pipe Supplemental Information

**Prepared for the Minerals Management Service
Under the MMS/OTRC Cooperative Research Agreement
1435-01-04-CA-35515
Task Order 35663
Project Number 509**

June 2007

Contents:

1. Production Riser Buoyancy & Thermal Insulation: Final Design Report, Prepared For FMC Technologies, Reed Hamm, Zac Rosenbaum, Daniel Yates, August, 2006.
2. Final Design Report: Manufacturing and Assembly of Interstitially Insulated Coaxial Pipe, Prepared For Lone Star Steel Company, Braz, Davis, Jackson, Summer, 2006.
3. Connections for Interstitially Insulated Coaxial Pipes, MEEN 685 Directed Studies Report, Michael Tillmann, May, 2007.

Final Design Report

Production Riser Buoyancy & Thermal Insulation

**Prepared For
FMC Technologies**



**Presented to
Mr. Gabriel Silva & Mr. Scott McKenzie
Mr. Charles Bollfrass, P.E.**

**Prepared by
Reed Hamm
Zac Rosenbaum
Daniel Yates**

**Texas A&M University
Department of Mechanical Engineering**

MEEN 402-Section 301 – Summer 2006

August 3, 2006

Executive Summary

A deep water production riser was designed for FMC technologies. The design was required to allow for production at 10,000 ft ocean depth, to increase the buoyancy of the current system, to provide added damage resistance and to reduce the heat loss to the environment. An interstitially insulated coaxial pipe design is presented that reduces the expected heat loss to the environment, while providing a large buoyant force. Additionally, this design improves damage resistance, as well as structural integrity to the overall system.

The purpose of this report is to explain the insulation process and overall design of the system. It begins by presenting the need statement formulated to solve the problem at hand, followed by the analysis of that need. The requirements of the design are then explained in further detail. The overall system design is presented followed by specifics on each aspect of the design, ranging from materials to manufacturing to test and assembly.

Table of Contents

Introduction (Need Statement).....	1
Background (& Need Analysis).....	1
Constraints	1
Assumptions.....	2
Definitions.....	2
Function Structure.....	3
Design Requirements	3
Overall System Description	4
Detailed Design Analysis.....	5
Detailed Development Plan	19
Summary	21
Appendix A: List of Abbreviations.....	22
Appendix B: Glossary.....	23
Appendix C: References	24
Appendix D: Detailed Calculations	25

Introduction (Need Statement)

Design and develop completion risers for deep water. This depth will be limited by material strength and buoyed weight, as well as sizes specified by FMC Technologies. The design should incorporate external coating materials that increase net buoyancy and physical protection. The design should also be able to withstand all environmental conditions in deep water, as well as incorporating a method to significantly reduce the heat loss from flowing fluids to the environment.

The objective of this report is to present the Interstitially Insulated Coaxial Pipe (IICP) technology and show provide reason why it should be used to insulate deep water production risers. In addition to its superior insulative properties, the riser's buoyancy can be greatly increased due to the extra material added outer diameter of the pipe.

It is our contention that FMC Technologies should fully investigate the benefits this new technology has to offer and employ its use in production risers. It can be shown by further examination that the utilization of this technology can significantly reduce the amount of maintenance time currently devoted to pigging the riser system due to the high level of thermal resistance provided by the insulation. Additionally, the technology offers an opening to design possibilities that may advance this field and unveil fresh engineering acumen previously suppressed. We would like to thank FMC Technologies for working with us and honoring the Texas A&M Mechanical Engineering Department with its attention and undoubtedly precious time.

Background (& Need Analysis)

Constraints

- The riser must be rugged and survive transportation without reducing its productivity or effectiveness
- The riser must be able to withstand both collapse pressure and well pressure from deep sea production wells
- The system must be able to operate in at least 10,000 ft of water
- The system must not require more external buoyancy than current systems

- The cost of production must be optimized
- The heat transfer of the riser must be improved compared to current systems
- The system must have an operational life equal to the current systems

Assumptions

- The well pressure will be at least 15,000 psi
- The riser will be designed to the well pressure but verified by the collapse pressure
- The weight of the connections per length of pipe is 10% of the length weight
- Operational depth is at least 10,000 ft
- The internal diameter of the riser must meet the current production requirements
- Average temperature in the Gulf of Mexico is 37°F

Definitions

Deep water – water that is 3,500 to 10,000 ft

System – production riser with insulation and any buoyancy devices in place

Well pressure – The shut in pressure of the formation

Collapse Pressure – Pressure created by the ocean at the deepest operational point

Connections – Any parts or extra material required to connect two sections of pipe together

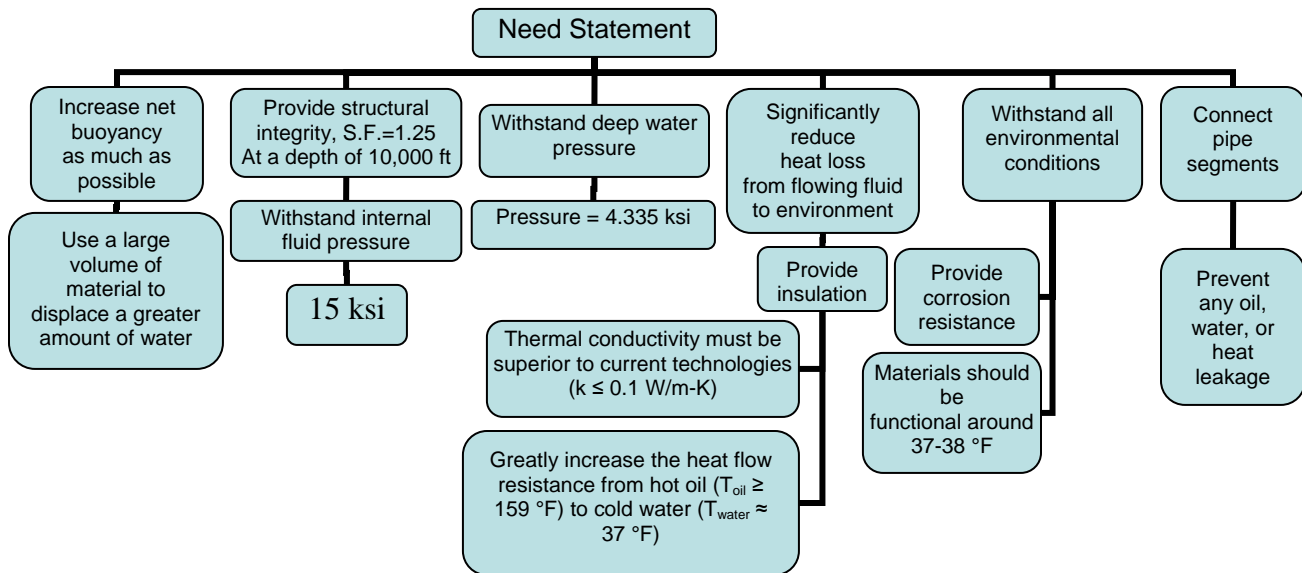
Section of pipe – a 60 ft length of pipe

Environmental Conditions – all environments under the surface of the ocean including ocean currents and temperatures

Operational Life – Amount of time the given system is functional and able to carry out its designed purpose without failure

Corrosion – any damage caused by contact with sea water or petroleum and side products of the well which will reduce the integrity of the system

Function Structure



Design Requirements

This riser design requires that certain specifications be met. A brief summary of the main points is presented here.

The riser system must accommodate the wire screen mesh insulation idea to maximize the heat flow resistance from the hot oil. In order to effectively insulate the oil, its temperature must remain above its cloud point (about 68°C), which is the point at which paraffins and asphaltenes can accumulate on the walls of the pipe. It is the goal of this design to prevent this from occurring so that the problems associated with this buildup are greatly reduced. The insulation design must, therefore, employ materials and parameters selected for optimal heat resistance performance. Parameters include mesh number, wire diameter, surface roughness, layer thickness, interface pressure, and number of layers.

The insulation should additionally be used to greatly increase the buoyancy of the system in order to decrease the total stress on the inner piping since it takes the entire load from weight. The inner pipe must be designed to an oil pressure of 15 ksi with a safety factor of 1.25. Conversely, the outer pipe must be designed to the water pressure at 10,000 pressure ft ($P \approx 4.335$ ksi), the pressure at which the pipe will collapse, with a safety factor of 1.25.

The riser system must also accommodate connectors for each joint of piping. These connectors must provide insulation to perform equally to the rest of the pipe's length without sacrificing the ability to give a secure connection and prevent any water, oil, or heat leakage at any point.

Overall System Description

The overall system contains specific design features that meet the given needs presented in the design problem. These main needs are outlined in the previous design requirements section.

In order to ensure structural integrity, multiple materials were researched. Of these materials, it is obvious that a high strength and low weight is desired, while keeping cost at a minimum. The system "begins" with the inner pipe, sized to withstand internal pressures. The inner pipe is the structural member, and it is desired that this member withstand the load of the entire system including the insulation and outer pipe.

Insulating the pipe to provide flow assurance is where a new innovative design is being applied. This design, called "Interstially Insulated Coaxial Pipe", incorporates multiple layers of wire mesh and liner material to achieve desired insulation properties. The basic premise behind the design lies in the creation of a thermal resistance as two materials contact each other. Separating these layers with a wire mesh moves the layers further apart, creating even more of a thermal resistance. Furthermore, the wire mesh helps to support the liner material and limits contact points, inhibiting heat transfer by conduction. The ends of the insulation are capped off, creating a large amount of stagnant air among the wire mesh, reducing heat transfer by convection. Finally the mesh and liner layers are surrounded on their outer and inner layers by an aluminized Mylar film which further inhibits heat transfer by radiation. Outside of this outer Mylar layer is an outer pipe which is sized to withstand the collapse pressure experienced at the desired depths of 10,000 ft. To shield the pipe from the ocean, and keep the sea water from "wetting" the surface and changing the heat transfer properties, the outside of the entire pipe is shielded by a polypropylene layer.

To insulate the flanges where the risers meet, there are two different designs presented. The first involves a vessel to be filled with a silica or polymer type jelly that

will provide heat transfer properties similar to the rest of the length of the pipe. The other design uses the layered mesh-liner concept identical to the rest of the pipe. The connector insulator is cut into two pieces and then in the field is placed around the flange and welded together to insulate the connector.

Detailed Design Analysis

Detailed design analysis of the production riser piping is found in Appendix D: Detailed Calculations .

One of the main sources of heat loss in the riser is the connections. Some of the difficulties involving insulating the connections are due to the very nature of the connections. The insulation must carry the same thermal resistance as the rest of the riser or else all of the heat loss will occur in the connections cause damage due to thermal stress and thermal expansion of a small region in the riser (Figure 1).



Figure 1. Insulated Riser with Non-Insulated Connections

Since the riser joints are not bolted together before they are shipped the insulation covering them must be removable and must be able to be installed in the field outside of a controlled environment.

Connection Insulation Requirements:

- Removable
- Easily attached in the field
- Same thermal resistance properties as the rest of the riser

The first design employs the same insulation used to cover the riser sections to insulate the connectors. The overall principal from the riser insulation is used, however for the connector insulation to be removable the insulation must be divided in half as seen in Figure 2.

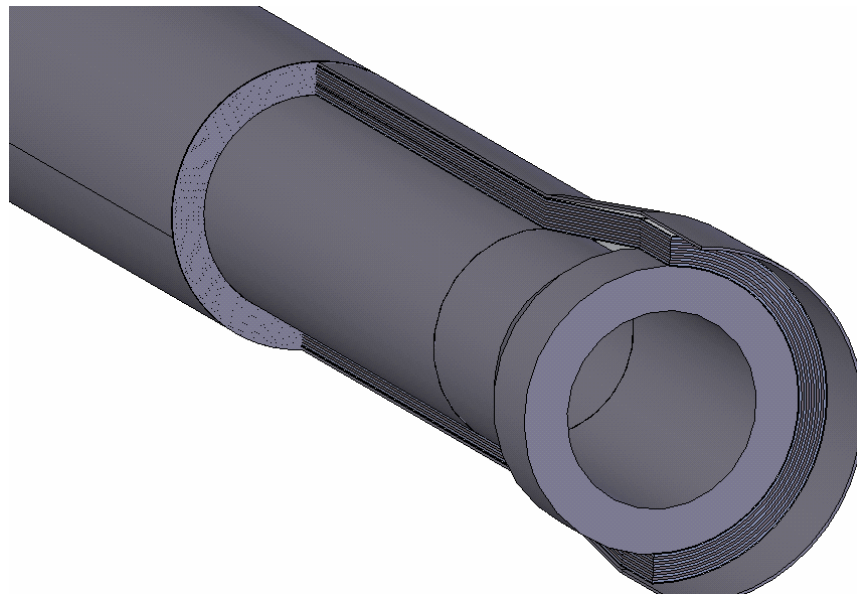


Figure 2. Half of the Connector Insulation in Place

The first half of the connector, as seen in Figure 2 is then welded to the existing insulation with a water resistant adhesive used between the butted joint to ensure no water infiltrates the joint. The adhesive will also need to possess adequate thermal resistance to ensure that weaknesses are not created in the insulation. Once the first half is in place the second half is attached in the same manner and then the two halves are welded together as seen in Figure 3.

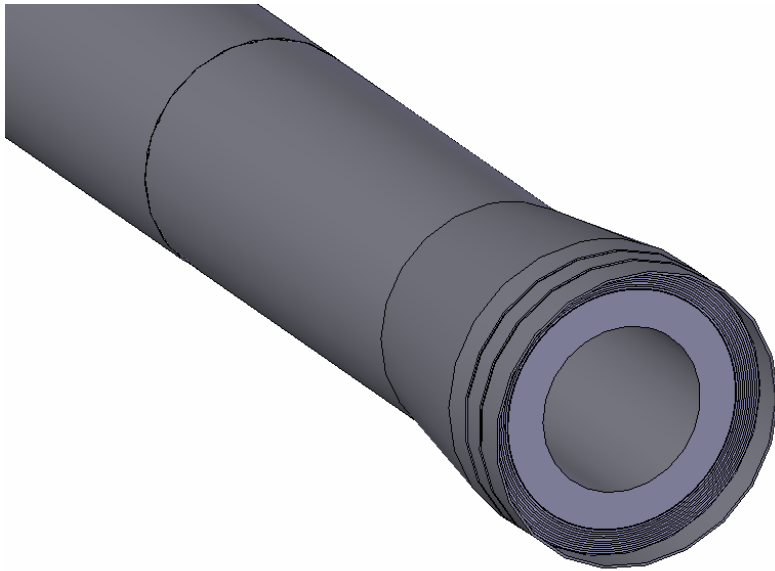


Figure 3. Connector Insulation Fully Assembled

The connection must be assembled in order, with the grooved half attached first and the outer portion applied second as seen in Figure 4. The outer portion is anchored in exactly the same way as the first, however it overlaps and completes the seal. Since the outer portion of the insulation is welded, the outer pipe will contract due to the thermal change, thus creating a pressure seal on the o-rings.

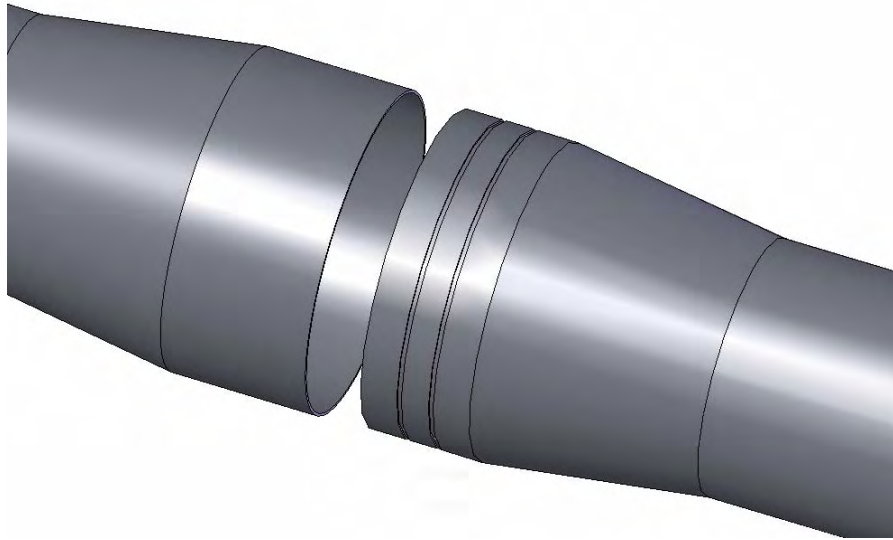


Figure 4. Exploded View of the Connection Insulation

The two slots on the outer pipe are seats for the o-rings seen in Figure 4 to seal the joint against leakage. A pipe clamp is used as an additional guard against leakage as seen in Figure 5.

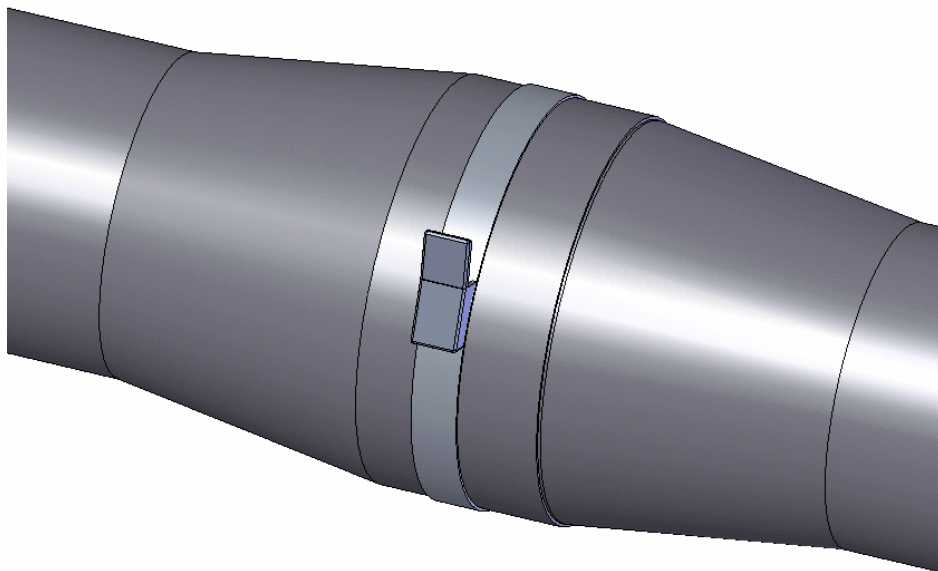


Figure 5. Fully Assembled Connection with Pipe Clamp

The benefits of using this insulation are:

- Uniformity of heat transfer resistance
- Compact design
- Rugged insulation which also protects the inner riser from damage

The connection insulation will be difficult to manufacture and install due to the half-and-half nature of the assembly. Since the setup will be cut in half an experiment will need to be performed in order to determine if that will affect the multi-layer vessel nature of the design, i.e. will the assembly stay together or will additional reinforcement be needed. Other investigations that need to be made include: testing the o-rings for longevity and pressure in 10,000 ft of water to ensure a water-tight seal and determining if welding the setup in place will affect the properties of the Mylar radiation film.

Clamp-On Insulation

A secondary option for insulating the connections is using a removable can filled with an insulating gel in order to match the insulative properties of the rest of the riser. In order to provide enough gel to match the thermal insulation properties for the riser, the can will need to be considerably larger than the riser itself. This design will also require the case to be in two pieces since the riser will need to be bolted together before any insulation is applied. The can is attached in the same manner as the previous insulation except the can is not welded to the previous insulation. Instead, the can is welded over the insulation. The welds will also provide a thermal shrink effect in order to seal the o-rings located in the neck of the can as seen in Figure 6. Valves will be located on the top and bottom of the can in order to allow the gel to be injected once the can has been welded in place. The gel will be inserted into the bottom valve while the top valve is opened to allow the air to escape as seen in Figure 7. Having the valves arranged in this manner will ensure the entire cavity is filled with gel and no air remains.

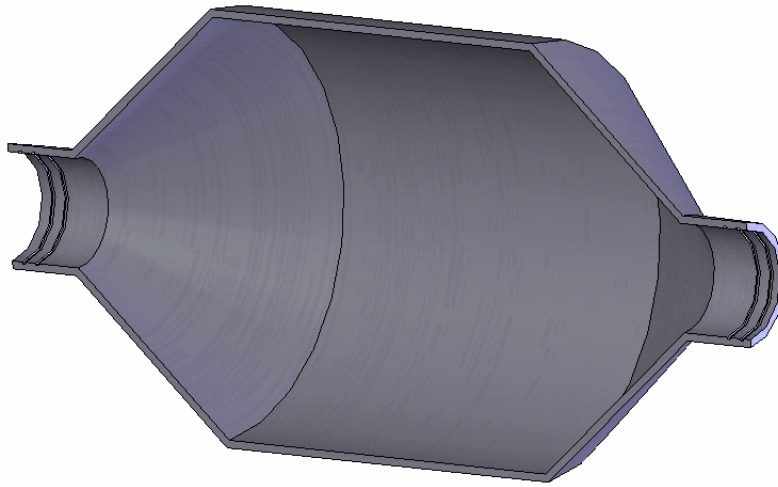


Figure 6. Cutaway View of the Insulation Can - Demonstrating the O-ring Placement



Figure 7. Clamp-On Insulation

Layered Wire Screen Mesh

The riser system design consists of 60 ft coaxial pipe segments connected by flanges. In the cavity formed between the outer diameter (OD) of the inner pipe (IP) and the inner diameter (ID) of the outer pipe (OP) lies insulation. The insulation is constructed by layers of mesh and liner, as follows, starting from the OD of the IP: Mylar® film, multiple concentric layers of mesh with layers of liner between each mesh, Mylar® film, OP, polypropylene layer. Figure 8 below shows a partially exploded view of this arrangement with 6 layers of mesh, the proposed design to maximize heat resistance.

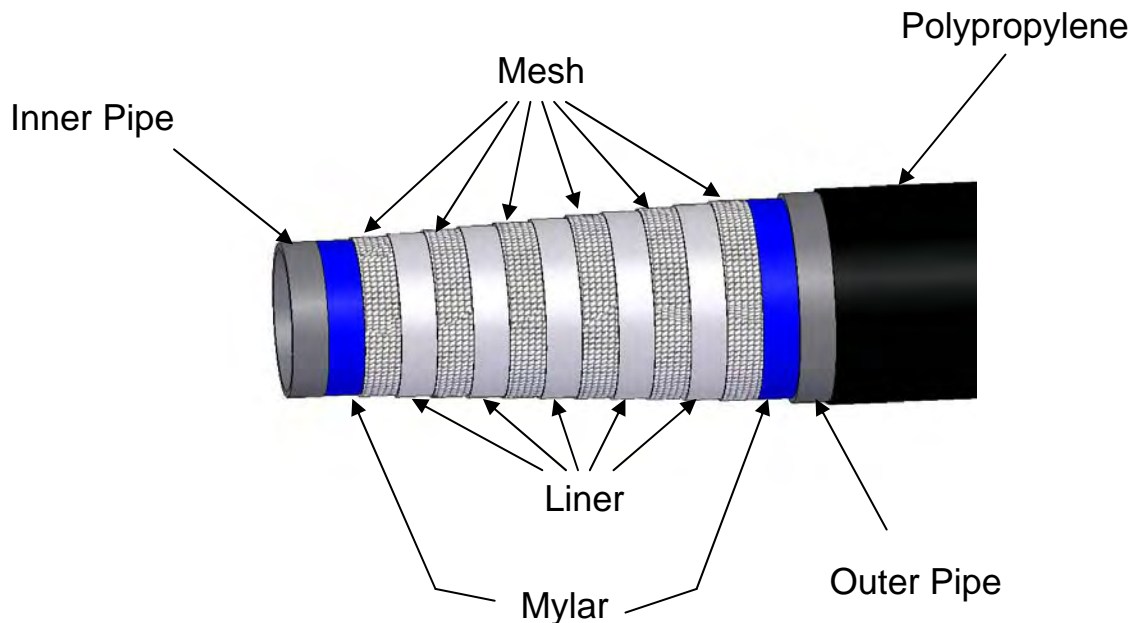


Figure 8. Coaxially insulated pipe with multiple layers of mesh liner.

The purpose of the liners is simply to provide surfaces by which the meshes can separate by its geometry. Figure 9 below shows this geometry and the screen mesh “sandwiched” between two mesh liners.

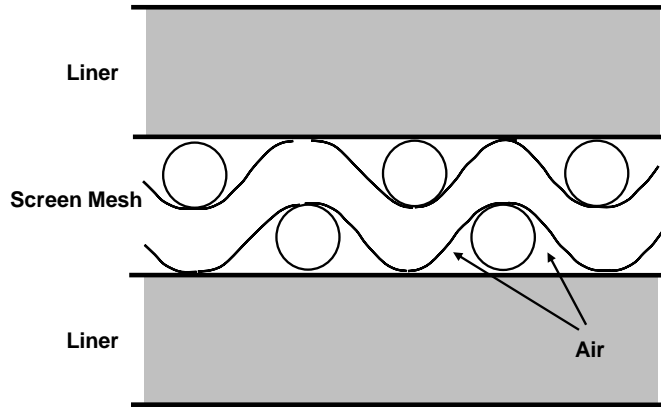


Figure 9. Cross-section of screen mesh between two mesh liners.

If a temperature difference is present across the screen mesh, heat flows across this material and the interstitial air mainly by conduction. The central idea of this arrangement is to separate the liner materials with air ($k = 0.08 \text{ W/m-K}$) (or some other low thermal conductivity gas, such as argon [$k = 0.016 \text{ W/m-K}$]) between them to provide a large amount of heat resistance. Heat resistance depends on the geometry involved. In this case, cylindrical geometry is employed. For a cylinder, the heat resistance is formulated as:

$$R_{\text{cyl}} = \frac{\ln(r_2/r_1)}{2\pi Lk}$$

where r_2 and r_1 are the outer and inner radii of the cylinder, L is the length of the cylinder, and k is the thermal conductivity of the material. The total heat resistance utilized in this design depends on the number of layers, since resistance increases with increasing cylindrical thickness. Therefore a good design will make use of multiple layers (Figure 1 shows 6). This equation for cylindrical heat resistance can be used for the liner, Mylar, and pipe materials, but more complex resistance equations exist when analyzing the mesh, so accommodation must be made for this.

Aluminized Mylar is a material with a low thermal conductivity ($\approx 0.16 \text{ W/m-K}$) in addition to the ability to reduce radiation heat transfer greatly. It is a good choice to accomplish this reduction in radiation for the design. Mylar is a proven material and is used on the International Space Station to greatly increase radiation heat transfer resistance. All three forms of heat transfer must be considered in this system:

conduction, convection, and radiation to work out all possible ways to increase the heat flow resistance.

Also, a layer of polypropylene is added to the exterior of the outer pipe to prevent the pipe from being wetted and provide corrosive resistance (in addition to thermal resistance).

The mesh consists of wire formed into a screen such as that seen below in Figure 10.

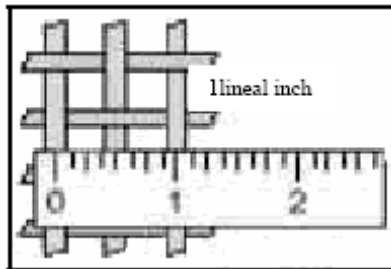


Figure 10. Screen mesh showing a mesh size of 2.

A mesh is described mainly by its mesh size, this being the number of spaces within 1 inch from the center of one wire to the center of parallel wire one lineal inch away. Figure 10 shows a mesh with a mesh size of 2. Additionally, wire mesh is spatially equivalent horizontally and vertically, so that the spaces between wires form squares.

Extensive testing has already been done, both physical and analytical, to assess the thermal resistance properties of the mesh-liner system. The physical testing performed involved measuring the thermal conductivity of one small circular-shaped layer of mesh with two layers of liner (modeled by two cylindrical inserts) squeezed between two cylindrical steel pieces (flux meters), one heated and the other cooled to approximate the temperatures present in the riser (hot oil and cold water). The flux meters were used to determine the heat flux through the mesh-liner arrangement by measuring the temperature distribution. Air was present interstitially in the mesh at about atmospheric pressure. Figure 11 and Figure 12 below show a picture of a mesh test specimen and the test apparatus, respectively.

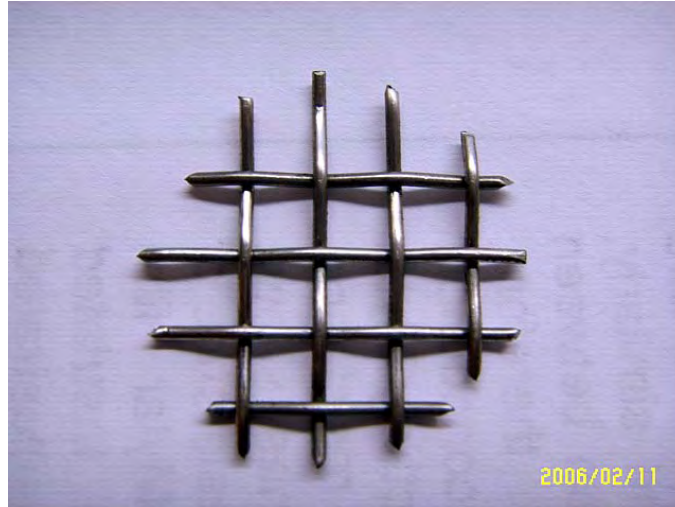


Figure 11. Circular mesh test specimen.

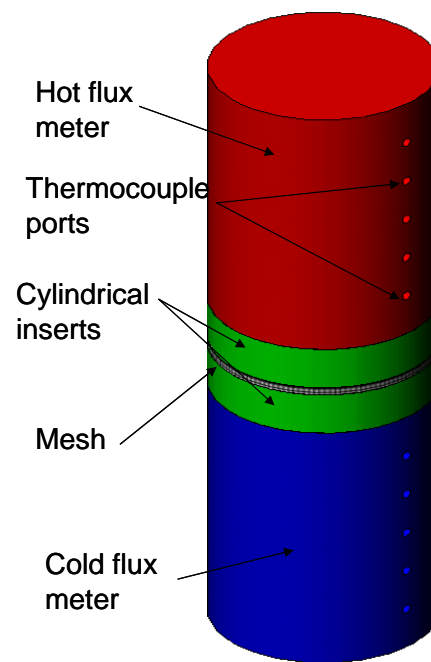


Figure 12. Test apparatus for determining the effective thermal conductivity of a mesh-liner system.

Varied parameters in testing include: mesh material, mesh diameter, mesh number, interface temperature, interface pressure, presence of mesh, presence of Mylar, and

surface roughness. Each of these parameters was tested to evaluate the optimum conditions to increase heat resistance. Tests conducted showed stainless steel ($k = 16.3 \text{ W/m-K}$) with a mesh number 5, at an interface pressure of 25 psi, an interface temperature of 39 °F, diameter 1/16", with Mylar, with maximum possible surface roughness exhibited the lowest thermal conductivity ($k = 0.08 \text{ W/m-K}$). Compared to the case without mesh ($k = 45 \text{ W/m-K}$), this is a significant reduction in conductivity. It must be noted that the mesh-liner system's heat resistance depends greatly on the properties of the materials chosen. Even saying stainless steel was found to be the best among the materials tested is vague since there are so many different types of stainless steel. The manufacturing technique used for any material, be it quenching, tempering, annealing, etc., affects the properties of the materials in use, therefore it is difficult to give a final choice of material since there are so many different possibilities.

Because of this problem of material properties, simulations of the test can be performed to evaluate the effective thermal conductivity of the test apparatus, while varying the materials and any other parameters that are desired. Before running the analysis, there are a few points that are easy to observe. First, it is proven experimentally that certain parameters affect the effective thermal conductivity in a foreknown way. For example, the heat resistance of the system decreases with increasing interface pressure. Also, the heat resistance increases with a decrease in the number of contact points (mesh number). A lower mesh number is desired because of a smaller number of contact points for the heat to flow through.

The simulation was done by varying the mesh material and interface pressure while evaluating the effective thermal conductivity of the arrangement. This simulation is merely an example of the analysis done. It takes into consideration the equivalent thermal circuit formed by the mesh-liner interface and the deformation caused by the interface pressure. (It was observed during physical testing that the mesh became deformed and decreased in thickness. This was accounted for by using a new mesh piece during every run.) The initial thicknesses of the mesh and liner were both 1/8", the interface temperature was assumed to be 200 °F (for material properties), the mesh number was set at 2, the contact area was about 0.785 in^2 , and all surfaces were assumed to have a roughness of $1.2 \text{ }\mu\text{m}$. The deformation of liner was taken into

consideration when analyzing the system. Also, the interstitial gas was taken as air, though this can vary. Argon is a possible substitute for air since it actually has a slightly lower thermal conductivity than air. The air was assumed to be stagnant in the interstitial gaps. All of the parameters assumed here can be varied and tweaked to achieve the best possible results. The following just shows examples of what is possible and what typical results show using the currently developing technology.

Figure 13 below shows the results for the effective thermal conductivity from analysis done for 5 different materials: titanium, 316 stainless steel, precipitation hardened (PH) 17-7 stainless steel, ductile iron, and Inconel Alloy 625 as they vary with interface pressure. As can be seen by the graph in Figure 13, Inconel displays the lowest thermal conductivity with titanium performing at the highest k-value. The graph also shows that thermal conductivity increases with increasing interface pressure.

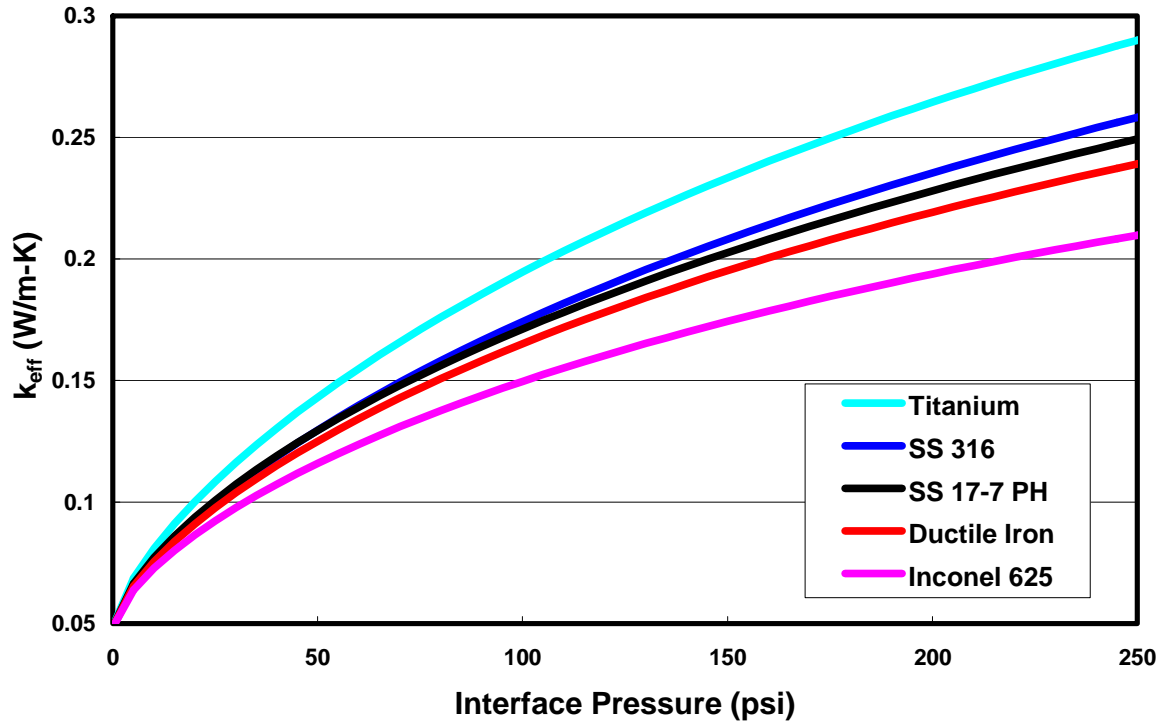


Figure 13. Effective thermal conductivity with interface pressure variance and material choice.

Due to the nature of this problem, a low interface pressure is desired because of the sharp increase in thermal conductivity that exists at higher pressures. Therefore, a more desirable range of thermal conductivities is shown in Figure 14 in a pressure range of 0-25 psi.

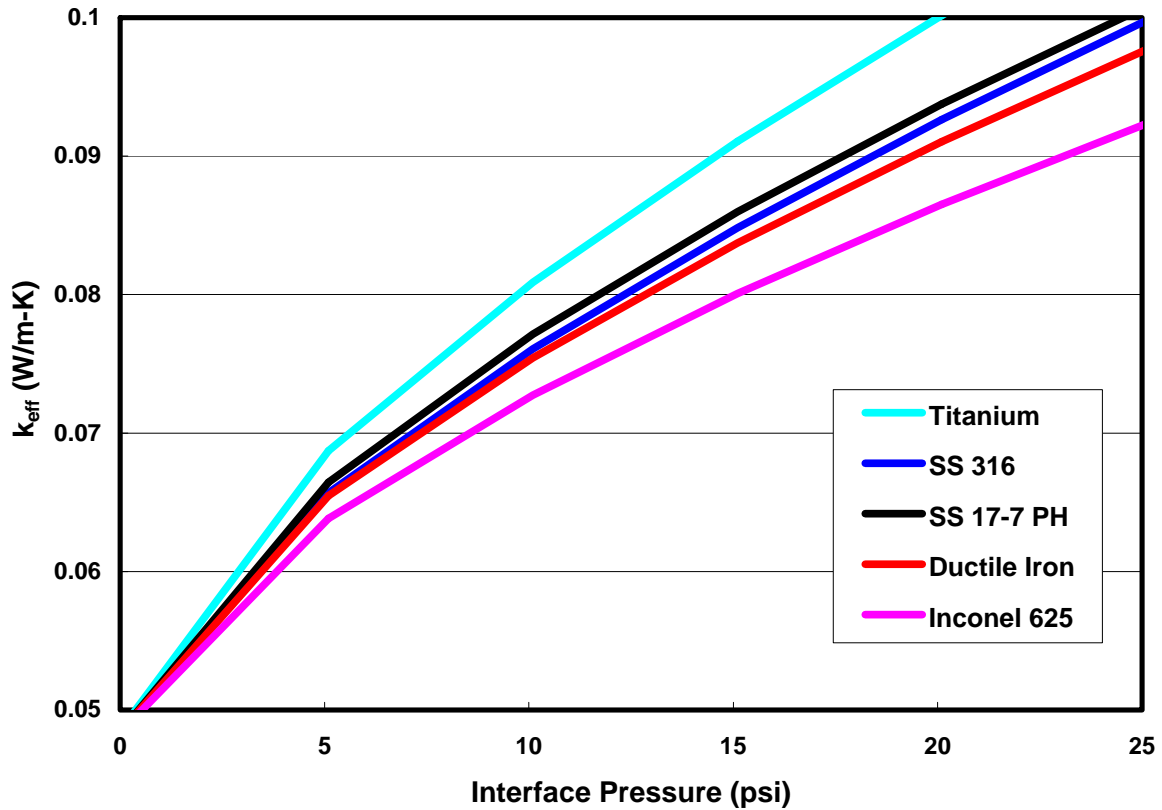


Figure 14. Effective thermal conductivity with interface pressure for various materials.

Interface pressure range of 0-25 psi.

As can be seen by Figure 14, the graph shows the same general trend at lower pressures, with Inconel displaying the most desirable thermal conductivities. Since the objective of the mesh design is to aim for an effective thermal conductivity superior to that of current insulation technologies, a suitable value is somewhere in this range, preferably below 0.08 W/m-K. This corresponds to an interface pressure less than 15 psi. This must be taken into consideration when manufacturing the riser system because the layers should not be pressed against each other with too great a pressure or else the heat resistance will largely increase and cause a major problem with the design. The design must be such that the inner pipe takes all of the pressure given by the oil as well as the total stress from the hanging weight, and the outer pipe must be designed to take all of the outer water pressure that tends to collapse the piping. Careful, precise manufacturing is therefore necessary to accomplish this design.

Furthermore, it must be noted that conclusive material choices for the arrangement cannot be stated quite yet due to the numerous possibilities in selecting proper materials. Relevant material properties include the thermal and mechanical varieties. Thermal conductivity, modulus of elasticity, Poisson's ratio, and hardness and other possible material properties all go into the analysis of this thermal design. Since this is a new technology, it is difficult to say with confidence what will be the most effective in real application due to the inexperienced nature of this idea and its new presence in the world of riser materials.

Detailed Development Plan

There are a few major portions of the piping that needs to be tested. Obviously, the materials should be pressure tested at the given conditions. This is common among current practice today in the design of production risers. The outer piping must be additionally tested in a similar way to take on the collapse pressure.

Connection Insulation Development

Since the insulation will be cut in half, prototype modeling will need to include an investigation into the ease of cutting through the assembly. If this portion of the insulation is also manufactured as a multi-layered vessel, the design must be completed such that cutting it in half will not cause the assembly to fall apart. Further testing should be performed verifying whether the o-rings can withstand the rigors of both the pressures experienced in 10,000 ft of water and at 15,000 psi internal pressure, as well as the longevity required to continually ensure a water tight seal. Welding the parts together will cause thermal contraction, but further testing should be performed to determine whether the contraction will cause the seals to leak. The manufacturing processes should be altered to make sure this isn't the case. Testing should be performed to determine whether a clamp is necessary to increase the contact pressure in the connection joint. If this clamp is necessary, it must be designed in order to impart the desired contact pressure on the o-rings. Another concern is welding on the layer touching the Mylar film. It should be determined whether welding the setup in place will affect the properties of the Mylar radiation film, therefore increasing the heat transfer of

the system. The only concern that differs with using the clamp on insulation is the need to find an appropriate insulating gel and vessel size. Depending on the heat transfer attained in the riser the connection gel insulation will have to be tailored to match that particular value and depending on the amount of gel needed will determine the vessel size.

Layered Wire Screen Mesh Development

Several things need to be tested to ensure the functionality of the mesh design. Physical testing and mathematical analysis should be extended on that already accomplished by the Texas A&M Mechanical Engineering Department to include all possibilities, perhaps ceramics and polymers as mesh material. Also, mechanical testing should be performed to show that the mesh insulation layers withstand any excessive bending or torsion forces exerted on the piping and stay in place. Since the outer pipe is designed to take the collapse pressure and the inner pipe the oil pressure, this should be tested as well to ensure that this does in fact work properly. Since deep sea environments tend to be rather brutal with the water pressures and corrosive natures involved, tests should be undertaken to mimic these conditions and evaluate how the mesh-liner system holds up under these circumstances.

It is desirable to create a prototype of a 60 ft length of pipe with insulation to perform these tests and give accurate results that will represent the actual conditions applied to this riser system. This life-size prototype is desired because of the need for an accurate model to recreate the probable stresses that the insulation may in reality endure. These stresses depend on the length of pipe involved, so a real prototype must be tested. Also, given the unknown behavior that this mesh system will exhibit under extreme manufacturing, installing, and operating conditions, tests should be conducted to explore this behavior and make the necessary adjustments to the design that will allow the technology to be employed in real application. Anticipated conditions include some “banging around” and bending/torsion stresses applied to undesirable areas in the mesh insulation. This is a crucial facet of testing to ensure the operability of this design in extreme and highly probable situations in a deep sea environment.

Possible failures associated with the mesh insulation may be attributed to these bending/torsion stresses that undoubtedly will occur while installation is taking place in

deep water pressures and currents. The mesh may want to deform greatly and cause non-uniform interface pressures anywhere in the insulation. This may largely affect the thermal resistance and instigate any number of problems. Again the behavior of this system is essentially unknown due to the complex mechanical nature of the numerous mesh-liner layers. The interface pressure will greatly affect this nature and the ability of the layers to retain their thermal properties upon deformation.

Summary

Using the Interstitially Insulated Coaxial Pipe insulation for a production riser will allow for deep sea production as well as providing a rugged alternative to present day insulation. The IICP design has added benefits because it takes into account all modes of heat transfer (conduction, convection and radiation) and has a method for reducing all three. The IICP system not only has better heat transfer characteristics compared to present day insulation, it is made out of steel increasing the overall durability and life of the system. There is no need to drastically change any of the present day service equipment because the overall dimensions do not differ greatly from production risers in use today. The IICP system is also designed to be effective independent of the water depth it is operating in since the outer layer is designed to withstand the collapse pressure at the specified depth and the inner pipe is designed to the well pressure. Due to this design there is a minimal transfer of stress to the layered insulation, therefore it still maintains all of its heat transfer characteristics. The insulation is also able to work in both sweet and sour wells due to the material used for the inner production riser.

Overall using the IICP system will:

- Decrease heat loss to the environment
- Increase the maximum water depth
- Increase riser life
- Increase resistance to wear
- Increase shut-in time
- Decrease the need for additional buoyancy devices

Appendix A: List of Abbreviations

PIP – Pipe in Pipe

IICP – Interstitially Insulated Coaxial Pipe

Appendix B: Glossary

Deep water – water that is 3,500 to 10,000 ft

System – production riser with insulation and any buoyancy devices in place

Well pressure – The shut in pressure of the formation

Collapse Pressure – Pressure created by the ocean at the deepest operational point

Connections – Any parts or extra material required to connect two sections of pipe together

Section of pipe – a 60 ft length of pipe

Environmental Conditions – all environments under the surface of the ocean including ocean currents and temperatures

Operational Life – Amount of time the given system is functional and able to carry out its designed purpose without failure

Corrosion – any damage caused by contact with sea water or petroleum and side products of the well which will reduce the integrity of the system

Interface pressure – the pressure by which the cylindrical layers of mesh are initially squeezed together during manufacture and which affects the thermal contact resistance of the two materials that are touching.

Pigging – the process of cleaning the walls of piping by sending an object called a “pig” down the length of the pipe to collect the buildup formed from the oil flow over time

Appendix C: References

Mylar properties - <http://www.yutopian.com/Yuan/prop/Mylar.html>

Marotta, Dr. Ed, Fletcher, Dr. L.S. "Interstitially Insulated Coaxial Pipe." Texas A&M University Department of Mechanical Engineering, 2005.

Material properties – www.matweb.com

Appendix D: Detailed Calculations

Final Design Report
**Manufacturing and Assembly of Interstitially
Insulated Coaxial Pipe**
Prepared For Lone Star Steel Company

EXECUTIVE SUMMARY

The Offshore Technology Research Center at Texas A&M University developed a new insulation design for line pipe to transport oil and gas at depths reaching up to 10,000 feet. This design is known as Interstitially Insulated Coaxial Pipe, and it has the potential to save oil companies millions of dollars by reducing the likelihood of paraffin or other flow buildup that causes lost production time by the use of an effective interior insulation design. One layer of the insulation contains an arrangement of Mylar© film, stainless steel wire mesh, Mylar©, and an intermediate stainless steel liner. The line pipe may contain up to six of these layers with an increase in thermal resistivity with each layer. The best insulation proved to be six layers of five-count mesh stainless steel wire screen equipped with Mylar© film that is inserted at the interface between two layers of pipe material (1).

Large and small line pipe models were designed to contain this optimum arrangement of insulation. The sizes designed were to compare to the standard 12 ¾ inch outer diameter line pipe and the standard 4 ½ inch outer diameter pipe. They'll be manufactured by drawing a mandrel through the inner diameter of the thick liner, which will plastically deform the insulation radially and make the pipe and insulation one component. During assembly, Chockfast Orange compound will be used to fill the void insulation space where two line pipes interface.

Final Design Report – Manufacturing and Assembly of Interstitally Insulated Coaxial Pipe

TABLE OF CONTENTS

EXECUTIVE SUMMARY.....	1
TABLE OF CONTENTS	2
LIST OF FIGURES AND TABLES	3
INTRODUCTION	4
<i>Need Statement</i>	5
<i>Need Analysis</i>	5
<i>Current Technology</i>	6
FUNCTION STRUCTURES.....	6
OVERALL SYSTEM DESCRIPTION	11
<i>Wire mesh</i>	13
<i>Mylar© Film</i>	15
<i>Insulation Layers</i>	16
<i>Method of Application</i>	17
<i>Component Specifications</i>	23
DETAILED DESIGN ANALYSIS	27
DETAILED DEVELOPMENT EVALUATION.....	35
<i>Failure Modes and Effects Analysis (FMEA)</i>	35
SUMMARY AND PERFORMANCE SPECIFICATIONS	35
APPENDIX A: LIST OF ABBREVIATIONS	39
APPENDIX B: GLOSSARY.....	39
APPENDIX C: REFERENCES	40
APPENDIX D: MATERIAL TABLES	40
APPENDIX E: MESH TYPE AND CONFIGURATION	43
APPENDIX F: DETAILED CALCULATIONS	44
APPENDIX G: DRAWINGS	54

LIST OF FIGURES AND TABLES

Figures

Figure 1. Top-level Functions 7
 Figure 2. Breakdown for providing a means to maintain required flow rate 7
 Figure 3. Breakdown of provide a means to prevent build-up formation of asphaltenes and paraffin 8
 Figure 4. Breakdown of provide a means to operate in 10,000 feet of water depth 9
 Figure 5. Breakdown of to provide a means to install on-site 10
 Figure 6. Breakdown of provide a means to prevent corrosion 10
 Figure 7. Configuration of one layer of Interstitially Insulated Coaxial Pipe (1) 12
 Figure 8. Definition of mesh count (1) 13
 Figure 9. As moisture content increases, the thermal conductivity decreases (3) 14
 Figure 10. Thermal conductivity various configuration of P110 pipe with stainless steel wire screen mesh and Mylar© (1) 16
 Figure 11. Overall thermal conductance as a function of wire screen mesh thermal 17
 Figure 12: Pre-expanded insulation to line pipe setup 18
 Figure 13: 2D Drawing Showing Product Ready for Expansion 19
 Figure 14: Unexpanded line pipe and insulation setup 20
 Figure 15: End of line pipe with prepared components 21
 Figure 16: 2D cross-section view of line pipe with insulation 21
 Figure 17. Illustration of filling void annulus 22
 Figure 18. Design of S-seal 25
 Figure 19. Cross-section of metal sealing sleeve 26
 Figure 20. 3D view of metal sealing sleeve 27
 Figure 21: Cross-section of pipe before expansion used for sizing 28
 Figure 22: Large pipe model data sheet 36
 Figure 23. Small pipe model data sheet 37
 Figure 25. Collection of mesh type and configuration (1) 43
 Figure 26. Examples of alternative to the conventional mesh (1) 43

Tables

Table 1: Mylar©, wire screen mesh and intermediate liner thickness 28
 Table 2: Large pipe model example for determining insulation thickness 29
 Table 3: Mylar© sheet specifications for large pipe (2 sheets per layer) 32
 Table 4: Mesh screen sheet specifications, five-count, AISI 430 stainless steel 33
 Table 5: Intermediate liner sizes – AISI 430 33
 Table 6: Production fluid liner – AISI 430 33
 Table 7: Mylar© specifications for small pipe (2 sheets per layer) 33
 Table 8: Mesh screen sheet specifications, five count, AISI 430 stainless steel 34
 Table 9: Intermediate liner sizes - AISI 430 34
 Table 10: Production fluid liner – AISI 430 34
 Table 11. Failure Modes and Effects Analysis (FMEA) 35
 Table 12. Mechanical and thermal properties of various metals 40
 Table 13. Stainless steel comparative landmark 40
 Table 14. Mechanical and thermal properties for Inconel and Incoloyl Alloys 41
 Table 15. Elemental break down of Inconel and Incoloyl Alloys 42

INTRODUCTION

Currently, many companies in the petroleum industry are expending greater effort for offshore exploration and production in deeper depths of the ocean, thus incurring greater expense for offshore drilling research and development. This has created a need for a more rugged insulated flow line design to provide lower overall cost for thermal resistance than current technologies. This design, developed by the Offshore Technology Research Center at Texas A&M University, is called the Interstitially Insulated Coaxial Pipe. The design takes into account the environmental condition experienced at these greater depths that include extremely hot and cold temperature conditions due to production flow and ocean water.

The following portions of the report include background information that contains a need statement and analysis that defines the scope of the project as well as a brief overview of current technologies. Following the background, the function structure will discuss the breakdown of the functions that are required for successful application of the design. Next, in the design requirements and specifications a table will display what each function must do and to what degree. Then, in-depth information on the design of Interstitially Insulated Coaxial Pipe will be presented in the overall system description, and the detailed design analysis will present the manufacturing and assembly design process. The report will be concluded with a summary and performance specifications.

BACKGROUND

In order to design the insulation, Texas A&M University's Offshore Technology Research Center developed a goal that would provide a similar performance to current technology with more advantages. This goal is stated below.

“The goal of this project was to reduce the overall thermal conductance of flow pipes through the insertion of one or more layers of a low thermal conductance screen mesh as a sleeve insert between an inner and outer pipe. This technology will offer a passive insulation solution to deep water flow-lines without the use of phase-change materials (e.g., paraffin waxes) or foam insulations, and minimizes solid deposits in the interior pipe.”- Offshore Technology Research Center at Texas A&M University

Need Statement

The goal of the Offshore Technology Research Center was used in the development of this projects scope. The first step in this process was to devise a broad statement that would encompass manufacturing and assembly process of the insulation. After much iteration, the final need statement was formed.

Final Need Statement

To design and develop a model for the application of a passive mechanical insulation inside standard sizes of line pipe. The selected size of pipe will be based on internal fluid flow area requirements as well as the heat loss rate to the sub-sea environment for various internal fluids. The amount of insulation used shall be sufficient to prevent asphaltenes and/or paraffin build-up inside the line pipe for a given minimum fluid temperature.

Need Analysis

With the development of this flow-line technology, there is a need for a manufacturing and assembly process because Lone Star Steel Company desires to install this Interstitially Insulated Coaxial Pipe technology. This new insulating technology is to be utilized in Lone Star Steel's fabrication process in order to provide fully insulated segments of line pipe, custom made to customer specifications at the mill. Comparisons were prepared for current insulating methods in the industry. Fabrication processes for installation were evaluated and presented, as well.

Definitions:

- *Design* – perform thermal analyses to provide adequate layers of insulation; perform deformation analysis on liner pipe for installation; research material properties.
- *Develop* – apply design to create a tangible product for mass production.
- *Sub-sea Environment* – approximately 38°F
- *Asphaltenes & Paraffin wax* – minerals that solidify and precipitate from liquid/gas phases inside of pipe surfaces due to declining de temperature difference.

- *Mean Fluid Temperature* – Insulated pipe must maintain a minimum temperature of 60°C for fluids flowing inside.

Current Technology

Current technologies used for flow assurance in transporting oil from a range of depths offshore include: pipe-in-pipe, exterior thermal insulation, external heating sources, and additives (chemicals). The concept of pipe-in-pipe is similar to the design of a heat exchanger in preventing oil from losing heat by conduction and convection. Next, exterior thermal insulation is located on the outside of the pipe wall, and it is currently the most common used method in the Gulf of Mexico (1). An external heating source uses power provided from the topside (rig) to maintain a specific temperature along the pipeline (2). Additives are used in combination with these other technologies. They are continuously added to production flow to aid in flow assurance. These current technologies share a common goal with Interstitially Insulated Coaxial Pipe in preventing production flow from blockage or build-up.

FUNCTION STRUCTURES

The function structure begins with a breakdown from the need statement. The top-level functions of the function structure are shown below in Figure 1. The top-level functions are the main functions that the insulated line pipe must fulfill. It must provide a means to: maintain required flowrate, prevent formation of asphaltens and paraffin, operate in 10,000 feet of water depth, install on-site, and prevent corrosion.

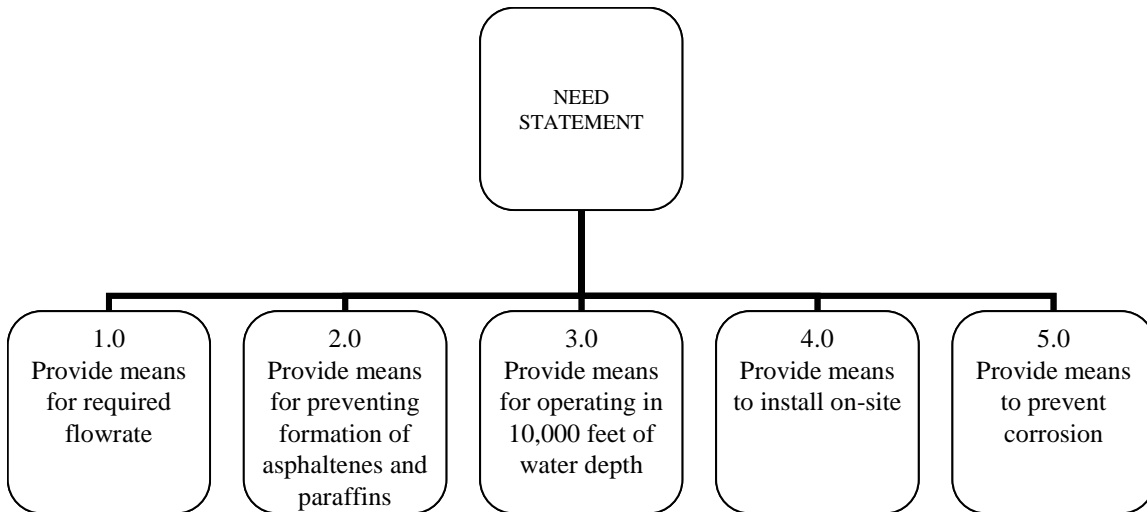


Figure 1. Top-level Functions

Figure 2 below shows a breakdown of a top-level function with its successive sub functions. Functional requirements are labeled by F.R. and performance requirements needed to be carried out by the function are labeled P.R. The first top-level function is to maintain a required flowrate. This may be accomplished in the pipeline by using standard sizes currently offered for this type of application in the oil industry, and maintaining a steady reservoir pressure.

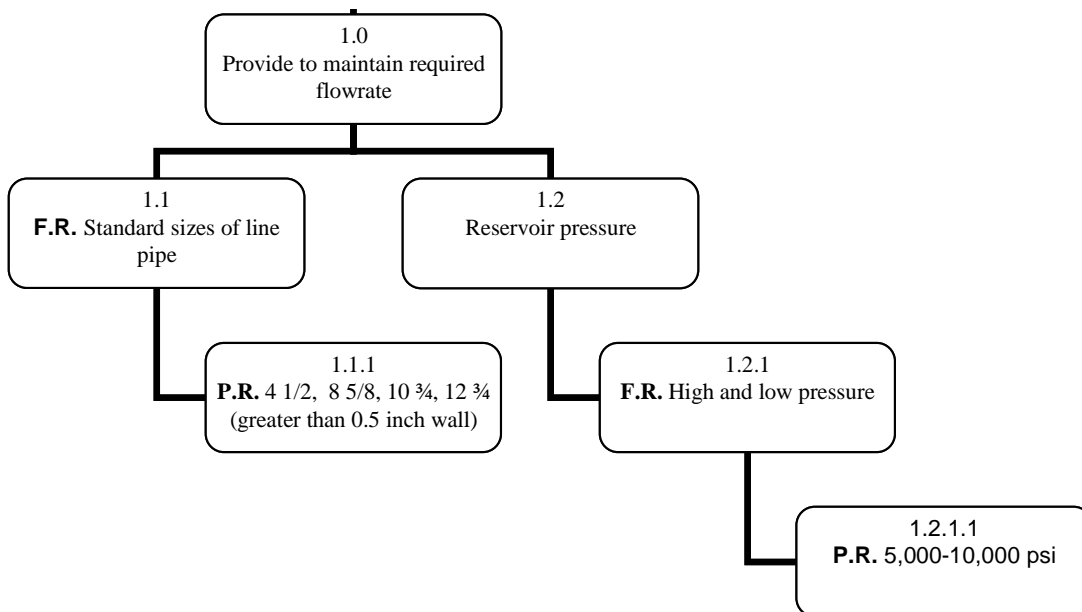


Figure 2. Breakdown for providing a means to maintain required flow rate

Figure 3 shows the next top-level function which is to prevent formation of asphaltenes and paraffin. By maintaining a temperature of 60 °C or higher with the use of some configuration of insulation in the line pipe, this build-up may be prevented.

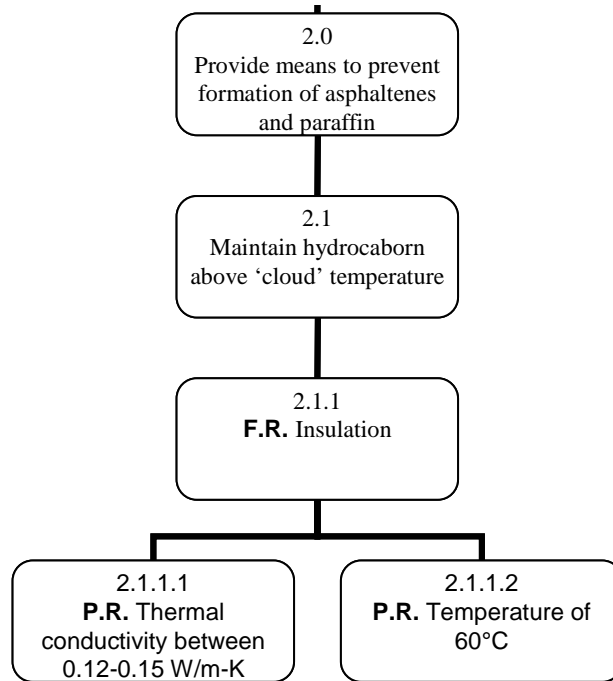


Figure 3. Breakdown of provide a means to prevent build-up formation of asphaltenes and paraffin

The line pipe must be able to withstand the environment and the large pressure at greater depths of operation. The third top-level function (Figure 4), to provide a means to operate in a large ocean depth of 10,000 feet, takes this point into account. By selecting a durable pipe material with a large enough wall thickness, this may be accomplished.

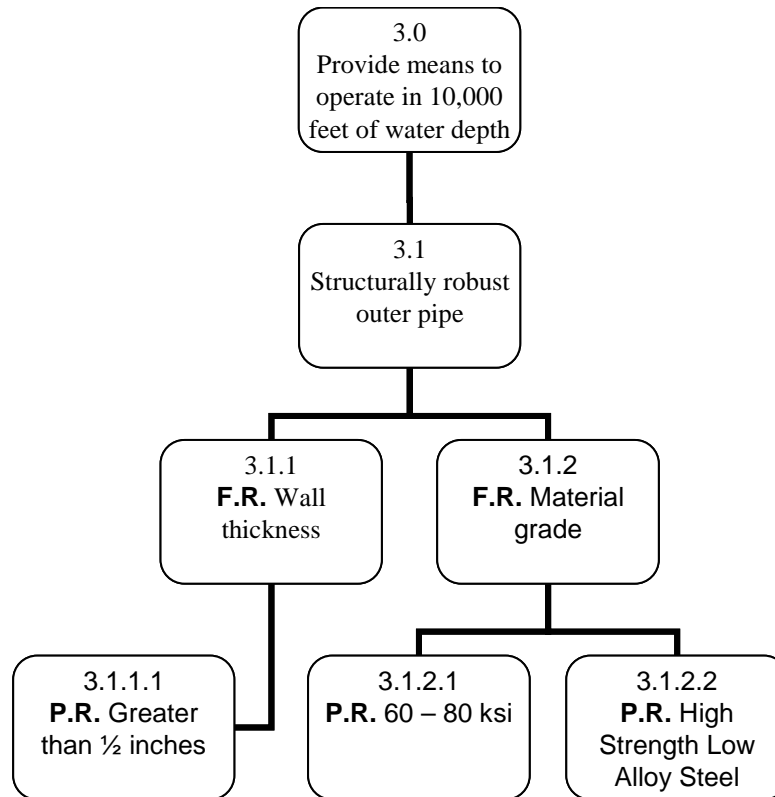


Figure 4. Breakdown of provide a means to operate in 10,000 feet of water depth

The design must be feasible in its assembly process. This idea has been captured in the fourth top-level function which is to provide a means to install on-site. The insulation must first be assemble by some process and placed in the line pipe. A device or process will create a proper resistance at the interface of the line pipe and insulation so that the insulation may plastically deform and stay intact with the line pipe. The breakdown of this function may be seen in Figure 5 below.

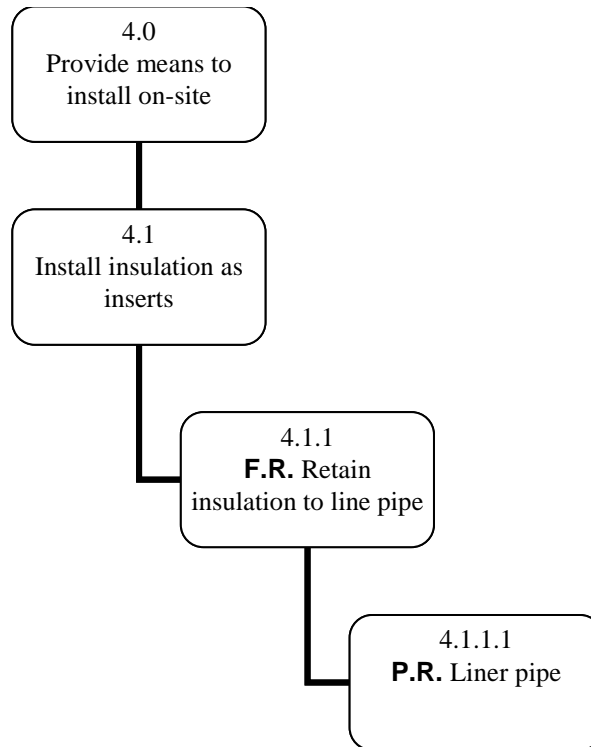


Figure 5. Breakdown of to provide a means to install on-site

The last top-level function involves preventing corrosion from occurring to the outer face of the line pipe that interface with the ocean water and to the inner surface interfacing with production flow. Corrosion may be prevented for a long time by coating the outer wall or cladding the inner pipe wall with some type of corrosion resistant material. Figure 6 below displays the breakdown of this function.

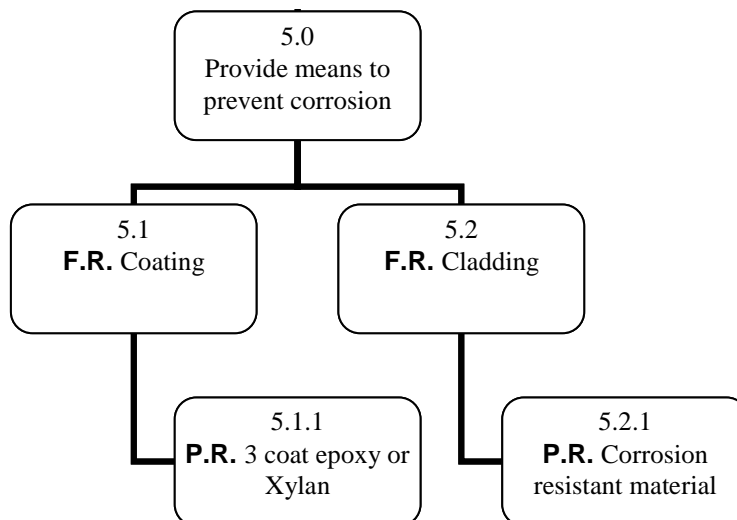


Figure 6. Breakdown of provide a means to prevent corrosion

Overall System Description

The product discussed in this report involved the adaptation of Texas A&M University's patented pipe insulation technology to line pipe for use in subsea applications. The ultimate goal of this technology is to effectively reduce the quantity of thermal energy (heat) leaving the production fluid. Keeping the heat trapped inside the line pipe prevents the formation of asphaltenes and paraffin waxes in the production fluid which could cause disruption of flow. Although this system adds to the capital cost of the product leaving the mill, it will save the customer time and money down the road compared to current insulating practices. There is a lot of money and time spent on preparing line pipe, not to mention the costly repairs to damaged insulation. With insulating materials on the outside of the pipe, it is subject to being struck by many objects (e.g. ship anchors). This technology is essentially maintenance free, as it is located inside the line pipe. This feature alone reduces cost because a customer would not have to worry about repairing damages (encountered in a subsea environment) to the insulation. In other words, the rugged line pipe protects the critical insulation which makes this product worry free to potential customers.

As mentioned previously, the insulation is located inside the pipe and was designed on the premise of contact resistance. Using several layers of stainless steel wire mesh, Mylar®, and intermediate liners, the heat can only travel through the system through distinct paths limiting the amount of energy that escapes. The material selection in the design also aids in keeping the production fluid above the clouding temperature by reducing heat transfer via conduction, convection and radiation. Current insulation in line pipe only reduces heat transfer in conduction. Moreover, the results seem to indicate superior insulating characteristics when compared to current available technologies that have far greater manufacturing complexities (1).

The design presented can be optimized even more upon customer interest. Currently, air is the gas present inside the insulation. Stagnant air has a very low thermal conductivity and acts as an element of insulation on its own. A severe drawback with using air, however, is moisture. Although the air's thermal conductivity decreases with increasing

percentages of moisture, it is only true for temperatures above the dew point. Once the air's temperature reaches the dew point, the moisture will condense and the insulation will have water inside. Obviously, water is extremely conductive and would really affect the performance of this technology. However, it is assumed that the temperature of the insulation will be much higher than the dew point of the air inside of it. As far as optimizing the insulation, gases with lower thermal conductivity than air such as argon can be used. No matter what is used, this insulation offers great flexibility in a way that a customer could customize the insulation for their needs.

This study involved the development of two line pipe models. A large pipe model was designed to compare to the standard 12 $\frac{3}{4}$ inch outer diameter line pipe, and a small pipe model was designed to compare to the standard 4 $\frac{1}{2}$ inch outer diameter pipe. When the term 'compared to' is used in reference to a standard line pipe size, it is referring to the flow rates. These models were sized from the inside expanding outward to ensure that customers retain their flow rate requirements. Regardless of the model's size, six layers of insulation were used. Figure 7 shows one layer of insulation that is composed of Mylar©, stainless steel wire mesh, Mylar© and an intermediate stainless steel liner (in order from center of pipe to outside of pipe).

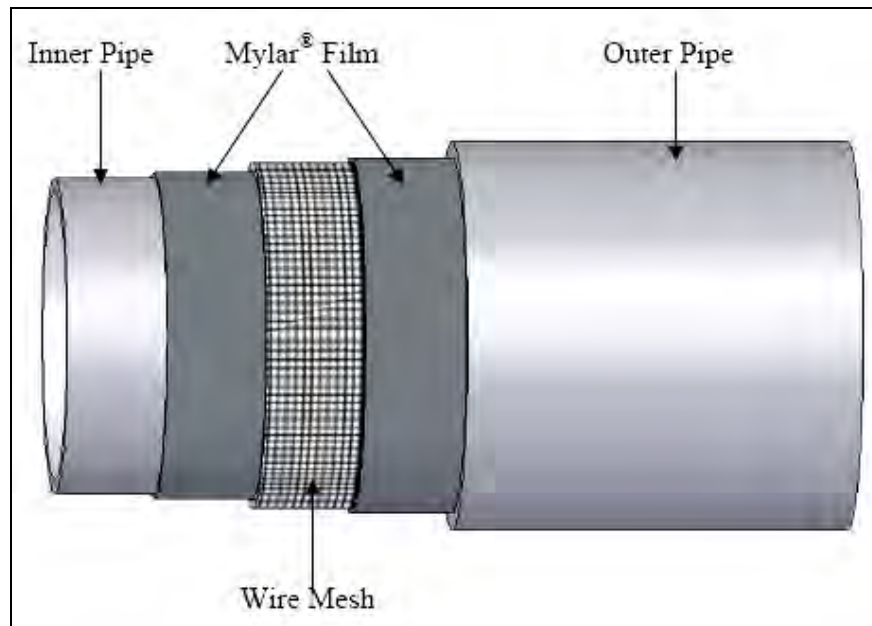


Figure 7. Configuration of one layer of Interstitially Insulated Coaxial Pipe (1)

All of the layers are secured to the outer diameter of another stainless steel liner (thicker than the intermediates). Four layers of insulation have shown to be the minimum amount of layers to gain sufficient amount of insulation to compare to what exists now. Six layers were chosen, as this is the optimized layer count. More layers can be used, but it is outside the scope of this project. Once all of the layers of insulation have been put together, the entire component is inserted inside a segment of line pipe. A mandrel drawn through the inner diameter of the thick liner will then plastically deform the insulation radially. The insulation (liners included) will expand until resistance is met in the inner diameter of the line pipe. The insulation will be trimmed per drawing instructions, specific surfaces will be polished and the insulation will be potted with Chockfast Orange. At this stage the line pipe and insulation are one component, and leaves the mill ready for installation.

Wire mesh

The wire mesh component makes this insulation design unique to other designs. Limited contact points of the wire mesh increase thermal resistance through the pipe wall and air gap, which lowers the heat transfer through both conduction and convection. In general, limiting the number of contact points will reduce heat transfer by conduction. Wire mesh is identified by the “mesh count” which corresponds to the number of contact points of the wire mesh in one linear inch. An illustration of two-count plain weave wire mesh is shown in Figure 8 below.

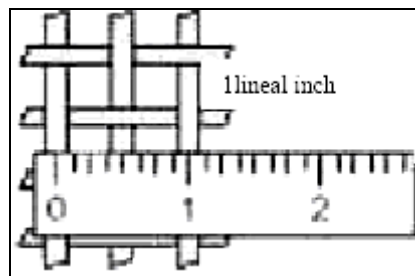


Figure 8. Definition of mesh count (1)

The material and configuration of the wire mesh impact the heat transfer. A set of selection criteria was used to determining the proper material for the wire mesh. The selection criteria included: geometry, material service and maximum temperatures,

manufacturability, and corrosion resistance. Although many materials meet the material properties required by the design (Appendix D), manufacturability ruled out all but stainless steel, titanium, and tungsten. Of these three materials, stainless steel proved to be the best selection based on the criteria and availability. The wire mesh comes in many different configurations (Appendix E). The best configuration that would optimize the insulation design demonstrated to be the plain weave style because of its simple design that would maximize the reduction of thermal conductivity through limited contact points and an air gap. Figure 8 above illustrates the design of a plain weave.

The air gap that the wire mesh creates could pose a problem if the air contains moisture, and it is aloud to reach the dew point temperature. Reaching the dew point temperature would allow the moisture to condense into water. Heat transfer would increase through the walls since water is a very good conductor. However, if the air never reaches the dew point temperature, moisture will not affect the heat transfer significantly. The rigid-sphere theory proves that as moisture increases in the air gap, the thermal conductivity will decrease slightly (3). This idea is shown by data presented in Figure 9 below.

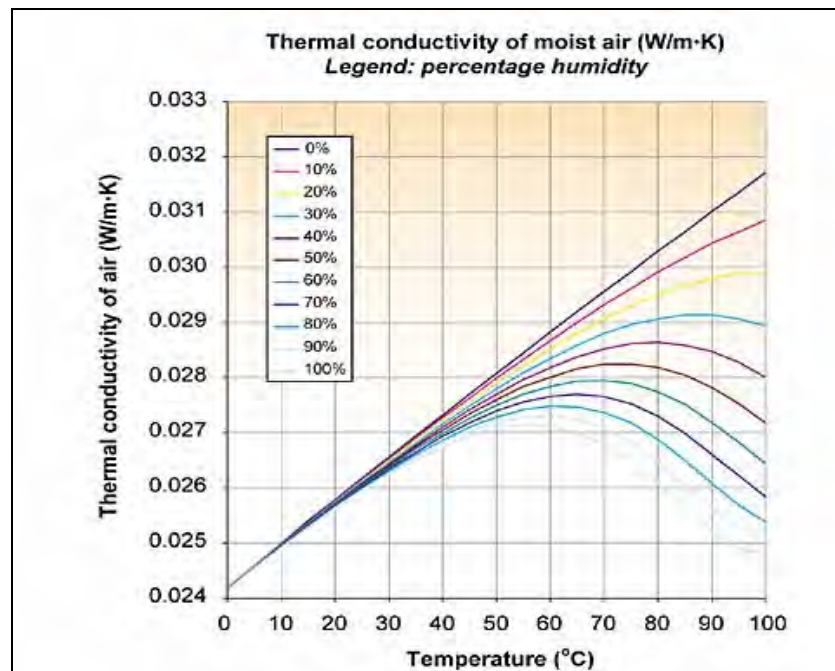


Figure 9. As moisture content increases, the thermal conductivity decreases (3)

Alternatives to the use of atmospheric air include: injecting dry air, injecting another gas such as Argon, or creating a vacuum in the void space. Dry air would eliminate any concern of water condensation, and injecting Argon would decrease heat transfer since Argon has a lower thermal conductivity than air.

Wire screen mesh has characteristics that include: the mesh count, configuration, and material. Testes were conducted to determine the optimum fit of these characteristics. The lowest equivalent heat transfer coefficient was determined from tests for plain weave stainless steel five-count mesh.

Mylar© Film

Mylar© is a very versatile material. Most importantly it is highly effective in temperature resistance, and it has an excellent oil or moisture barrier resistance. These properties make Mylar© an ideal candidate for additional aid in decreasing heat transfer. In the Interstitially Insulated Coaxial Pipe the Mylar© film was placed at the two interfaces of the liner pipe for to reduce radiation and conduction created across the air gap by the wire screen mesh. Tests determined that a 20% reduction of heat transfer occurred from the addition of these layers. Below, in Figure 10, is a comparison of experimental data from various configurations of pipe, wire screen mesh, and Mylar©.

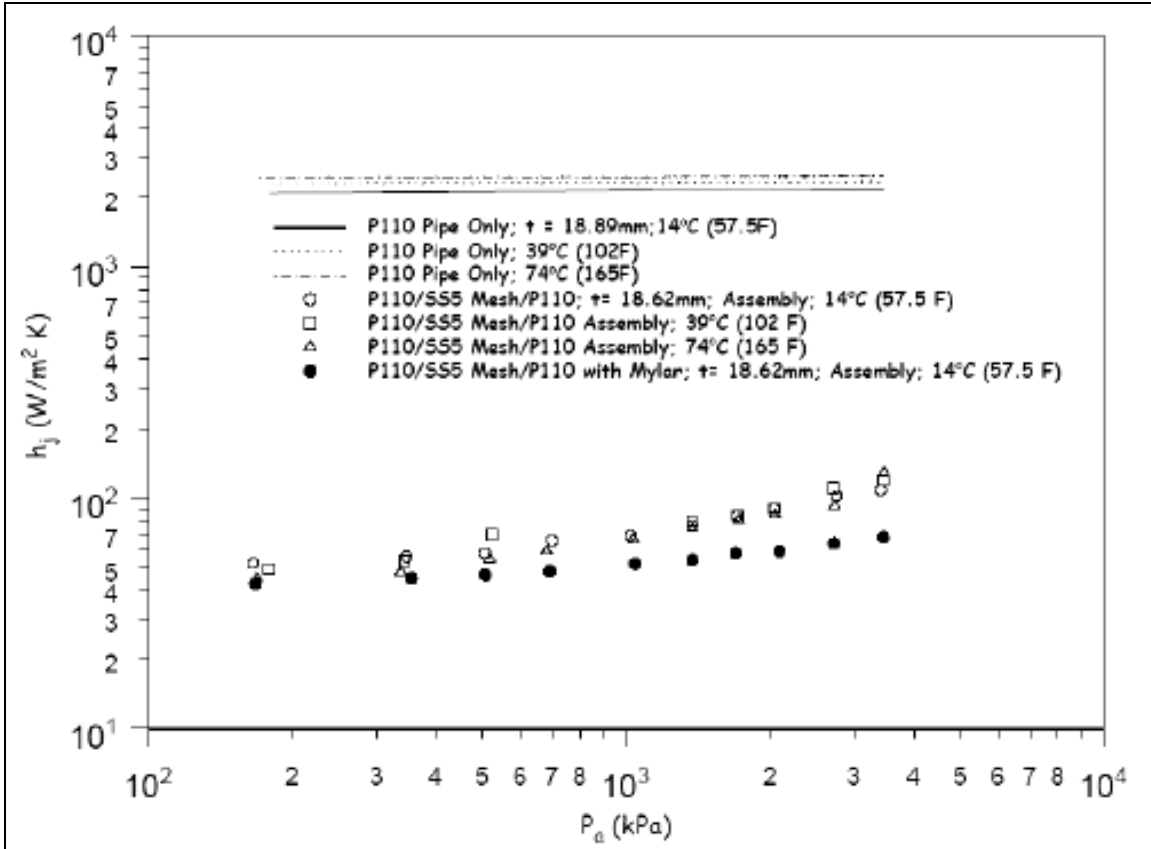


Figure 10. Thermal conductivity various configuration of P110 pipe with stainless steel wire screen mesh and Mylar© (1)

Results from the tests found that including Mylar© film with the five-count mesh, there was two orders of magnitude reduction in thermal contact resistance. The new design proves more beneficial by adding the two layers of Mylar© at the interface of the liner pipe between wire screen mesh.

Insulation Layers

Figure 11 below displays the test results when the insulation layers and mesh count were varied in order to determine the most effective and efficient configuration for the entire insulation. The data demonstrated that six layers of five-count mesh made of stainless steel wire screen and a Mylar© film at the interface pipe layer would provide the best insulation (1).

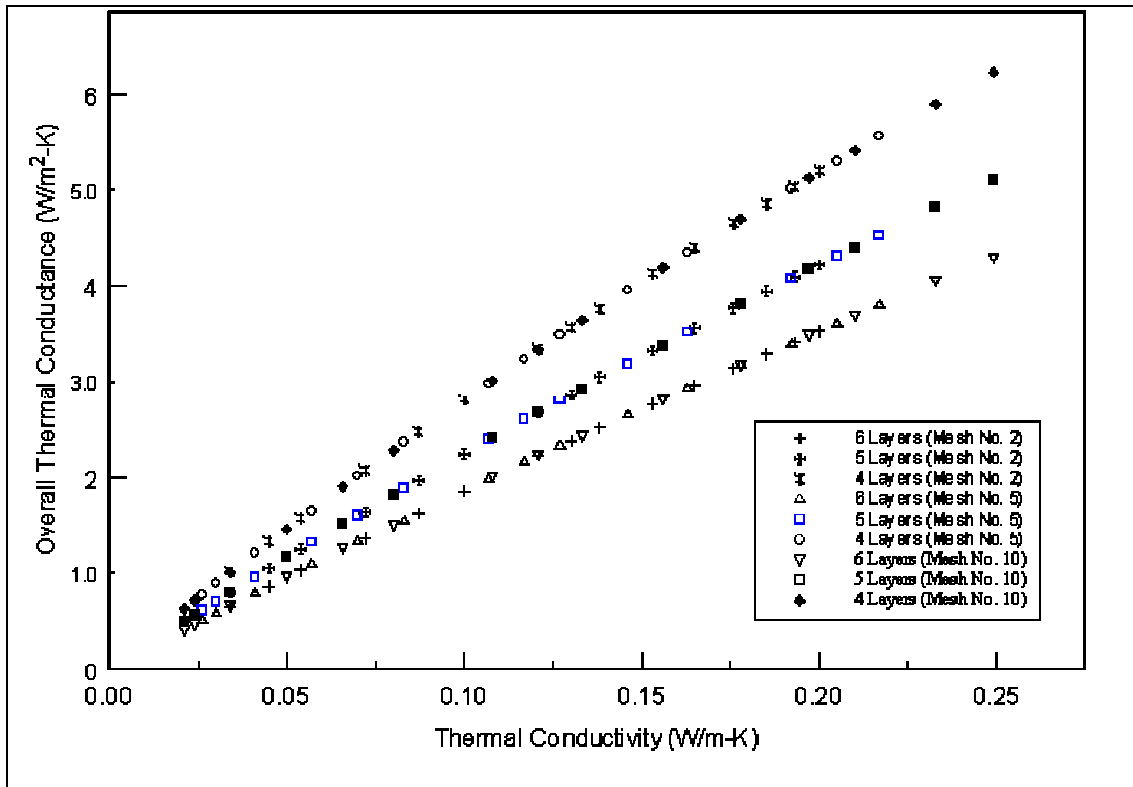


Figure 11. Overall thermal conductance as a function of wire screen mesh thermal conductivity (1)

This arrangement provided a thermal conductivity of 0.08 W/m-K (0.05 Btu/ft hr °F) at an interface pressure of 172.3 kPa (25.0 psi). This is comparable to current technologies, which range from 0.12 to 0.15W/m-K (0.07 Btu/ft hr °F to 0.09 Btu/ft hr °F) in effective thermal conductivity (1).

Method of Application

The first step in preparing this product for manufacturing is to acquire the appropriate materials and cut them to their appropriate sizes (see product specification sheets in appendix). Each segment of line pipe is assumed to be made in forty-two feet segments. Since the liners will decrease in length when expanded, they will need to be cut to forty-three feet lengths for the large pipe model and forty-four feet lengths for the small pipe model. Once the insulation layers are wrapped around the inner liner and secured, it can be inserted inside the segment of line pipe. At one end of the line pipe, the insulation will be offset outwards by two inches and structural steel ribbing will be welded on (see

Figure 12). It should be noted that the three-dimensional figures are not modeled to the specified lengths. They are shown shorter for clarity.

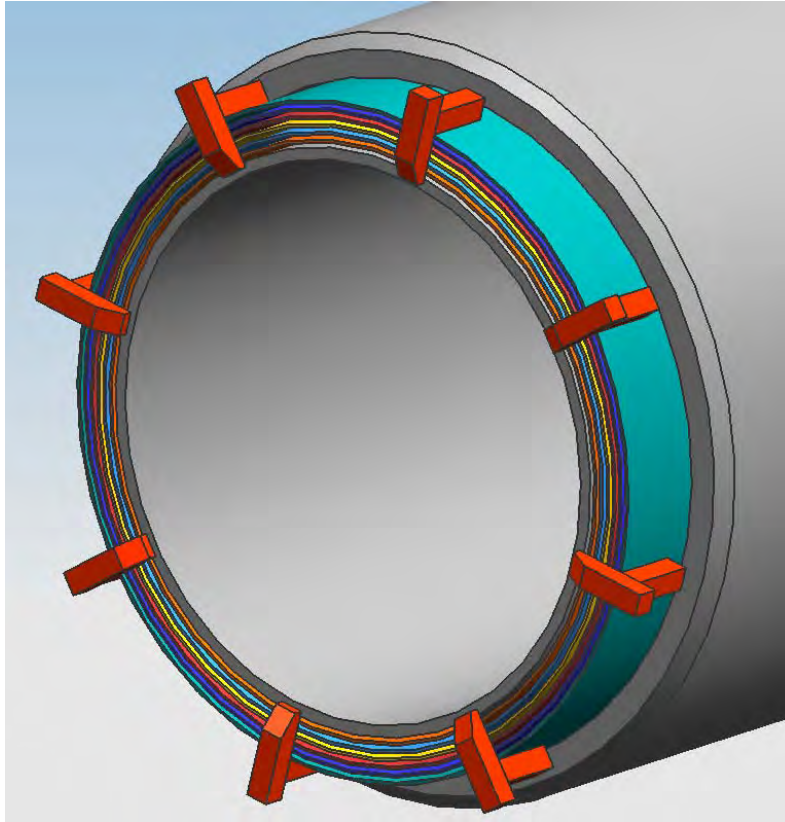


Figure 12: Pre-expanded insulation to line pipe setup

The steel ribbing will provide two functions as the insulation and liner are expanded. First, the members oriented radially will keep all of the layers flush and will also eliminate any relative axial slipping during expansion. These would be fillet welded around their perimeters to the steel liners. Second, the members that are oriented axially ensure that the insulation will not slide axially relative to the line pipe. These would also be fillet welded around their perimeters. See Figure 13 below.

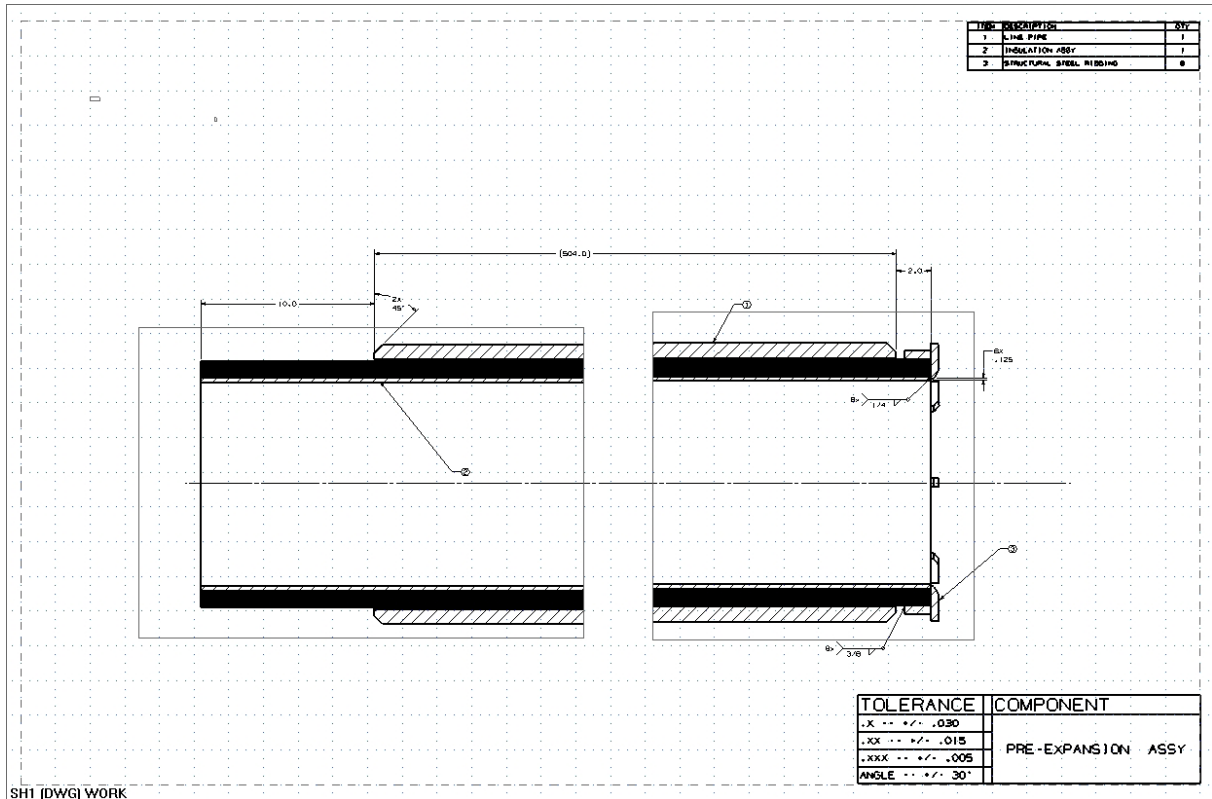


Figure 13: 2D Drawing Showing Product Ready for Expansion

The process chosen to secure the insulation and liner to the inside of the line pipe is to draw a mandrel (internally) through the liner. The mandrel would be sized to create the necessary interference to retain and plastically deform the insulation with liners to the line pipe. As the mandrel is pulled through the pipe, the layers of liner and insulation will naturally want to slide axially instead of expanding. The ribbing will serve as a reaction component so that the mandrel can begin to enter the bore to expand all components. The opposite end of the line pipe is free to move and is offset outwards ten inches to allow for the reduction in length. Having the assembly set up in this manner will force the liners to shrink at the free end only. Figure 14 shows the set up for expansion.

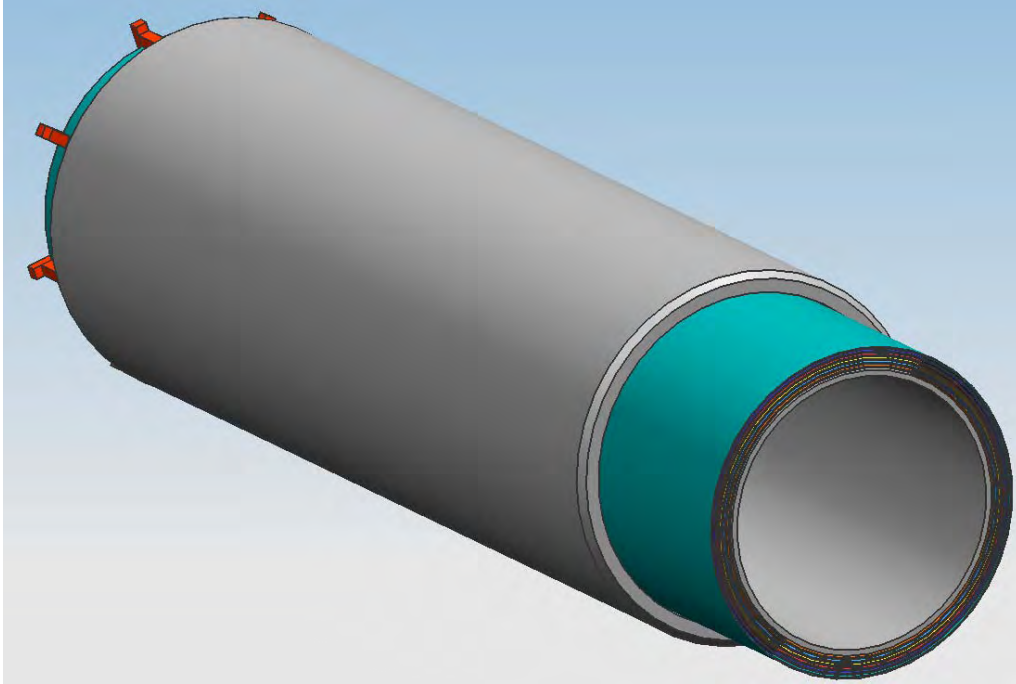
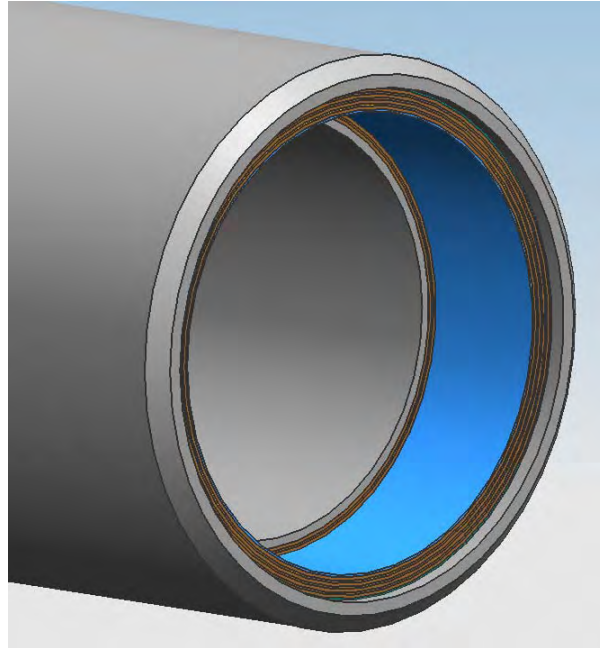


Figure 14: Unexpanded line pipe and insulation setup

After the mandrel has been pulled through and the insulation with liners has expanded, the pipe can now be prepped for a finished product. The insulation will be cutoff to achieve an inward offset of half an inch (from the end of the line pipe) at both ends. There will be another cut made four and a half inches from the ends removing two of the inner most layers (production liner included). The exposed surface will be polished smooth to a surface finish of 63 micro-inches (minimum). Figure 15 and Figure 16 below show the cross section of the pipe with these features added.



**Figure 15: End of line pipe with prepared components
(Both ends prepped as shown)**

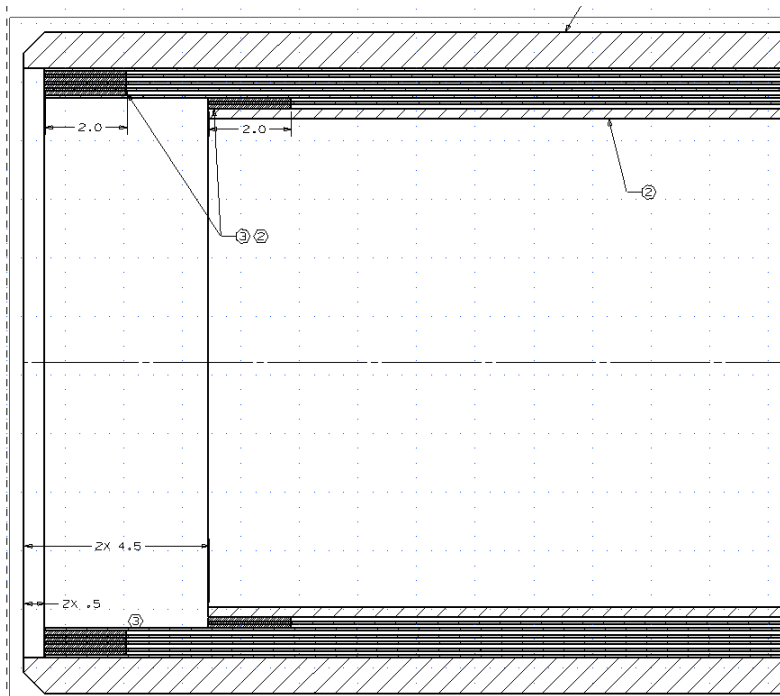


Figure 16: 2D cross-section view of line pipe with insulation

The final procedure in completing a segment of insulated pipe is applying a casting compound material, called Chockfast Orange, to the ends of the pipe inside the

insulation. See Figure 15 and 16 above. Chockfast Orange is designed to withstand severe marine and industrial environments involving a high degree of both physical and thermal shock. The casting compound material will be potted inside the void spaces between the layers of insulation. The extent of how far the compound is applied inside the insulation is not critical, as long as the gaps are filled. The compound filled ends will not only serve as additional insulation, but also as a barrier preventing the liquid injected polymer from running the length of the pipe. It also maintains the gas trapped and stagnant within the layers of insulation.

After the installation of the sealing sleeve into the end of one pipe and the connection with another, a void annulus between the outside diameter of the sealing sleeve and the inner diameter of the flow line must be filled. To begin, a consumable insert will be tacked nearly the entire circumference of the gap between the two pipes leaving a 3-4 inch space at the top. Next, Chockfast Orange compound, the same material that is used to pot the ends of the insulation in the pipes, will be poured into the annulus volume until full. The remaining gap can then be filled with nonconsumable insert. Finally, the butt joint can be fully welded and inspected to complete the assembly of the two members of the flow line. Figure 17 illustrates representing this process.

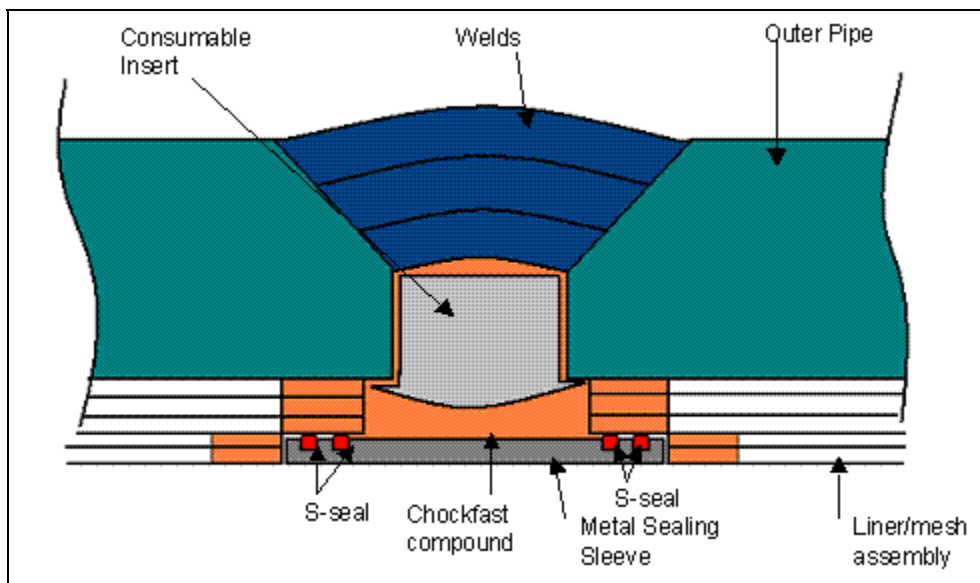


Figure 17. Illustration of filling void annulus

Component Specifications

The liners were chosen to be made from AISI 430 which is a special grade of stainless steel. The reason this steel was chosen was due to its anti-corrosive properties; mainly, not being susceptible to hydrogen induced cracking. Any steel with a hardness value below 22 HRC is not attacked by hydrogen at the grain boundaries (which leads to material failure).

The grade of line pipe was contingent upon the stress analysis performed on collapse pressure and limited by an upper bound with respect to yield strength. Designing the system to operate in depths of up to 10,000 feet, grades of X80 and X60 high strength low alloy steel were selected for large and small pipe models, respectively. Yield strengths of 80,000 pounds per square inch (psi) could not be surpassed as it would lead to hard points in the heat affected zone of welds. These hard points usually lead to cracking and can also cause material failure.

Several combinations of materials and wire screen mesh types were tested by Texas A&M researchers to achieve the lowest rate of heat transfer possible. It was determined that a five mesh stainless steel wire screen with an aluminized Mylar© film inserted at the interface between the two layers of pipe material provided the best insulation characteristics (1). The reflective side of the Mylar© would be facing the heat source to aid in radiating the heat leaving the fluid back to itself. Air is used as the gas trapped between all of the layers due to it being readily available and thermal properties. Other gases could be used in the place of air, and the air itself could be placed under vacuum if desired.

Chockfast Orange casting compound was used for added insulation and to provide a means of keeping the air trapped and stagnant. It will also serve as insulation and a barrier preventing hydrocarbons from getting inside the insulation. The compound will be potted in between the layers of insulation at each end before leaving the mill. Chockfast Orange is pour-able and will be dispensed into the annulus when two pipes are

made up to provide insulation. This material was chosen due to years of successful in-service experience.

The wire mesh/Mylar© thermal insulator concept is a novel idea and highly effective for the length of the pipe. However, the pipe ends must be connected for the assembly of a pipeline, and these connections can pose problems from a thermal aspect. As the fluid flows through the pipeline, the heat energy cannot escape effectively through the mesh insulator, and therefore must go somewhere. A poorly insulated connection would act as a heat sink, focusing all the heat energy at the pipeline connections.

Pipelines are most commonly connected by butt-welding two lengths together. This is the case when joining the rugged insulated flow lines; however, special considerations must be taken into account because of the insulation.

A sealing mechanism of some kind must be used to prevent fluid from entering the wire mesh layers of insulation. Metal to metal seals as well as elastomeric seals were considered for this. The metal-to-metal seal provide long life, reliable seals. One downside found was the installation of these types of seals since the pipelines are assembled in a horizontal fashion. A special tool would need to be designed to install the seals with the press fit required for an initial preload for them to be effective. This was decided against because of labor and time constraints.

Thermal expansion of the pipe joints also posed a possible problem for the metal seals. Distortion of the metal-to-metal seal contact point dimensions could compromise the entire seal, allowing fluid leaks as well as thermal leaks through the connection.

The seal design decided upon is a metal sleeve insert with double S-seals on each end that seal against the inner insulation liner. Figure 18 below illustrates the design.

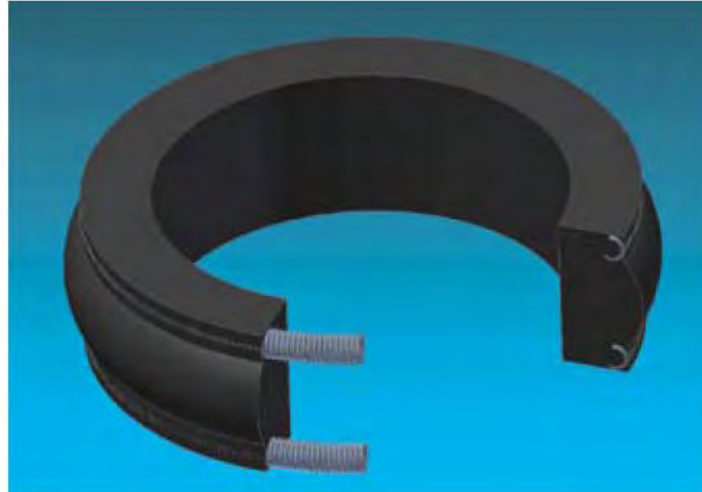


Figure 18. Design of S-seal

An S-seal, or spring seal, is a static elastomer seal that seals pressure in the radial direction. Sealing is accomplished by significant interference between the radial “bump” of the s-seal and the opposing metal wall. S-seals are considered a pressure-energized seal; however, a substantial initial interference of squeeze is needed for the seal to function properly. S-seals perform the same sealing characteristics as O-rings but exhibit much broader temperature and pressure capability. The S-seal is a compact, single piece design featuring a molded elastomer with two metal spring anti-extrusion rings molded into the outer edges of the elastomer. This simple construction is advantageous as opposed to a three-piece assembly associated with o-rings and their backup seals. Finally, the s-seal is easily installable by simply stretching it over an OD. Figure 19 shows an S-seal with a cross sectional cutaway view.

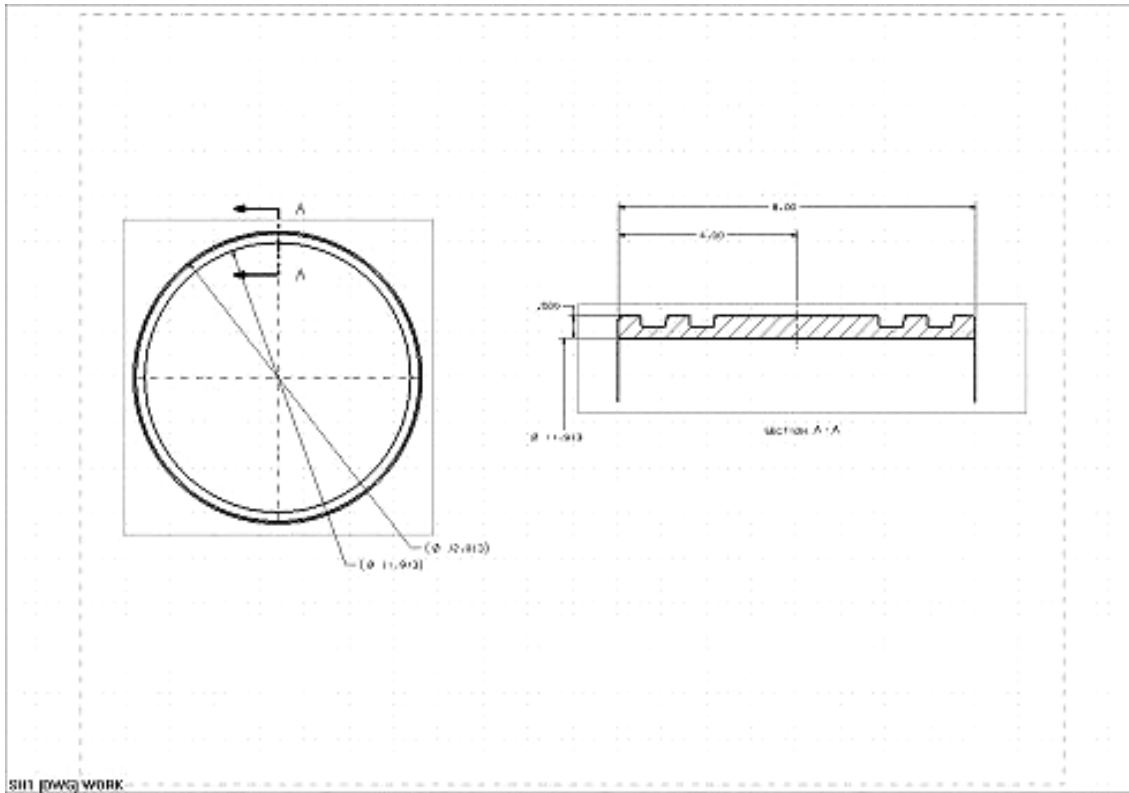


Figure 19. Cross-section of metal sealing sleeve

A ¼ nominal cross section standard S-seal from Parker Hannifin Corporation was chosen for the four seals to be used on the sealing insert. Furthermore, a special high tensile, heat resistant HNBR elastomer S-seal was chosen for the high temperature application. High tensile strength coupled with high resistance to heat, plus compatibility with hydrogen sulfide, corrosion inhibitors, steam and oil were selling features of this S-seal.

The metal sealing sleeve that the S-seals are assembled on is a solid, machined piece of 430 AISI Stainless Steel material coated with Xylan. The AISI 430 Stainless Steel material chosen is resistant to sulfide stress corrosion cracking, a major concern in the oil industry for sour service wells. The Xylan coating will aid in wear resistance, heat resistance, and corrosion issues for the sealing sleeve.



Figure 20. 3D view of metal sealing sleeve

Detailed Design Analysis

The design analysis began by determining the most commonly ordered sizes of line pipe for sub-sea applications. Having acquired that information, two sizes were selected for a large pipe and small pipe model. The large pipe model was based off of the 12 $\frac{3}{4}$ inch (outer diameter) pipe with a $\frac{1}{2}$ inch wall thickness, and the small pipe model was based off of the 4 $\frac{1}{2}$ inch (outer diameter) pipe with a $\frac{1}{2}$ inch wall thickness. The flow diameter was then determined for both models. The models (with liner and insulation) were sized for each specific flow diameter from the inside to the outside. Figure 21 shows a cross section of an arbitrary pipe with the pertinent radii denoted by R_n .

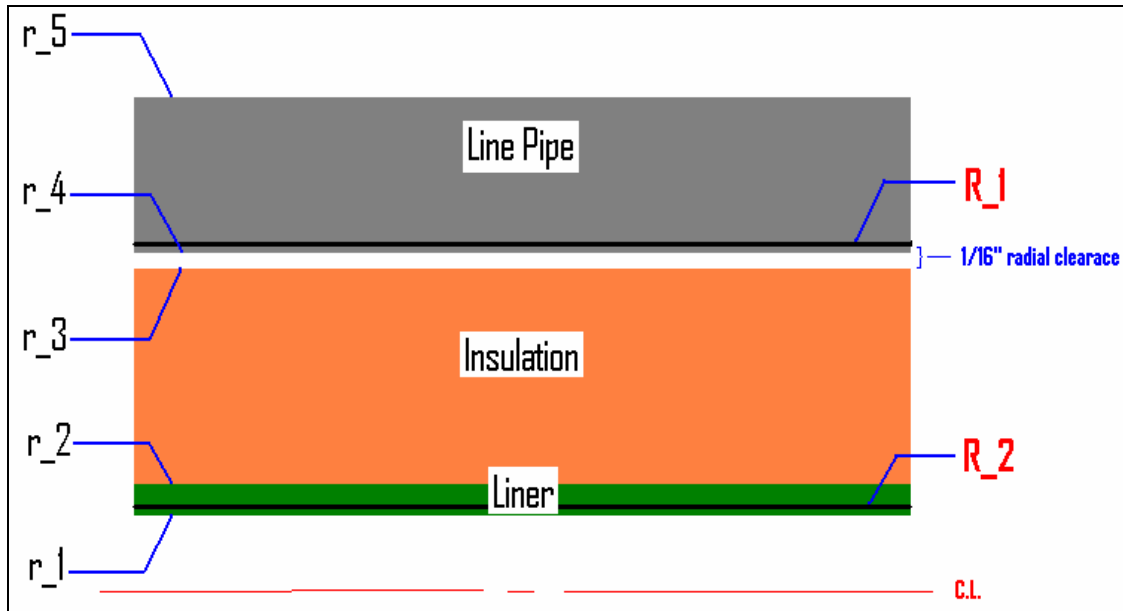


Figure 21: Cross-section of pipe before expansion used for sizing

The layers were all sized before the expansion occurred. Beginning with r_1 , it was half of the flow diameter of the standard size pipe. The production fluid liner was $\frac{1}{4}$ inch thick which determined r_2 . The insulation thickness was determined by adding the thickness of the steel wire screen mesh, Mylar© film and intermediate liner for each of the six layers used.

Table 1 gives the measured thickness for each of these components.

Table 1: Mylar©, wire screen mesh and intermediate liner thickness

Insulation Layer Specs		
Mylar© Thickness	0.015	in
Wire Mesh Thickness	0.072	in
Intermediate Liner Thickness	0.0625	in

A spreadsheet was created and all layers and components that made up a layer were summed up to determine the wall thickness of the insulation (before expansion). Table 2 shows that the thickness for all six layers was 0.9870 inches ($R_x - r_{outer}$). The addition of this value to r_2 determined r_3 .

Table 2: Large pipe model example for determining insulation thickness

Pre-Expansion	Radius			Circumference			
Inner-most Liner Outer Radius	r_{outer}	6.125	in				
First Layer	Ra	6.1400	in	Mylar©	Ca	38.5788	in
	Rb	6.2120	in	Mesh	Cb	39.0311	in
	Rc	6.2270	in	Mylar©	Cc	39.1254	in
	Rd	6.2895	in	Liner	Cd	39.5181	in
Second Layer	Re	6.3045	in	Mylar©	Ce	39.6123	in
	Rf	6.3765	in	Mesh	Cf	40.0647	in
	Rg	6.3915	in	Mylar©	Cg	40.1590	in
	Rh	6.4540	in	Liner	Ch	40.5517	in
Third Layer	Ri	6.4690	in	Mylar©	Ci	40.6459	in
	Rj	6.5410	in	Mesh	Cj	41.0983	in
	Rk	6.5560	in	Mylar©	Ck	41.1926	in
	RI	6.6185	in	Liner	Cl	41.5853	in
Fourth Layer	Rm	6.6335	in	Mylar©	Cm	41.6795	in
	Rn	6.7055	in	Mesh	Cn	42.1319	in
	Ro	6.7205	in	Mylar©	Co	42.2261	in
	Rp	6.7830	in	Liner	Cp	42.6188	in
Fifth Layer	Rq	6.7980	in	Mylar©	Cq	42.7131	in
	Rr	6.8700	in	Mesh	Cr	43.1655	in
	Rs	6.8850	in	Mylar©	Cs	43.2597	in
	Rt	6.9475	in	Liner	Ct	43.6524	in
Sixth Layer	Ru	6.9625	in	Mylar©	Cu	43.7467	in
	Rv	7.0345	in	Mesh	Cv	44.1991	in
	Rw	7.0495	in	Mylar©	Cw	44.2933	in
	Rx	7.1120	in	Liner	Cx	44.6860	in
Line Pipe							

Due to the drift clearance requirement of 1/16 inch (radially), r_4 was determined by adding 1/16 inch to r_3 . The wall thickness of the line pipe was determined by performing a collapse pressure analysis. Through trial and error, the wall thickness was determined for a specific grade of line pipe as well as the outer diameter. The collapse pressure analysis used was from API Bulletin on Formulas and Calculations for Casing, Tubing,

Drill Pipe and Line Pipe Properties (5C3). The models were evaluated at a maximum water depth of 10,000 feet. The type of collapse pressure equation depends on the diameter to thickness ratio (D/t). For the large pipe model, the D/t value was within the range of 13.88 to 22.47. The D/t value specified the equation, type of analysis, formula factors and pipe grade. Equation 1 shows the formula for the minimum collapse pressure, P_p , for plastic range of collapse on the large pipe.

$$P_p = \sigma_y * \left(\frac{A}{(D/t)} - B \right) - C$$

Equation 1: Collapse pressure equation for large pipe model

Where

A, B, & C = Formula Factors (Table 1.1.2.1, API 5C3)

σ_y = Yield Strength for Specific Grade

For the small pipe model, the D/t ratio was below 11 so the collapse pressure formula used can be referenced by Equation 2. This formula determines the external pressure, P_{yp} , required to generate the minimum yield stress on the inside wall of a tube.

$$P_{yp} = 2\sigma_y * \left[\frac{(D/t) - 1}{(D/t)^2} \right]$$

Equation 2: Collapse pressure equation for small pipe model

In 10,000 feet of depth, the external load put on any segment of pipe is 5,000 psi. This value was obtained by applying a rule of thumb that states a 1/2 psi per foot of water depth (sea water) acting on the outside of a component submerged. The collapse pressure for the large pipe model was 6,145 psi with a wall thickness of 0.875 inches. The collapse pressure for the small pipe model was 10,670 psi with a 0.75 wall thickness.

The proceeding analysis focused on the expansion of the internal components (production fluid liner and insulation) inside the line pipe. The process of expanding these components was by drawing a mandrel (internally) through the length of the pipe. The outer diameter of the mandrel was larger than the inner diameter of the production fluid liner, and would essentially provide a press fit to secure the layers of components to the

inside of the line pipe. The analysis began by arbitrarily choosing a radial interference value of 1/128 inches. Running the mandrel through the pipe would expand the components to new radii referred to as R_1 and R_2 , and may be referred to in Figure 21. Determining the outer diameter of the mandrel required adding the interference and drift clearance values to r_1 and converted to a diameter. This diameter was 11.891 inches and 3.641 inches for the large pipe and small pipe, respectively. These values also served as the transition radii for both models denoted as R_2 in Figure 21.

In order to ensure that the liners remained at their new diameters, the mandrel needed to impose enough pressure to plastically deform the materials. The interface pressure was calculated using Equation 3 below.

$$P_{R2} = \frac{E\delta_{tot}}{R_2} * \left[\frac{(r_3^2 - R_2^2) * (R_2^2 - r_{i,die}^2)}{2R_2^2 * (r_3^2 - r_{i,die}^2)} \right]$$

Equation 3: Interface pressure formula at R2

Where

E = Modulus of Elasticity of AISI 430

δ_{tot} = Interference + drift clearance values

$r_{i,mandrel}$ = Inner Diameter of Mandrel (assumed)

Next, the hoop stress was calculated with the known pressure using Equation 4 below. This equation is known as Lamé's Theory of Stress Analysis for Thick Walled Cylinders. The stress calculated was much larger than the yield strength of the large and small pipe which confirmed that the stainless steel liners would plastically deform.

$$\sigma_{hoop} = \frac{P_{R2}d_i^2}{d_o^2 - d_i^2} + \frac{d_i^2d_o^2}{d^2} * \left(\frac{P_{R2}}{d_o^2 - d_i^2} \right)$$

Equation 4: Hoop stress at internal wall of liner

Where

d_i = Inside Diameter

d_o = Outside Diameter

d = Transition Diameter

An analysis of vessel strength was also performed to determine the beginning of liner yielding. There are various theories of failure for combined stresses based upon the yield strength of the material have been applied to determine the beginning of yield of cylinders subjected to internal pressure. Out of all the theories, Lamé's was chosen upon recommendation and accuracy for determining stresses. This formula is based upon the stress, shear, strain, strain energy and distortion energy theories for elastic failure. See Equation 5 below.

$$P = \sigma_y \left(\frac{\left(\frac{d_o}{d_i} \right)^2 - 1}{\left(\frac{d_o}{d_i} \right)^2 + 1} \right)$$

Equation 5: Pressure based upon beginning of yielding

Inserting this pressure into Equation 4, the necessary hoop stress was determined. This stress validated that the stress imposed on the system must exceed the yield strength. Finally, a calculation was performed to determine the percentage of length that the liner would shrink as they expanded. This was performed assuming that the wall thickness of the liners did not change. Therefore, mass conservation was applied to the system and the percent of shrink was determined for both models. The detailed calculations for this project may be referenced in the Appendix for both pipe models.

The tables below list the sizes of Mylar©, wire screen mesh screen and liners for the large pipe model.

Table 3: Mylar© sheet specifications for large pipe (2 sheets per layer)

Layer	Sheet Width (inches)	Sheet Length (feet)
1	38.6, 39 1/8	43
2	39.6, 40.2	43
3	40.7, 41.2	43
4	41.7, 42.2	43
5	42.7, 43.3	43
6	43 3/4, 44.3	43

Table 4: Mesh screen sheet specifications, five-count, AISI 430 stainless steel

Layer	Sheet Width (inches)	Sheet Length (feet)
1	39.1	43
2	40.1	43
3	41.1	43
4	42.2	43
5	43.2	43
6	44.2	43

Table 5: Intermediate liner sizes – AISI 430

Layer	Pipe Outer Diameter (in) x Wall Thickness (in)	Pipe Length (feet)
1	12 37/64 x 1/16	43
2	12 29/32 x 1/16	43
3	13 15/64 x 1/16	43
4	13 9/16 x 1/16	43
5	13 8/9 x 1/16	43
6	14 7/32 x 1/16	43

Table 6: Production fluid liner – AISI 430

Parameter	Value
Inner Diameter	6.125inches
Wall Thickness	0.25inches
Length	43 feet
Percent Reduction in Length After Radial Expansion:	1.158%

The tables below list the sizes of Mylar®, wire screen mesh and liners for the small pipe model.

Table 7: Mylar® specifications for small pipe (2 sheets per layer)

Layer	Sheet Width (inches)	Sheet Length (feet)
1	12.7, 13.3	44
2	13.7, 14 ¼	44
3	14 ¾, 15.28	44
4	15.8, 16 1/3	44
5	16.8, 17.35	44
6	17.83, 18.38	44

Table 8: Mesh screen sheet specifications, five count, AISI 430 stainless steel

Layer	Sheet Width (inches)	Sheet Length (feet)
1	13.12	44
2	14.15	44
3	15.19	44
4	16 ¼	44
5	17 ¼	44
6	18.3	44

Table 9: Intermediate liner sizes - AISI 430

Layer	Pipe Outer Diameter (in) x Wall Thickness (in)	Pipe Length (feet)
1	4 17/64 x 1/16	44
2	4 19/32 x 1/16	44
3	4 59/64 x 1/16	44
4	5¼ x 1/16	44
5	54/7 x 1/16	44
6	529/32 x 1/16	44

Table 10: Production fluid liner – AISI 430

Parameter	Value
Inner Diameter	2.0 inches
Wall Thickness	0.25inches
Length	44 feet
Percent Reduction in Length After Radial Expansion:	3.614%

Because hot fluid will be in direct contact with the stainless steel liner, the thermal expansion was calculated. Equation 6 shows how this value was calculated, and provisions were made to ensure that the design would not be affected by elongating pipe. The liner pipe will expand by half of an inch is subjected to a temperature difference of 300 degrees Fahrenheit.

$$\Delta L = \alpha L_o \Delta T$$

Equation 6: Thermal expansion of pipe (linear)

Where,

ΔL = Change in Pipe Length, inches

α = Thermal Expansion Coefficient, $1/^\circ\text{F}$

ΔT = Temperature Difference

Detailed Development Evaluation

This project is meant to inform the industry of the capability and application of this new technology. The product will not be physically constructed this semester, but will be investigated further by customers who decide to use this technology.

Failure Modes and Effects Analysis (FMEA)

Table 11. Failure Modes and Effects Analysis (FMEA)

Item	Failure	Severity	Likelihood	Solution
Sliding Seal	Fluid Leak	med	low	Design, Polymer back seal, casting compound filled cavity, weld, chockfast potting, surface finish
Insulation	Heat Leak	high	low	Six layers, chockfast potting, materials, casting compound filled cavity
	Air condenses; loss of contact resistance	high	high	Injection of gas (argon), ceramic powder, vacuum, or dry air pump
	Liner buckling; thermal expansion	high	med	Floating connection, sliding seal sleeve, offset of insulation
	Corrosion	med	low	AISI 430 liner material
Pipe	Crack at weld (hard points)	high	low	Material selection
	Corrosion	med	low	3-part epoxy coating applied to outer surface
	Collapse	high	low	Sufficient wall thickness

SUMMARY AND PERFORMANCE SPECIFICATIONS

A summary of the large and small pipe specifications is summarized in Figure 22 and **Error! Reference source not found.** below.

Large Pipe Performance Specifications:

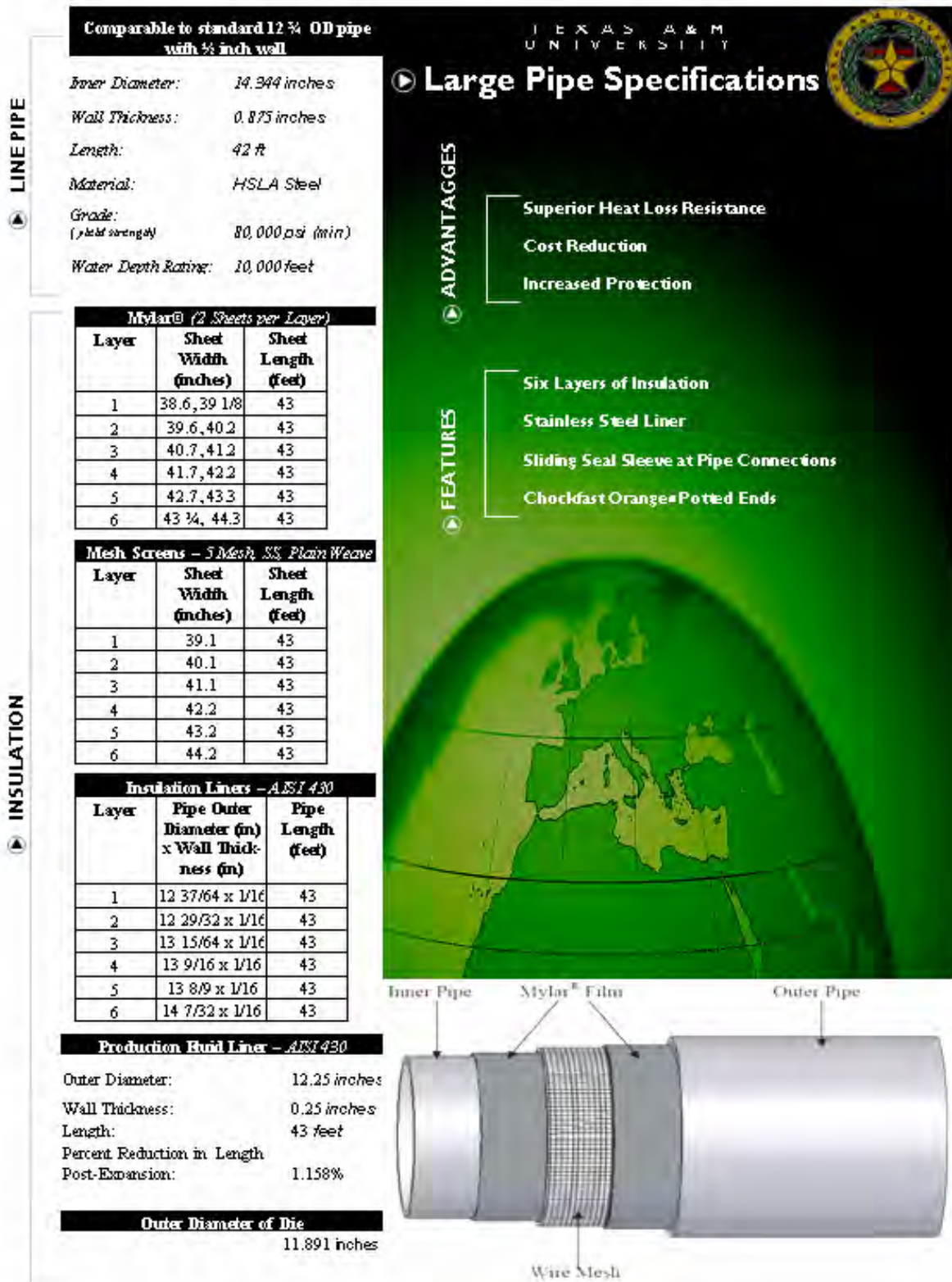


Figure 22: Large pipe model data sheet

Small Pipe Specifications:

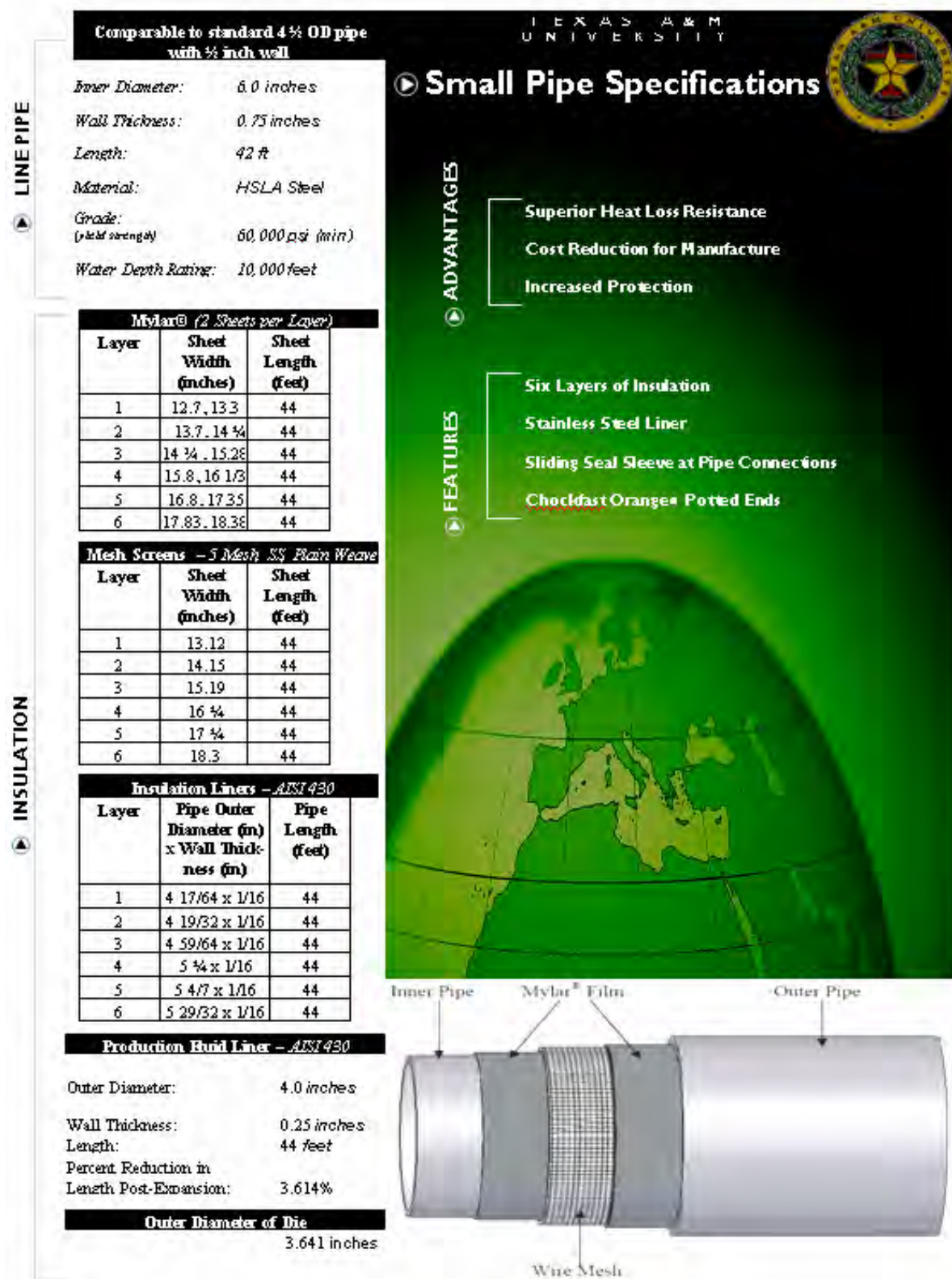


Figure 23. Small pipe model data sheet

Environmental Impact Statement:

The only item that has any environmental effect is the Chockfast Orange casting compound. Special care should be taken when handling and applying this product. Refer to the manufacturers precautions.

The production of this new flow-line design, Interstitially Insulated Coaxial Pipe, will bring many advantages to the oil industry. By using stainless steel wire mesh with Mylar© at the pipe interface, heat transfer will be effectively cut off. The hot temperatures of the production flow will be isolated from the cold temperatures of the ocean water preventing paraffin waxes or other build-up from occurring. This intern limits the amount of maintenance needed decreasing lost production time there by increasing profits. The rugged insulation would be manufactured and pre-assembled at the manufacturing site. This creates ease for installation and handling of the pipe when it is being used offshore. The insulation design also consists of common materials which allow for material availability and a consistent production process. Multiple layers of insulation are possible depending on the need and budget of the project and with the insulation located between an inner liner pipe and outer line pipe the product is very durable. This technology also accommodates pigging without damage to the interior. The production of Interstitially Insulation Coaxial Pipe will be as effective as current technologies, but it will provide more advantages to the customer.

We would like to thank our sponsors at Lone Star Steel for the tremendous amount of help over the term, and also for making the long drive to meet with us for the presentation.

A special thanks also goes out to our professor, Mr. Buddy Bollfrass. Mr. Bollfrass was very helpful, patient and kind. He was always willing to meet with us and discuss issues that arose.

Appendix A: List of Abbreviations

HSLA – High Strength Low Alloy

Appendix B: Glossary

1. Conduction - The transmission or conveying of something through a medium or passage, especially the transmission of electric charge or heat through a conducting medium without perceptible motion of the medium itself.
2. Convection - Heat transfer in a gas or liquid by the circulation of currents from one region to another.
3. Mandrel - A device used for cutting out, forming, or stamping material
4. Hoop stress - Mechanical stress applied in a direction perpendicular to the radius of the item in question.
5. Lamé's Theory of Stress Analysis for Thick Walled Cylinders
6. Mylar© film - Biaxial oriented, thermoplastic film made from ethylene glycol and dimethyl terephthalate (DMT)
7. Paraffin - A waxy white or colorless solid hydrocarbon mixture used to make candles, wax paper, lubricants, and sealing materials
8. Plastic deformation - Deformation that is not reversible
9. Radiation - Mission and propagation and emission of energy in the form of rays or waves
10. Rigid-sphere theory - Thermal conductivity is proportional to the specific heat by volume and inversely proportional to the square of the diameter of the molecules. Water vapor has a higher specific heat by volume and a smaller diameter
11. Thermal conductivity - k , is the intensive property of a material that indicates its ability to conduct heat.
12. Topside – Above water
13. Yield strength - The stress at which a material begins to plastically deform. Prior to the yield point the material will deform elastically and will return to its original shape when the applied stress is removed. Once the yield point is passed some fraction of the deformation will be permanent and non-reversible.

Appendix C: References

- [1] Marrota, Fletcher, Ed, L.S. "Interstitially Insulated Coaxial Pipe." MEEN CHTL-05-509-35663.13 Nov 2005
- [2] Howard, Brett. "Electrical Trace heating adapts to pipe-in-pipe stems." Reduces risk of pipeline blockage, optimizes production May 2006: 112-113.
- [3] Lasance, Clemens J.M.. "The Thermal Conductivity of Moist Air." Electronics Cooling. Nov 2003. The Central Resources for Practioners in the Field of Electronics Thermal Management. 29 Jul 2006 <http://www.electronics-cooling.com/html/2003_november_techdata.html>.
- [4] Technical Bulletin A4., "High Temperature Potting and Casting Materials." Aremco Products, INC Jan 2006
- [5] Cengel, Yunus. Heat Transfer: A Practical Approach. New York: McGraw, 2003.

Appendix D: Material Tables

Table 12. Mechanical and thermal properties of various metals

Metal or Alloy	Hardness (Brinell)	Modulus of Elasticity (GPa)	Poisson's Ratio	Melting Point (C)	Thermal Conductivity (W/m-K)
Titanium	70	116	0.34	1650-1670	17
Yttrium	40	63.5	0.243	1515-1531	14.6
Zirconium	145	94.5	0.34	1852	16.7
Tellurium	25	40	0.33	449.5	3.38
Terbium	38 (Vickers)	55.7	0.26	1356-1364	11.1
Samarium	38 (Vickers)	49.7	0.274	1067-1077	13.3
Scandium	132 or 36 (Vickers)	74.4	0.279	1539	6.3
Plutonium	242	96.5	0.15-0.21	640	8.4
Praseodymium	20 (Vickers)	37.3	0.281	927-935	11.7
Neodymium	18 (Vickers)	41.4	0.281	1010	13
Bismuth	7	31.7	0.33	271.3	10
Erbium	42 (Vickers)	69.9	0.237	1522	9.6
Europium	17 (Vickers)	18.2	0.152	817-827	13.9
Gadolinium	37 (Vickers)	54.8	0.259	1310-1312	8.8
Holmium	46 (Vickers)	64.8	0.231	1470	16.2

Table 13. Stainless steel comparative landmark

Stainless Steel	Density (g/cm ³)	Elastic Modulus (GPa)	Specific Heat (20 °C) (J/(Kg·K))	Hardness	Thermal Conductivity (20 °C) W/(m·K)
18-S	8.03	190	500	145-160 HB	18

Table 14. Mechanical and thermal properties for Inconel and Incoloyl Alloys

Alloy	UNS no.	Density (g/cm ³)	Elastic Modulus (GPa)	Specific Heat (20 C) (J/(Kg*K))	Hardness ⁵	Thermal Conductivity (20C) (W/(m*K)) ⁶
Inconel Alloy 600	N0660	8.47	207	444	36 HRC	14.9
Inconel Alloy 625	N06625	8.44	207	410	190 HB	9.8
Inconel Alloy 718	N07718	8.19	211	450	45 HRC	11.4
Inconel Alloy X-750	N07750	8.25	207	431	330 HB	12
Inconel Alloy MA 754	N07754	8.3	160	440	25 HRC	14.3
Incoloyl Alloy 825	N08825	8.14	206	440	75 HRB	11.1
Incoloyl Alloy 909	N19909	8.3	159	427	38 HRC	14.8

Table 15. Elemental break down of Inconel and Incoloy Alloys

Alloy	UNS no.	Nickel	Copper	Iron	Chromium	Molybdenum	Aluminum	Silicon	Magnesium	Carbon	Cobalt	Niobium	Titanium	Strontium Oxide
Inconel Alloy 601	N06601	73.5	0.5	8	15.5	*	*	0.2	0.5	0.08	*	*	*	*
Inconel Alloy 625	N06625	62	*	25	22	9	0.2	0.2	0.2	0.05	*	3.5	0.2	*
Inconel Alloy 718	N07718	53.5	*	18.5	19	3	0.5	0.2	0.2	0.04	*	5	0.9	*
Inconel Alloy 738	N07738	71	0.5	7	15.5	*	0.7	0.5	1	0.08	*	*	2.5	*
Inconel Alloy 825	N07825	78.5	*	*	20	*	0.3	*	*	0.05	1	*	0.5	0.6
Incoloy Alloy 825	N8025	42	2.2	30	21	3	0.1	0.25	0.5	0.02	*	*	0.9	*
Incoloy Alloy 909	N10909	38	*	42	*	*	*	0.4	*	0.1	13	4.7	1.5	*

Appendix E: Mesh Type and Configuration

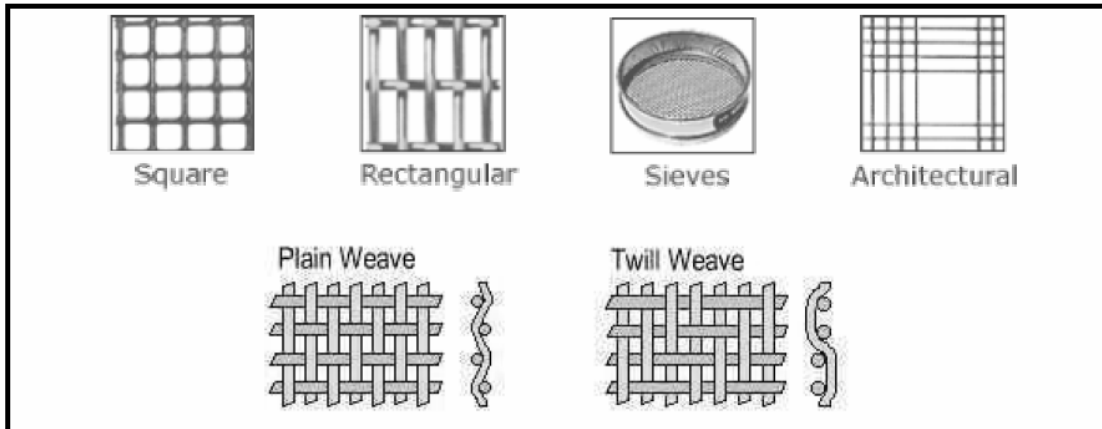


Figure 24. Collection of mesh type and configuration (1)

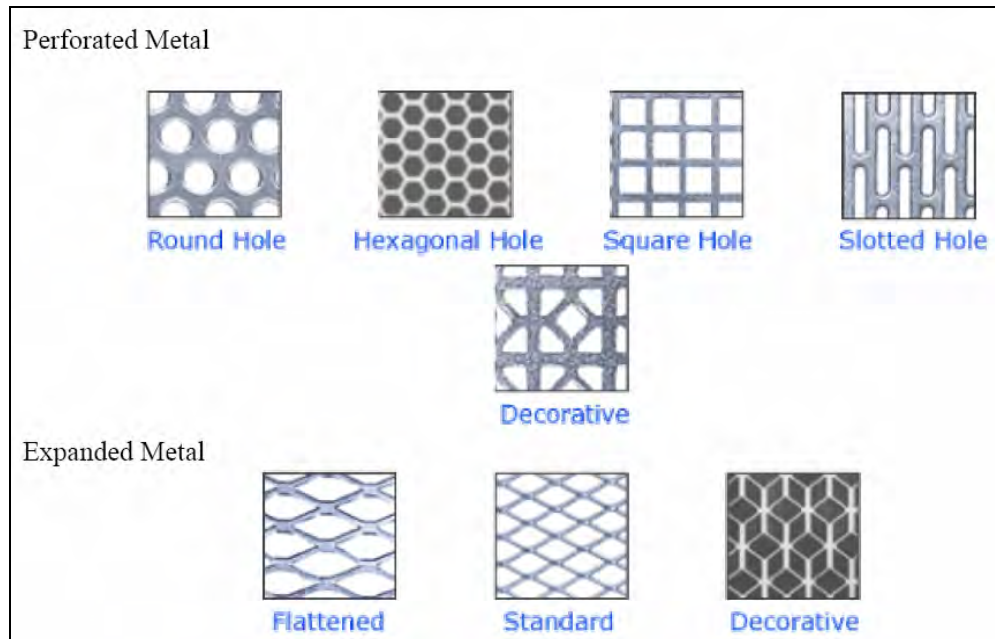


Figure 25. Examples of alternative to the conventional mesh (1)

Appendix F: Detailed Calculations

Large Pipe Calculations:

Rugged Insulation for Flow Assurance Project Analysis Document

Section 1.0 - Collapse Pressure Analysis

Line Pipe Specifications:

Grade 80 (Table 2, ASTM Spec: A 984/A 984M-03)

Yield Strength $\sigma_{y,pipe} := 80\text{ksi}$

Outer Diameter $OD_{pipe} := 16.00\text{in}$

Wall Thickness $t_{pipe} := .875\text{in}$

Collapse Pressure
in Salt Water $P_{col} := 0.5 \frac{\text{psi}}{\text{ft}}$

Max Water Depth $h_{max} := 10000\text{ft}$

External Load on
Pipe $P_{ext} := P_{col} \cdot h_{max}$

$$P_{ext} = 5 \times 10^3 \text{ psi}$$

D/t ratio $k_{pipe} := \frac{OD_{pipe}}{t_{pipe}}$

$$k_{pipe} = 18.286$$

Following Data and Equations from API Bul 5C3, Section 1.1.2 (Plastic Collapse)

Formula Factors $A_{pc} := 3.071$

$$B_{pc} := 0.0667$$

$$C_{pc} := 1955\text{psi}$$

(for D/t range 13.38 to 22.47)

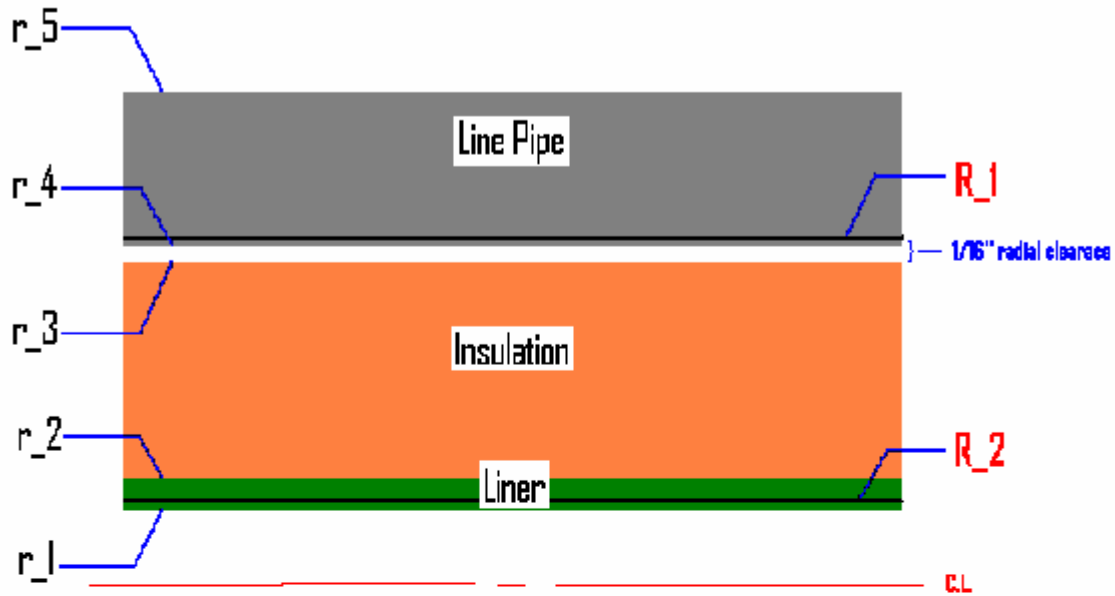
Min Collapse Pressure
for Plastic Range of
Collapse

$$P_p := \sigma_{y,pipe} \cdot \left(\frac{A_{pc}}{k_{pipe}} - B_{pc} \right) - C_{pc}$$

$$P_p = 6.145 \times 10^3 \text{ psi}$$

Section 2.0 - Press Fit Analysis

Cross Section of Components Pre-Die Draw:



Parameters from Figure:

Radii		Component Thicknesses	
$r_1 := \frac{11.75\text{in}}{2}$	$r_1 = 5.875\text{ in}$		$t_{\text{liner}} := 0.25\text{in}$
$r_2 := r_1 + t_{\text{liner}}$	$r_2 = 6.125\text{ in}$		$t_{\text{insulation}} := .9870\text{in}$
$r_3 := r_2 + t_{\text{insulation}}$	$r_3 = 7.112\text{ in}$		$t_{\text{gap}} := \frac{1}{16}\text{in}$
$r_4 := r_3 + t_{\text{gap}}$	$r_4 = 7.174\text{ in}$		$t_{\text{pipe}} = 0.875\text{ in}$
$r_5 := r_4 + t_{\text{pipe}}$	$r_5 = 8.05\text{ in}$		

INPUT

Radial Interference Required (at R1 and R2)

$$\delta_{\text{inter}} := \frac{1}{128}\text{in} \quad \text{Arbitrarily Chosen}$$

Total Radial Expansion Required $\delta_{tot} := \delta_{inter} + t_{gap}$

$$\delta_{tot} = 0.07 \text{ in}$$

Diameter of Die Required

$$D_{die} := 2 \cdot (r_1 + \delta_{tot})$$

$$D_{die} = 11.891 \text{ in}$$

Inner Diameter of Die (assumed)

$$ID_{die} := \frac{D_{die}}{2}$$

Inner Radius of Die

$$r_{i,die} := \frac{ID_{die}}{2}$$

$$r_{i,die} = 2.973 \text{ in}$$

Transition Radius at R1

$$R_1 := r_3 + \delta_{tot}$$

$$R_1 = 7.182 \text{ in}$$

Transition Radius at R2

$$R_2 := r_1 + \delta_{tot}$$

$$R_2 = 5.945 \text{ in}$$

Modulus of Elasticity

$$E_{steel} := 300000000 \text{ psi}$$

CALCULATIONS

Interface Pressure at R1

$$P_{R1} := \frac{E_{steel} \delta_{tot}}{R_1} \cdot \left[\frac{(r_5^2 - R_1^2) \cdot (R_1^2 - r_1^2)}{2 \cdot R_1^2 \cdot (r_5^2 - r_1^2)} \right]$$

$$P_{R1} = 2.12 \times 10^4 \text{ psi}$$

Interface Pressure at R2

$$P_{R2} := \frac{E_{steel} \delta_{tot}}{R_2} \cdot \left[\frac{(r_3^2 - R_2^2) \cdot (R_2^2 - r_{i,die}^2)}{2 \cdot R_2^2 \cdot (r_3^2 - r_{i,die}^2)} \right]$$

$$P_{R2} = 4.855 \times 10^4 \text{ psi}$$

Following calculation from:

- 1) 'High Pressure Monobloc Vessels', Ch. 14 - Lamé's Theory of Stress Analysis for Thick Walled Cylinders
- 2) 'Design of Thick-Walled Pressure Vessels Based Upon Plastic Range - Lamé's

$$\text{Inner Diameter of Liner (pre-drift)} \quad d_i := 2r_1 \quad d_i = 11.75 \text{ in}$$

$$\text{Outer Diameter of Liner (pre-drift)} \quad d_o := 2r_2 \quad d_o = 12.25 \text{ in}$$

$$\text{Transition Diameter} \quad d := 2R_2 \quad d = 11.891 \text{ in}$$

Hoop Stress at Liner-Die Interface (ref. 1)

$$\sigma_{\text{hoop.lame1}} := \frac{P_{R2} \cdot d_i^2}{d_o^2 - d_i^2} + \frac{d_i^2 \cdot d_o^2}{d^2} \left(\frac{P_{R2}}{d_o^2 - d_i^2} \right)$$

$$\sigma_{\text{hoop.lame1}} = 1.152 \times 10^6 \text{ psi}$$

Pressure Based Upon Beginning of Yielding (ref. 2)

$$\text{Yield Strength of Liner} \quad \sigma_{y.\text{liner}} := 39900 \text{ psi}$$

$$\text{Pressure at Yield} \quad P_{\text{lame}} := \sigma_{y.\text{liner}} \frac{\left(\frac{d_o}{d_i} \right)^2 - 1}{\left(\frac{d_o}{d_i} \right)^2 + 1}$$

$$P_{\text{lame}} = 1.662 \times 10^3 \text{ psi}$$

Section 3.0 - Mass Conservation, Initial Volume = Final Volume

$$\text{Length of Liner Before Expansion} \quad L_i := 43 \text{ ft}$$

$$L_i = 516 \text{ in}$$

Pre-Expansion Dimensions of Liner:

Inner Radius $r_{1,i} := r_1$
 $r_{1,i} = 5.875 \text{ in}$

Outer Radius $r_{2,i} := r_2$
 $r_{2,i} = 6.125 \text{ in}$

Post Expansion Dimensions of Liner:

Inner Radius $r_{1,f} := r_{1,i} + \delta_{\text{tot}}$
 $r_{1,f} = 5.945 \text{ in}$

Outer Radius $r_{2,f} := r_{2,i} + \delta_{\text{tot}}$
 $r_{2,f} = 6.195 \text{ in}$

CALCULATION:

Initial Volume $V_i := \pi \cdot (r_{2,i}^2 - r_{1,i}^2) \cdot L_i$
 $V_i = 4.863 \times 10^3 \text{ in}^3$

Liner Length (Post Expansion) $L_{\text{post}} := \frac{V_i}{\pi \cdot (r_{2,f}^2 - r_{1,f}^2)}$
 $L_{\text{post}} = 510.023 \text{ in}$

Percent Shrink $\%_{\text{shrink}} := \left(1 - \frac{L_{\text{post}}}{L_i} \right) \cdot 100\%$

$\%_{\text{shrink}} = 1.158\%$

New Liner Length

$$L_{\text{after}} := L_i - \left(L_i \cdot \frac{\% \text{shrink}}{100\%} \right)$$

$$L_{\text{after}} = 42.502 \text{ ft}$$

Small Pipe Calculations:

Rugged Insulation for Flow Assurance Project Analysis Document

Section 1.0 - Collapse Pressure Analysis

Line Pipe Specifications:

Grade 80 (Table 2, ASTM Spec: A 984/A 984M-03)

Yield Strength $\sigma_{y,\text{pipe}} := 60\text{ksi}$

Outer Diameter $OD_{\text{pipe}} := 7.6\text{-in}$

Wall Thickness $t_{\text{pipe}} := .75\text{in}$

Collapse Pressure
in Salt Water $p_{\text{col}} := 0.5 \frac{\text{psi}}{\text{ft}}$

Max Water Depth $h_{\text{max}} := 10000\text{ft}$

External Load on
Pipe $p_{\text{ext}} := p_{\text{col}} \cdot h_{\text{max}}$

$$p_{\text{ext}} = 5 \times 10^3 \text{ psi}$$

D/t ratio $k_{\text{pipe}} := \frac{OD_{\text{pipe}}}{t_{\text{pipe}}}$

$$k_{\text{pipe}} = 10.133$$

Following Equation from API Bul 5C3, Section 1.1.1 (Yield Strength Collapse)

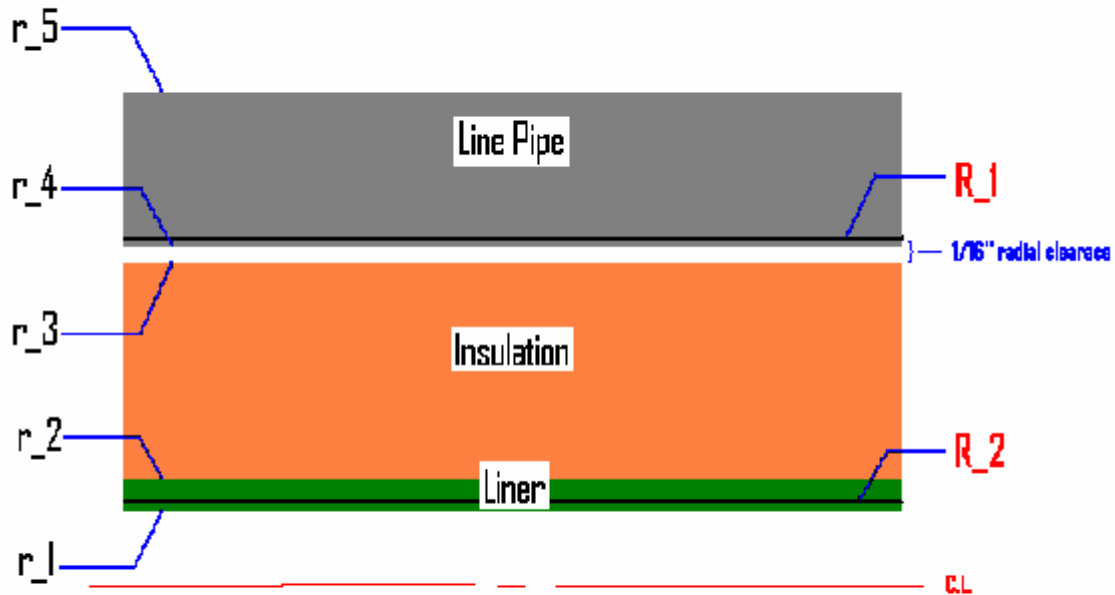
Collapse Pressure $P_p := 2\sigma_{y,\text{pipe}} \cdot \frac{k_{\text{pipe}} - 1}{k_{\text{pipe}}^2}$

$$P_p = 1.067 \times 10^4 \text{ psi}$$

The external pressure that generates
minimum yield stress on the inside wall

Section 2.0 - Press Fit Analysis

Cross Section of Components Pre-Die Draw:



Parameters from Figure:

Radii

$$r_1 = \frac{3.5}{2} \text{ in} \quad r_1 = 1.75 \text{ in}$$

$$r_2 = r_1 + t_{\text{liner}} \quad r_2 = 2 \text{ in}$$

$$r_3 = r_2 + t_{\text{insulation}} \quad r_3 = 2.987 \text{ in}$$

$$r_4 = r_3 + t_{\text{gap}} \quad r_4 = 3.05 \text{ in}$$

$$r_5 = r_4 + t_{\text{pipe}} \quad r_5 = 3.8 \text{ in}$$

Component Thicknesses

$$t_{\text{liner}} = 0.25 \text{ in}$$

$$t_{\text{insulation}} = .9870 \text{ in}$$

$$t_{\text{gap}} = \frac{1}{16} \text{ in}$$

$$t_{\text{pipe}} = 0.75 \text{ in}$$

INPUT

Radial Interference Required (at R1 and R2)

$$\delta_{\text{inter}} = \frac{1}{128} \text{ in} \quad \text{Arbitrarily Chosen}$$

Total Radial Expansion Required $\delta_{\text{tot}} := \delta_{\text{inter}} + t_{\text{gap}}$

$$\delta_{\text{tot}} = 0.07 \text{ in}$$

Diameter of Die Required

$$D_{\text{die}} := 2 \cdot (r_1 + \delta_{\text{tot}})$$

$$D_{\text{die}} = 3.641 \text{ in}$$

Inner Diameter of Die (assumed)

$$ID_{\text{die}} := \frac{D_{\text{die}}}{2}$$

Inner Radius of Die

$$r_{i,\text{die}} := \frac{ID_{\text{die}}}{2}$$

$$r_{i,\text{die}} = 0.91 \text{ in}$$

Transition Radius at R1

$$R_1 := r_3 + \delta_{\text{tot}}$$

$$R_1 = 3.057 \text{ in}$$

Transition Radius at R2

$$R_2 := r_1 + \delta_{\text{tot}}$$

$$R_2 = 1.82 \text{ in}$$

Modulus of Elasticity

$$E_{\text{steel}} := 30000000 \text{ psi}$$

CALCULATIONS

Interface Pressure at R1

$$P_{R1} := \frac{E_{\text{steel}} \delta_{\text{tot}}}{R_1} \left[\frac{(r_5^2 - R_1^2) \cdot (R_1^2 - r_1^2)}{2 \cdot R_1^2 \cdot (r_5^2 - r_1^2)} \right]$$

$$P_{R1} = 1.038 \times 10^5 \text{ psi}$$

Interface Pressure at R2

$$P_{R2} := \frac{E_{\text{steel}} \delta_{\text{tot}}}{R_2} \left[\frac{(r_3^2 - R_2^2) \cdot (R_2^2 - r_{i,\text{die}}^2)}{2 \cdot R_2^2 \cdot (r_3^2 - r_{i,\text{die}}^2)} \right]$$

$$P_{R2} = 3.011 \times 10^5 \text{ psi}$$

Following calculation from:

- 1) 'High Pressure Monobloc Vessels', Ch.14 - Lamé's Theory of Stress Analysis for Thick Walled Cylinders
- 2) 'Design of Thick-Walled Pressure Vessels Based Upon Plastic Range - Lamé's

Inner Diameter of Liner (pre-drift)	$d_i := 2r_1$	$d_i = 3.5 \text{ in}$
Outer Diameter of Liner (pre-drift)	$d_o := 2 \cdot r_2$	$d_o = 4 \text{ in}$
Transition Diameter	$d := 2 \cdot R_2$	$d = 3.641 \text{ in}$

Hoop Stress at Liner-Die Interface (ref. 1)

$$\sigma_{\text{hoop.lame1}} := \frac{P_{R2} \cdot d_i^2}{d_o^2 - d_i^2} + \frac{d_i^2 \cdot d_o^2}{d^2} \cdot \left(\frac{P_{R2}}{d_o^2 - d_i^2} \right)$$

$$\sigma_{\text{hoop.lame1}} = 2.171 \times 10^6 \text{ psi}$$

Pressure Based Upon Beginning of Yielding (ref. 2)

Yield Strength of Liner $\sigma_{y.\text{liner}} := 39900 \text{ psi}$

Pressure at Yield
$$P_{\text{lame}} := \sigma_{y.\text{liner}} \cdot \frac{\left(\frac{d_o}{d_i} \right)^2 - 1}{\left(\frac{d_o}{d_i} \right)^2 + 1}$$

$$P_{\text{lame}} = 5.296 \times 10^3 \text{ psi}$$

Section 3.0 - Mass Conservation, Initial Volume = Final Volume

Length of Liner Before Expansion $L_i := 44 \text{ ft}$

$$L_i = 528 \text{ in}$$

Pre-Expansion Dimensions of Liner:

$$\begin{aligned} \text{Inner Radius} \quad r_{1,i} &:= r_1 \\ r_{1,i} &= 1.75 \text{ in} \end{aligned}$$

$$\begin{aligned} \text{Outer Radius} \quad r_{2,i} &:= r_2 \\ r_{2,i} &= 2 \text{ in} \end{aligned}$$

Post Expansion Dimensions of Liner:

$$\begin{aligned} \text{Inner Radius} \quad r_{1,f} &:= r_{1,i} + \delta_{\text{tot}} \\ r_{1,f} &= 1.82 \text{ in} \end{aligned}$$

$$\begin{aligned} \text{Outer Radius} \quad r_{2,f} &:= r_{2,i} + \delta_{\text{tot}} \\ r_{2,f} &= 2.07 \text{ in} \end{aligned}$$

CALCULATION:

$$\begin{aligned} \text{Initial Volume} \quad V_i &:= \pi \cdot (r_{2,i}^2 - r_{1,i}^2) \cdot L_i \\ V_i &= 1.555 \times 10^3 \text{ in}^3 \end{aligned}$$

$$\begin{aligned} \text{Liner Length (Post Expansion)} \quad L_{\text{post}} &:= \frac{V_i}{\pi \cdot (r_{2,f}^2 - r_{1,f}^2)} \\ L_{\text{post}} &= 508.916 \text{ in} \end{aligned}$$

$$\text{Percent Shrink} \quad \% \text{shrink} := \left(1 - \frac{L_{\text{post}}}{L_i} \right) \cdot 100. \%$$

$$\% \text{shrink} = 3.614 \%$$

Appendix G: Drawings

MEEN685: Directed Studies

Connections for Interstitially Insulated Coaxial Pipes

Michael Tillmann

Supervisor: C.A. "Buddy" Bollfrass, P.E.

May 24th, 2007

Texas A&M University

Abstract

In this project, the connections for the Interstitially Insulated Coaxial Pipe (IICP) were designed to deal with both structural and heat transfer issues. Since no assembled pipe prototype with the desired number of insulation layers was available, a pipe model including plastic deformation needed to be set up as a first step. In the second step, the connection was designed using the systematic approach according to G. Pahl and W. Beitz. The mechanical strength of the final design was verified using FEM.

Table of Contents

Abstract	ii
1. Introduction.....	1
2. Requirements	2
2.1 Requirements List	2
2.2 Thermal Expansion	3
3. Pipe Model.....	4
3.1 Assumptions	4
3.2 Material Model	5
3.3 Pipe Measurements and Materials.....	5
3.4 Plastic Collapse Pressure of the Structural Pipe	7
4. Functions and Working Principles	8
4.1 Pipe Sealing.....	8
4.2 Insulation Face Sealing.....	12
4.3 Thermal Insulation	14
4.4 Screen wire mesh protection from the welding heat	18
4.5 Selected Working Principles	19
5. Preliminary Layout.....	20
5.1 Arrangement of the Seals	20
5.2 Selection of a preliminary layout for definitive design	23
6 Definitive Design.....	24
6.1 Insulation of the Connection.....	24
6.2 Design Iteration with FEM	26
6.3 Final Design	30
7. Discussion	34
8. Future Work.....	35
8.1 Pipe Model	35
8.2 Finite Element Analysis.....	35
8.3 Experiments	35
8.4 Expansion Bellows	36
8.5 Diameter Variation	36
References	37

Appendix A: Preliminary Layouts 1&239
Appendix B: Thermal Conductivity.....43
Appendix C: Final Design44
Appendix D: Preliminary Layout with Expansion Bellows48

1. Introduction

The high demand for oil around the world requires exploration and transportation even in deep seawaters. Paraffin in the oil builds up at the inner diameter of the pipe and reduces the effective cross section if the oil temperature falls below the cloud point. Hence, a proper insulation is required in order to keep the oil temperature above the paraffin formation. Texas A&M researchers have developed a new form of insulation material utilizing stainless steel screen wire mesh and Mylar®. Applying this technology to pipelines, the IICP (Interstitially Insulated Coaxial Pipe) was developed and its effectiveness was proven in experiments.

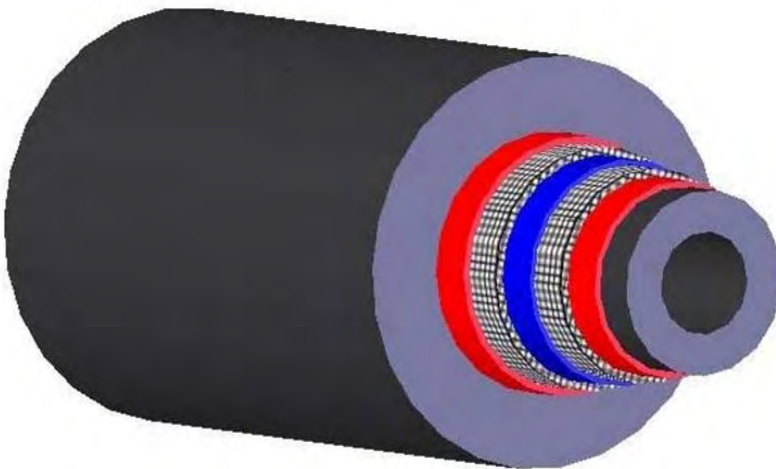


Figure 1.1: IICP in double layer configuration

This project deals with the design of the IICP connections. The options for the design strongly depend on the pipe setup, i.e. the number of layers of screen wire mesh and Mylar® and the measurements and materials of the utilized pipes. Therefore, a typical pipe setup was created using 6 layers of screen wire mesh, 5 intermediate liners and 2 layers of Mylar® (on the outside of the liner and on the inside of the structural pipe). A 6 5/8" OD standard pipe was selected as the structural pipe.

The connections were designed according to the systematic approach by G. Pahl and W. Beitz. This includes listing the requirements, identification of functions, finding working principles, selecting working principles and embodiment design.

2. Requirements

2.1 Requirements List

The following requirements were identified in an iterative process, i.e. some requirements were known from the outset, some were added during the design process.

User: Michael Tillmann		Requirements List for Interstitially Insulated Coaxial Pipe Connections	
Property / Subject	D/W	Requirements (quantitative or qualitative)	
Design / Materials	W	transferability to high pressure - high temperature applications	
Design	W	ease of machining by additional connector parts	
Design / Safety	D	redundant sealing with 2 different working principles	
Assembled Pipe	W	no protruding machined outer surfaces (to avoid damage during transport)	
Assembled Pipe	D	behavior as one structural part	
Assembled Pipe	D	internal pressure rating at 5000 psi with margin 1.25	
Structural Pipe	D	6 5/8" standard size pipe according to API SPEC 5L	
Structural Pipe	D	segments of 42 ft length	
Structural Pipe	D	collapse pressure > 6000 psi (10,000 ft water pressure with margin 1.2)	
Structural Pipe	D	corrosion allowance of 0.063" (= 1,6mm)	
Structural Pipe	D	pipe ends are butt-welded	
Structural Pipe	W	use of a consumable welding insert	
Insulation	D	6 Layers of 5 count stainless steel screen wire mesh	
Insulation	W	minimum necessary Mylar use for easy assembly	
Insulation	D	Intermediate Liners between screen wire mesh layers	
Insulation	D	ends of int. liner and wire mesh layers sealed (to avoid air circulation)	
Ambient Temperature	D	37°F (= 3°C) Gulf of Mexico	
Max Fluid Temperature	D	325°F (= 163°C)	
Min Fluid Temperature	D	140°F (= 60°C) cloud point of paraffin	
Thermal Conductivity	D	≤ 0.08 W/m-K	
Thermal Expansion	D	allowance of 0.55" (=14mm) thermal expansion of the liner (per pipe end)	
Materials	W	standard pipeline steel for liners	
Materials	D	oil resistant materials for polymeric seals	
Materials	D	insulation material must withstand the welding heat	
Production	W	pipe assembly by internal fluid pressure	
Maintenance	D	design must allow pigging	

Table 2.1.1: requirements list

2.2 Thermal Expansion

The need to deal with thermal expansion has not been sufficiently considered in previous studies on the design of the connections. The temperature of the liner varies between 3°C (=37°F) in deep seawater and 25°C (=77°F) during manufacturing. The temperature of the liner is the same during manufacturing, while in utilization, it can be assumed to be the fluid temperature which is up to 162°C (=325°F). These assumptions are made since a poor heat conductor (the screen wire mesh insulation) is placed between the pipes. Relative to the structural pipe, the liner expands in axial direction according to [1]:

$$\Delta L = \alpha * \Delta T * L \quad (2.2.1)$$

Where: $\alpha = 7.22 * 10^{-6} \text{ } ^\circ\text{F}^{-1}$
 $\Delta T = 325^\circ\text{F} - 37^\circ\text{F} = 288^\circ\text{F}$
 $L = 42 \text{ ft}$

$$\Delta L = 1.048 \text{ in}$$

Hence, the connection must accommodate a differential thermal expansion of the liner of 1.048 in for pipe sections of 42 ft.

3. Pipe Model

As mentioned in the introduction, the created pipe model features a fluid liner (1/8" wall-thickness), 6 layers of 5 count stainless steel screen wire mesh with 5 intermediate liners of 1/16" wall-thickness in between and a structural pipe. The structural pipe is a 6 5/8" standard line pipe with a wall-thickness of 1/2". Aluminized Mylar® films are applied on the outside of the fluid liner and on the inside of the structural pipe. There are 2 ways to assemble the pipe; driving a mandrel through the liner's bore or applying a high internal fluid pressure to make the stresses in the liners exceed the yield strength.

3.1 Assumptions

The pipe model was created using the following assumptions:

1. The plastic deformation behavior was represented by a tangential modulus. It was calculated from the yield point and the point characterized by the tensile strength and 0.5 times the minimum elongation value given in [2]. The factor 0.5 was chosen in order to avoid necking since no further information was available for pipeline steel A25. It was assumed that the Poisson's ratio for plastic deformation is the same as for elastic deformation, i.e. $\nu_p = \nu_e$. This is not true since it is approx. 0.3 for elastic and 0.5 for plastic deformation.

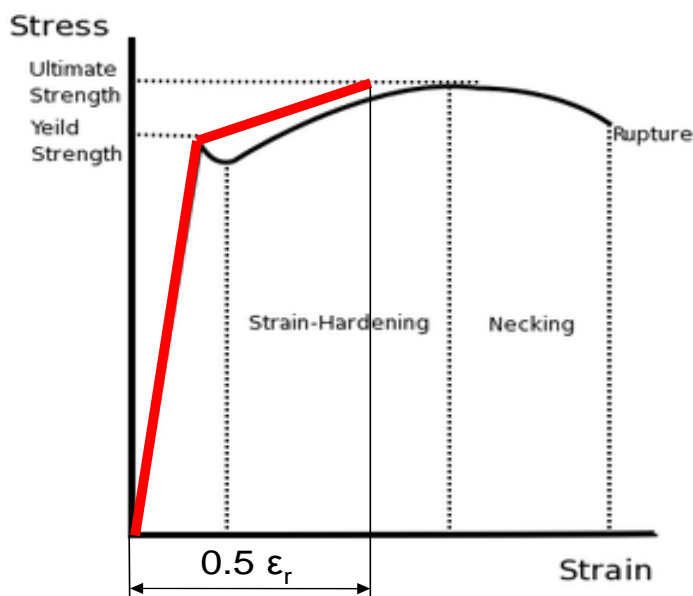


Figure 3.1.1: assumed stress-strain behavior

2. The pipes were assumed to be thin walled cross sections ($D > 10 \cdot s$). This was not true for the structural pipe. For the manufacturing process no values larger than 70% of the yield stress in the structural pipe were obtained from this assumption, i.e. an appropriate safety factor was included.

3. During the manufacturing process the screen wire mesh is exposed to very high surface pressure. It is assumed that it deforms plastically and its thickness is reduced from 2 wire diameters to a single wire diameter.

3.2 Material Model

Calculations were conducted based on the formulas for plane stress [3] neglecting radial stresses from the compression of the fluid liner and the intermediate liners. Attention should be paid to the fact that the liners must be free to reduce their length, i.e. the fluid liner may not be exposed to the axial loads that may come from the fluid pressure that is used to assemble the pipe.

3.3 Pipe Measurements and Materials

Using these pipes for the model before the assembly:

$d_{o, \text{st. pipe}} =$	6.625	in	168.275	mm
$d_{i, \text{st. pipe}} =$	5.625	in	142.875	mm
$s_{\text{st. pipe}} =$	0.5	in	12.7	mm
$d_{o, \text{liner}} =$	4.076	in	103.53	mm
$d_{i, \text{liner}} =$	3.818	in	96.95	mm
$s_{\text{liner, bd}} =$	0.129	in	3.29	mm

Table 3.3.1: pipe measurements before assembly

And insulation material of the following thicknesses:

$S_{\text{int.liner}}$	0.0625	in	1.588	mm
$S_{\text{wire mesh}}$	0.072	in	1.829	mm
S_{mylar}	0.015	in	0.381	mm

Table 3.3.2: insulation material measurements

The following pipe measurements for after the assembly were obtained:

$d_{\text{o,st.pipe}}$	6.625	in	168.275	mm
$d_{\text{i,st.pipe}}$	5.625	in	142.875	mm
$S_{\text{st.pipe}}$	0.5	in	12.7	mm
$d_{\text{o,liner}}$	4.517	in	114.719	mm
$d_{\text{i,liner}}$	4.267	in	108.382	mm
$S_{\text{liner,d}}$	0.125	in	3.175	mm

Table 3.3.3: pipe measurements after assembly

The structural pipe only deforms elastically and its wall thickness is very large compared to the liners'. So it is assumed that it does not change its measurements.

The material chosen for the fluid liner and the intermediate liners was A25 pipeline steel. For the structural pipe, X60 was selected [4].

The obtained fluid pressure for manufacturing was 17,000 psi (=117 MPa). After the assembly process, the screen wire mesh and the liners protruding from the ends of the structural pipe must be cut off. Subsequently the cavities for the connection can be milled into the insulation, and the ends off the fluid liners can be removed by turning or milling.

3.4 Plastic Collapse Pressure of the Structural Pipe

For the collapse pressure analysis the formulas given in [5] were applied. In this case the D/t ratio was $k_{\text{pipe}} = 15.16$ since a corrosion allowance of 0.063" was considered. Thus, the formula factors were applied:

$$\begin{aligned} A &= 3.071 \\ B &= 0.0667 \\ C &= 1955 \text{ psi} \end{aligned}$$

The external load on the pipe is approximately (including safety factor 1.2):

$$P_{\text{ext}} = 1.2 * 10,000 \text{ ft} * 0.5 \frac{\text{psi}}{\text{ft}} = 6000 \text{ psi} \quad (3.4.1)$$

And the yield strength of X60 is:

$$\sigma_{y.X60} = 60,000 \text{ psi}$$

Applying the formula:

$$P_p = \sigma_{y.\text{pipe}} * \left(\frac{A_{pc}}{k_{\text{pipe}}} - B_{pc} \right) - C_{pc} \quad (3.4.2)$$

Returned:

$$P_p = 6197.21 \text{ psi} > P_{\text{ext}}$$

Hence, the pipe can withstand the external pressure.

4. Functions and Working Principles

According to Pahl/Beitz (see [6]), from the requirements and constraints of an engineering task, functions can be formulated and solved separately. After that, the consistency of the solutions must be checked in order to obtain reasonable working structures when combining them.

In the following paragraphs, the determined functions are introduced and possible working principles are discussed.

4.1 Pipe Sealing

Function description:

- radial sealing of a gap between two steel pipes
- allowing relative axial displacement
- redundant seals; the fluid is oil
- internal fluid pressure: 6,250 psi

Solution 1: PTFE O-Ring

PTFE O-Rings cannot not be used because they deform visco-plastically in high pressure applications. Thus, reliable sealing would not be assured (Information provided by [7], [8]).

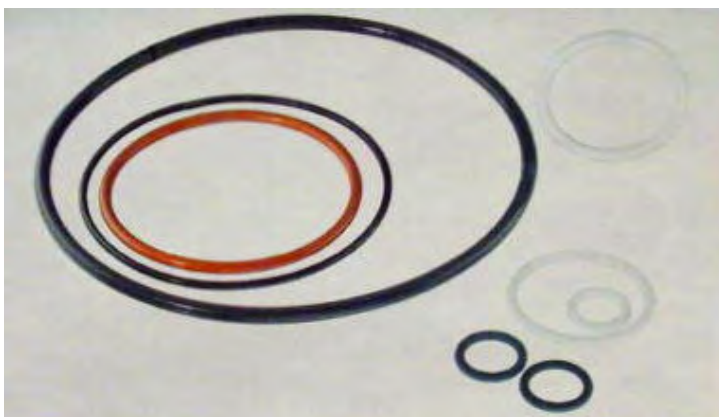


Figure 4.1.1: PTFE o-rings

Solution 2: FEP-Covered Elastomeric O-Ring

Even using back-up rings, the service pressure is limited to 3,500 psi. Hence, this seal does not meet the requirements.

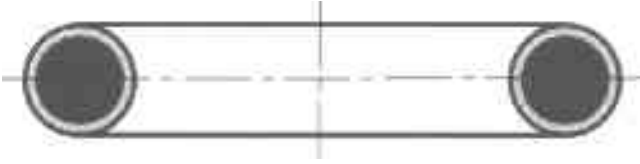


Figure 4.1.2: FEP-covered elastomeric o-ring

Solution 3: PTFE-Covered Metallic C-Ring

Metallic C-Rings are pressure-energized seals available for sealing internal, external and radial pressure. The PTFE-cover limits the allowable surface pressure to 11,000 psi, but it provides a very low coefficient of friction and a lower minimum surface pressure compared to an uncovered seal. C-Rings were developed as static seals [9]. Their utilization in dynamic applications requires further research.



Figure 4.1.3: Metallic c-ring for radial sealing

Solution 4: PTFE Hydraulic Seal

Hydraulic seals are usually made of PTFE, so they are chemically inert in this service. They are considered pressure-energized since they have a slight sealing effect at low pressures, and as pressure increases, the sealing effect goes up as well. An example for such seals is the Turcon[®] Variseal[®] H series available from Busak+Shamban. They can be operated at temperatures from -248°F (= -120°C) up to 500°F (= 260°C) [10]. In static applications the maximum pressure is 11,600 psi (= 80 MPa); for dynamic applications (up to 5 m/s) the pressure is limited to 5,800 psi (= 40 MPa) [10]. These seals are equipped

with a helical metallic spring for improved reliability. The choice of the spring material depends on the type of oil conveyed by the pipe. For crude oil the chemical resistance of Elgiloy® is required. Otherwise the standard spring material, stainless steel 301, is sufficient. [11]. A surface finish of the mating surface with $R_{\max} \leq 4.0 \mu\text{m}$, $R_z \leq 2.5 \mu\text{m}$ and $R_a \leq 0.4 \mu\text{m}$ is necessary. This type of seal also qualifies for high pressure-high temperature applications if reinforced with back-up rings.

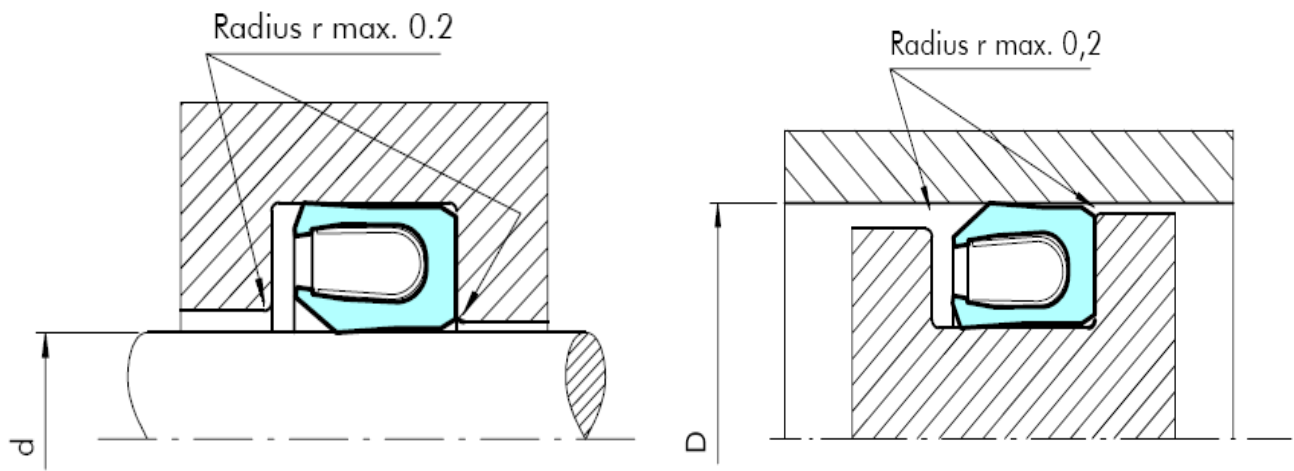


Figure 4.1.4: hydraulic rod-seal (left) and piston-seal (right)

Solution 5: Metal-to-Metal Sliding Seals

“Metal seals meet the long-term sealing challenges presented by high pressures, extreme operation temperatures and corrosive chemicals. They are normally manufactured from high strength, low alloy steel or corrosion-resistant alloy” [12]. For utilization in this project, they should be designed with a low self-energization factor. The shape of the mating surfaces can be varied according to the requirements of the application. Small contact areas (e.g. from curved surfaces) mean a large factor of pressure amplification, i.e. the internal fluid pressure strongly enhances the pressure in the sealing. Metal-to-metal seals qualify for utilization in high pressure-high temperature applications.

The eventual design of the mating surfaces must be iterated using FEM, considering different scenarios of loads from pre-tension and fluid pressure and states of thermal expansion.

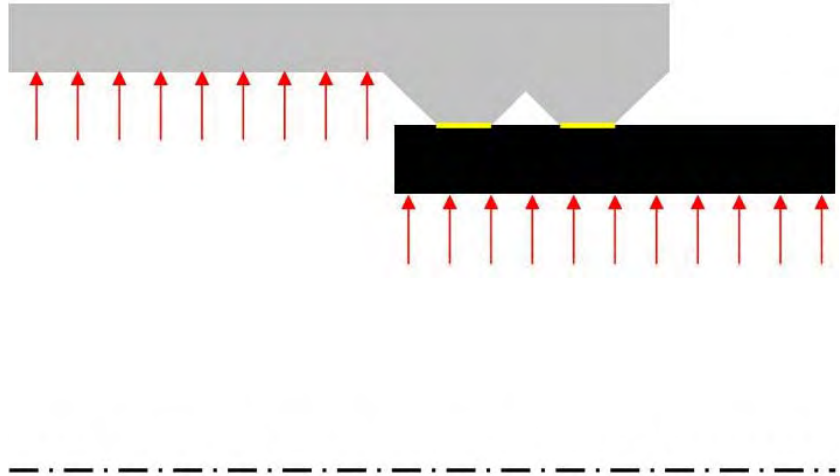


Figure 4.1.5: Metal-to-Metal sliding seal

Solution 6: Expansion Bellow

Due to the high operating pressures of pipelines only metallic multi-layer expansion bellows (see Figure 5.1.6) can be utilized. The advantage of this technology is that no sliding is necessary and so no wear of sealing surfaces can occur. Both of the sub functions, 'allowing expansion' and 'sealing,' are solved by one part; they are hermetic seals. Expansion bellows are available with weld preps, so they can be welded onto the liner ends. In order to avoid damage to the bellow from pigging, thin steel pipes on the bellow's inside are necessary. According to [13] edge-welded metal bellows allow larger strokes than convoluted bellows. In a double-ply configuration, pressures up to 70 MPa (=10,000 psi) can be handled [13].

There is almost no information available concerning the measurements of an expansion joint meeting the requirements of this project. That is why it has not been chosen for the final design.

However, it is highly recommended to consider patent protection of this option.

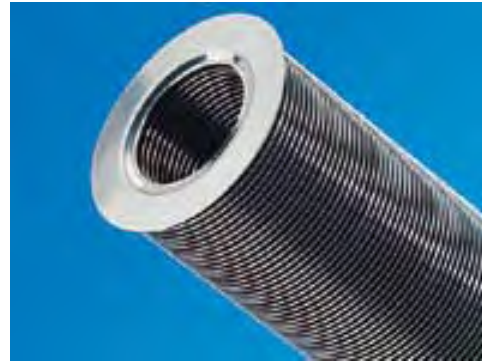
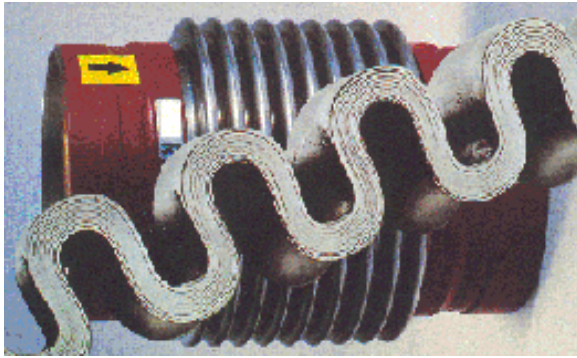


Figure 4.1.6: convoluted expansion bellow (left) and edge-welded expansion bellow (right)

4.2 Insulation Face Sealing

- Function description:
- sealing of the spot faces of the intermediate liner / screen wire mesh insulation in order to avoid air circulation and fluid leakage into the insulation layers
 - no high pressure service.

Solution 1: Seal Welding

The faces of the intermediate liners and screen wire mesh could be seal welded. But this would not allow axial thermal expansion, and a continuous welding seam would mean a highly thermal conductive connection between the liner and the structural pipe. This would lead to thermal leakage.

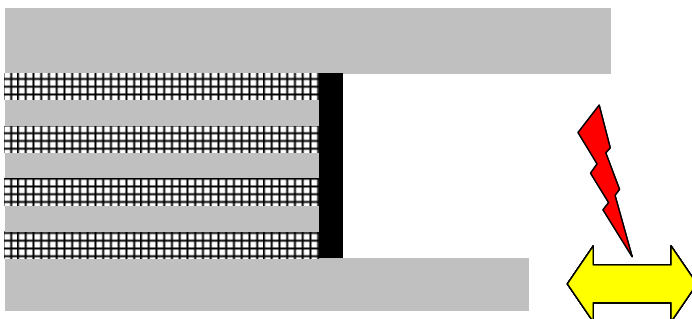


Figure 4.2.1: seal-welded insulation

Solution 2: Inject Silicone Sealant

By injecting a silicone sealant into the gaps in the spot faces these can be made airtight and watertight. Since silicone is very flexible, so it allows deformation of the faces from thermal expansion. Its thermal conductivity is 0.146-0.314 W/m-K, which is larger than the average target value for the pipe [14]. However, since only a thin layer needs to be applied, it will not contribute a critical heat leakage. An available low conductivity sealant is RTVS-61 from ITW Polymer Technologies. It features a thermal conductivity of 0.19 W/m-K and an elongation of 150%. The maximum operation temperature is 399°F (=204°C) [15], which means it does not qualify for high pressure-high temperature service.

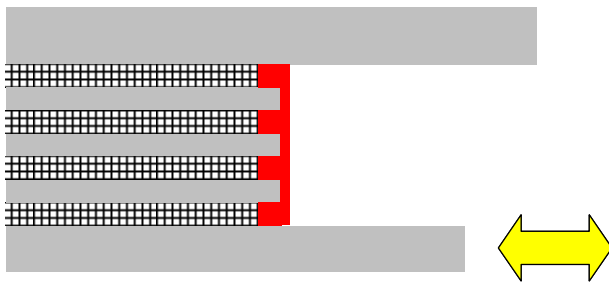


Figure 4.2.2: injected silicone sealant

Solution 3: Polymeric Seal

A polymeric radial sealing ring could be placed between the liner and the structural pipe near the faces of the screen wire mesh insulation. In the case of axial thermal expansion it would move away from the deforming insulation layer face and so it would allow air circulation between different screen wire mesh layers. Fluid leakage into the insulation, however, could be prevented safely.

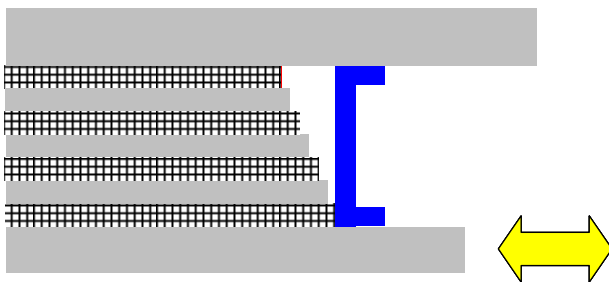


Figure 4.2.3: polymeric seal

4.3 Thermal Insulation

- Function description:
- thermal insulation of a cavity of unstable volume
 - must be able to withstand the high temperature of the structural welding process

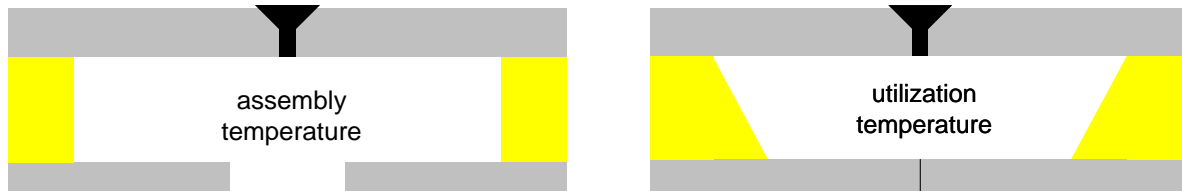


Figure 4.3.1: volume change due to temperature changes; seals are not shown

Solution 1: Ceramic Powder

Depending on the material, ceramic powder can provide good insulation properties. Since the particles are arbitrarily shaped, the areas of contact are small and air is trapped between the particles. However, the density of ceramic powders is high compared to other insulation materials which leads to a higher thermal conductivity. Also, ceramic powder is not compressible, i.e. the cavity could not be filled completely in order to allow axial thermal expansion of the insulation material between the fluid liner and the structural pipe. Small ceramic particles could cause increased wear of the polymeric seal.

Solution 2: Ceramic Fabrics

Ceramic fabrics meet the requirements of this function. Their coefficient of thermal conductivity is temperature-dependent and increases for higher temperatures. Typical values for a fire resistant material are 0.0342 W/m-K (at 68°F=20°C) and 0.06 W/m-K (at 392°F=200°C) [16]. The range of available thicknesses of the FireMaster607™ Blanket offered by Thermal Ceramics is 6mm (~1/2") to 100mm (~4"). It can be ordered with coverings like aluminum foil in order to reduce heat loss from radiation. The fabric has a low bending stiffness, so it can be wrapped around cylindrical objects if necessary. Information concerning the bounce-back behaviour after deformation and the transverse stiffness were not on-hand.

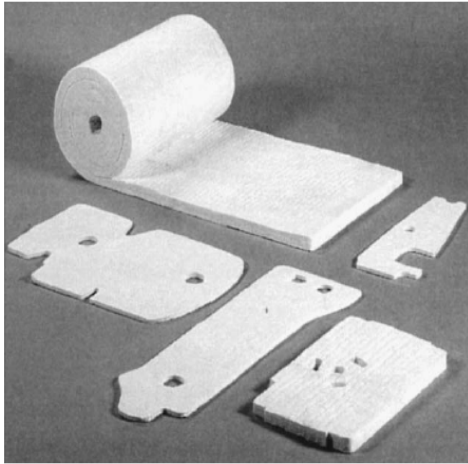


Figure 4.3.2: ceramic fabric

Solution 3: Nanoporous Aerogel

“The nanoporous aerogels available from aspen aerogels consist of lightweight silica solids derived from a gel in which the liquid component has been replaced with gas. The silica solids, which are poor conductors, consist of very small, three-dimensional, intertwined clusters that comprise only 3% of the solids. Volume conduction through the solid is therefore very low. The remaining 97% of the volume is composed of air in extremely small nanopores. The air has little room to move, inhibiting both convection and gas phase conduction. That makes nanoporous aerogels the most effective thermal insulator” (see Figure 4.3.3) [17].

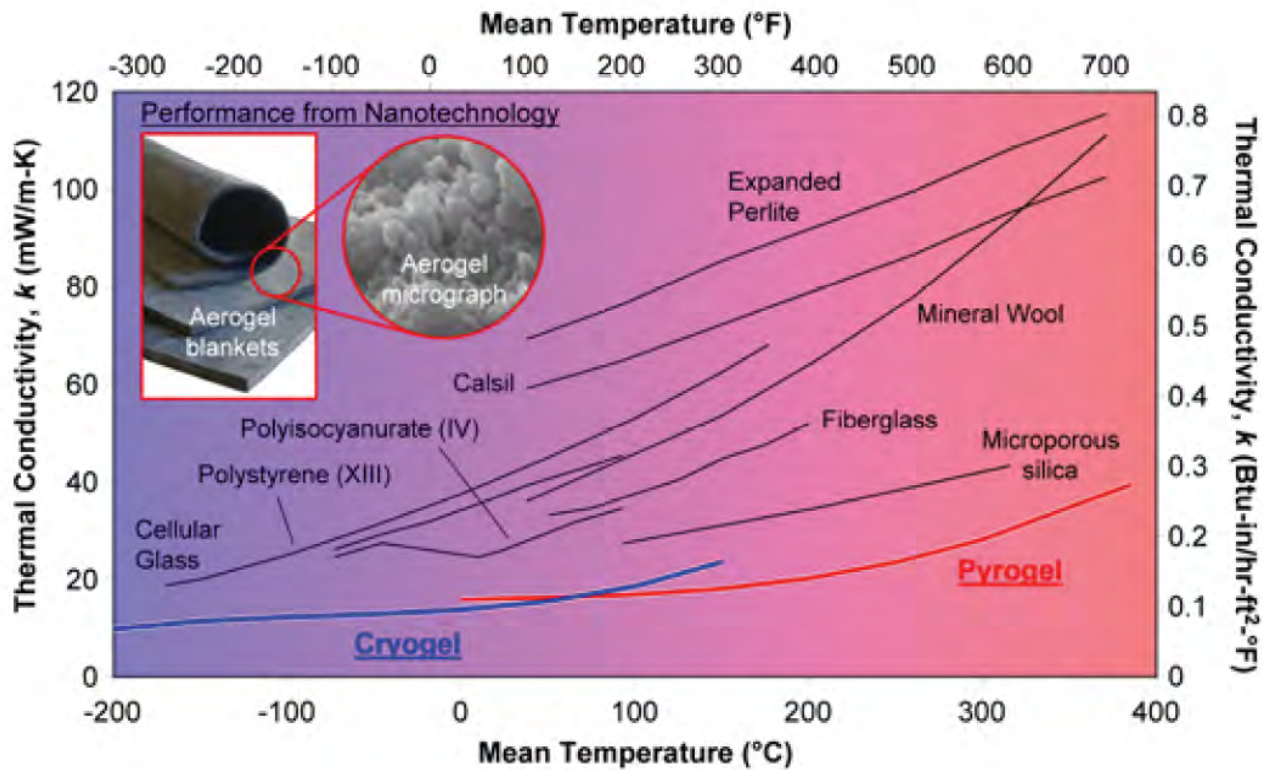
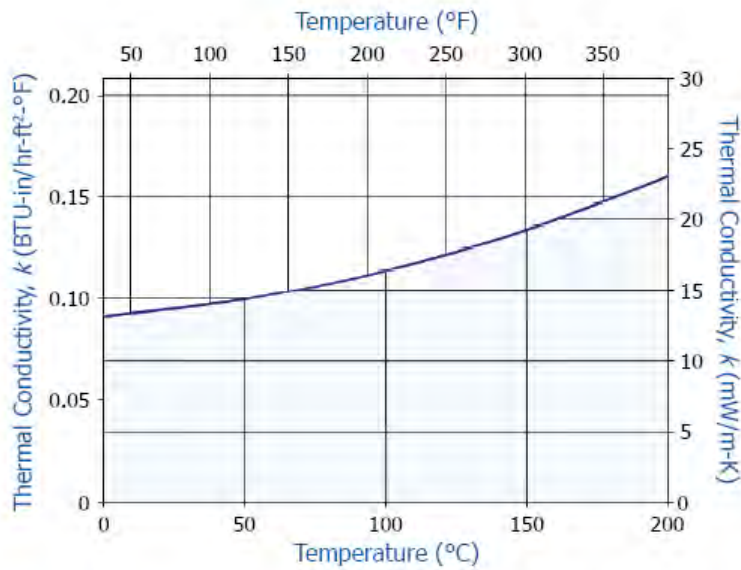


Figure 4.3.3: thermal conductivity of nanoporous aerogels from aspen aerogels

Aspen aerogels is offering 3 different types of insulation materials, each optimized for a certain range of operation temperatures. For application in pipeline insulation, Spaceloft™ has the lowest thermal conductivity (values see Figure 4.3.4). Nanoporous aerogels can protect pipes in hydrocarbon fires [18], so it is assumed that Spaceloft™ can withstand the heat of the welding of the structural pipe, although its long-term service temperatures is limited to maximum 390°F (=200°C) [19]. If it cannot withstand the temperatures of the welding process, a small stripe of ceramic fabric could be applied locally around the welding seam in order to protect the aerogel from the welding heat. Spaceloft™ has an excellent springback so changes of the volume of the insulated cavity will not lead to unfilled spots. However, the impact that compression causes on the thermal conductivity is not known. Spaceloft™ is available in form of blankets with thicknesses of 0.12", 0.24" and 0.36" (= 3mm, 6mm and 9mm).



Mean Temp.	°C	0	25	50	75	100	125	150	175	200
	°F	32	77	122	167	212	257	302	347	392
k	mW/m-K	13.1	13.6	14.3	15.3	16.4	17.7	19.3	21.0	23.0
	BTU-in/hr-ft²-°F	0.091	0.094	0.099	0.106	0.114	0.123	0.134	0.146	0.160



Figure 4.3.4: thermal conductivity of Aspen Spaceloft™ (left) and Aspen Spaceloft™ blanket (right)

For high pressure-high temperature applications the use of Pyrogel® is required because temperatures exceed the maximum utilization temperature of Spaceloft™. Another option would be using multiple layers of different types of aerogels.

Solution 4: Aluminized Mylar®

“Mylar® is a biaxially oriented, thermoplastic film made from ethylene glycol and dimethyl terephthalate (DMT).” It can be metal-coated and has excellent resistance to oil, water, chemicals and temperature [20]. Aluminized Mylar® can be utilized in order to reduce heat loss from radiation.

Utilization of Mylar® in high pressure-high temperature applications must be well considered since the service temperature is limited to 440°F (=227°C) [21].



Figure 4.3.5: metallized Mylar®

4.4 Screen wire mesh protection from the welding heat

Function description: The wall-thickness of the liner ends is too small to withstand the internal fluid pressure. Therefore its ends must be removed by turning or milling so that connection parts with larger wall-thicknesses can be welded onto the fluid liner.

Solution 1: Inject Ceramic Potting Material

In order to protect the screen wire mesh from the welding heat, a ceramic paste like Aremco Ceramacast™ 589 can be injected into the insulation material locally. Its major constituent Silica melts at 3326°F (=1830°C) [22]. However, the maximum utilization temperature given by Aremco is 2400°F (=1316°C). But even if the binder fails due to the high temperatures during the welding, the ceramic paste will prevent melting of the screen wire mesh. Experiments are necessary to figure out whether the heat loss caused by a welded connection to the first layer of the screen wire mesh or by the conduction through the injected ceramic paste is larger. It was assumed that using a ceramic paste would mean a benefit since the thermal conductivity of Silica 1.3 W/m-K [22] compared to 46 W/m-K [23] for steel.

4.5 Selected Working Principles

Weighing the pros and cons of the above mentioned solutions, the following selections were made:

For sealing the fluid liners PTFE hydraulic seals and metal-to-metal sliding seals were chosen. It was decided to seal the spot faces of the screen wire mesh insulation injecting RTVS-61 from ITW Polymer Technologies. For thermal insulation of the connections, Spaceloft™ was chosen. In order to reduce heat loss from radiation, the decision to apply a layer of aluminized Mylar® was made. Aremco Ceramacast™ 589 was selected to protect the screen wire mesh from the heat from welding on the liner connection parts.

The compatibility of the selected working principles was reviewed and no conflicts were found.

5. Preliminary Layout

In preliminary layout the optimal arrangement of the parts was determined.

5.1 Arrangement of the Seals

For the design of the connection, three different load cases had to be considered:

1. pre-tension of the metal-to-metal seal, no fluid pressure
2. pre-tension of the metal-to-metal seals and maximum fluid pressure
3. pre-tension of the metal-to-metal seal, maximum fluid pressure for failure of the metal-to-metal seal

It turned out that for optimal performance the metal-to-metal seal must be the primary seal in order to keep the surface pressure in the seal in the desired range. Hence, two preliminary layouts were created; one utilizing a rod seal and the other a piston seal.

The PTFE hydraulic seals had to be accommodated in a groove that is machined into one of the mating connectors. In general, not all sizes of seals can be placed into a closed groove because large deformation can damage the seal. For rod-seals this is more critical than for piston-seals. The Turcon® Variseal® H RVE3 series minimum diameter for installation in closed grooves was approx. 9" (230mm) [24]; the connection diameter was approx. 4". Therefore the groove had to be split and a threaded seal support was introduced. Welding on the additional part was not an option since the welding heat would have destroyed the polymeric seal. The minimum diameter for the Turcon® Variseal® H PVE3 series was approx. 2 ½" (60mm) [24], so that the seal could be accommodated in a closed groove.

Preliminary Layout:

Combining the results of the previous steps, two preliminary layouts were created. In Figure 6.1.1 the numbers denote the following parts (for larger figures see Appendix A):

- 1- structural pipe
- 2- fluid liner
- 3- Mylar®
- 4- male connection part
- 5- female connection part
- 6- silicone sealant RTVS-61
- 7- threaded seal support
- 8- PTFE hydraulic seal
- 9- metal-to-metal sliding seal
- 10- consumable welding insert
- 11- screen wire mesh insulation
- 12- Spaceloft™ insulation (the lines denote the direction of the material)

The ceramic paste that protects the screen wire mesh during the liner connection part welding is not shown in the layouts.

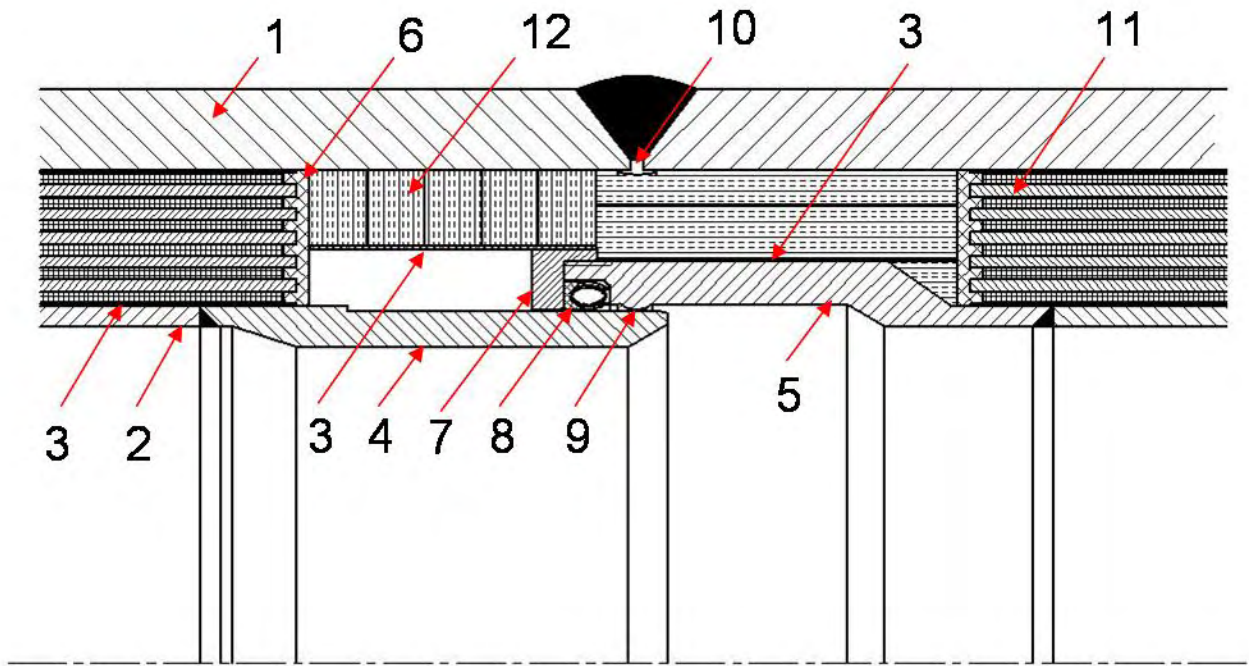


Figure 5.1.1: preliminary layout 1

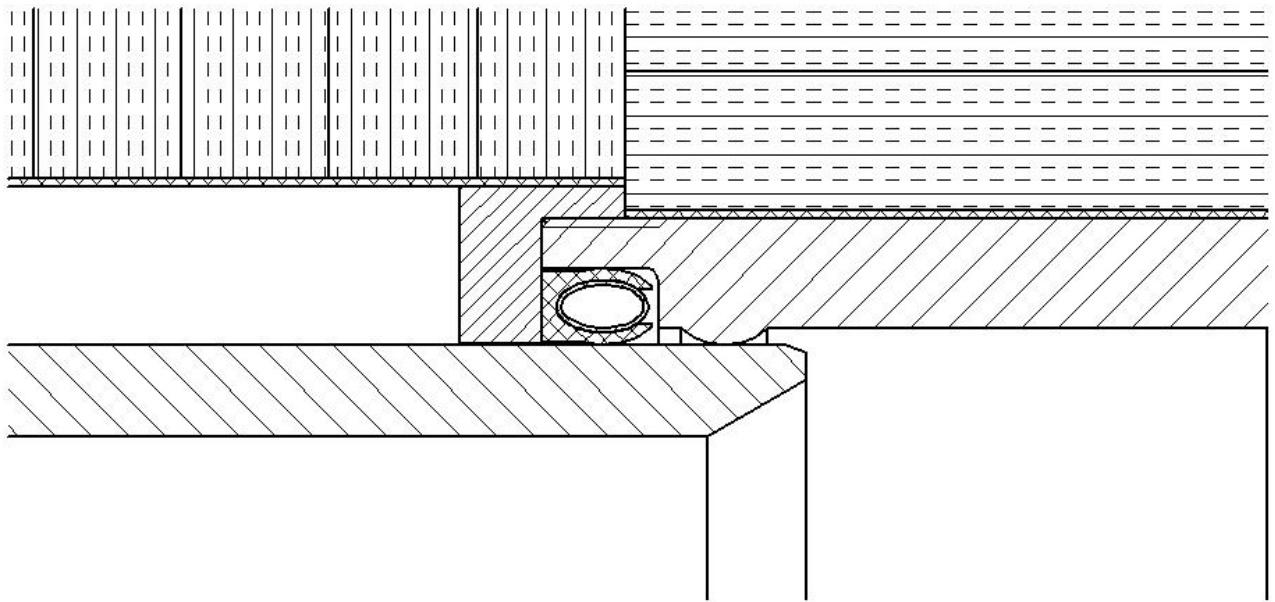


Figure 5.1.2: seals in preliminary layout 1

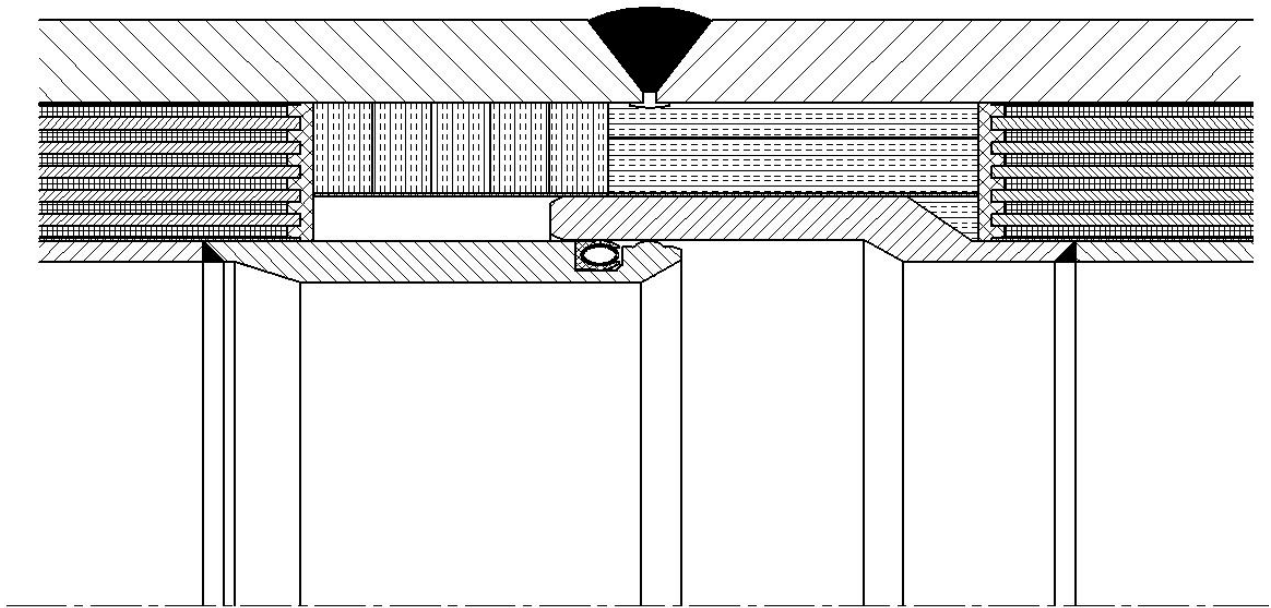


Figure 5.1.3: preliminary layout 2

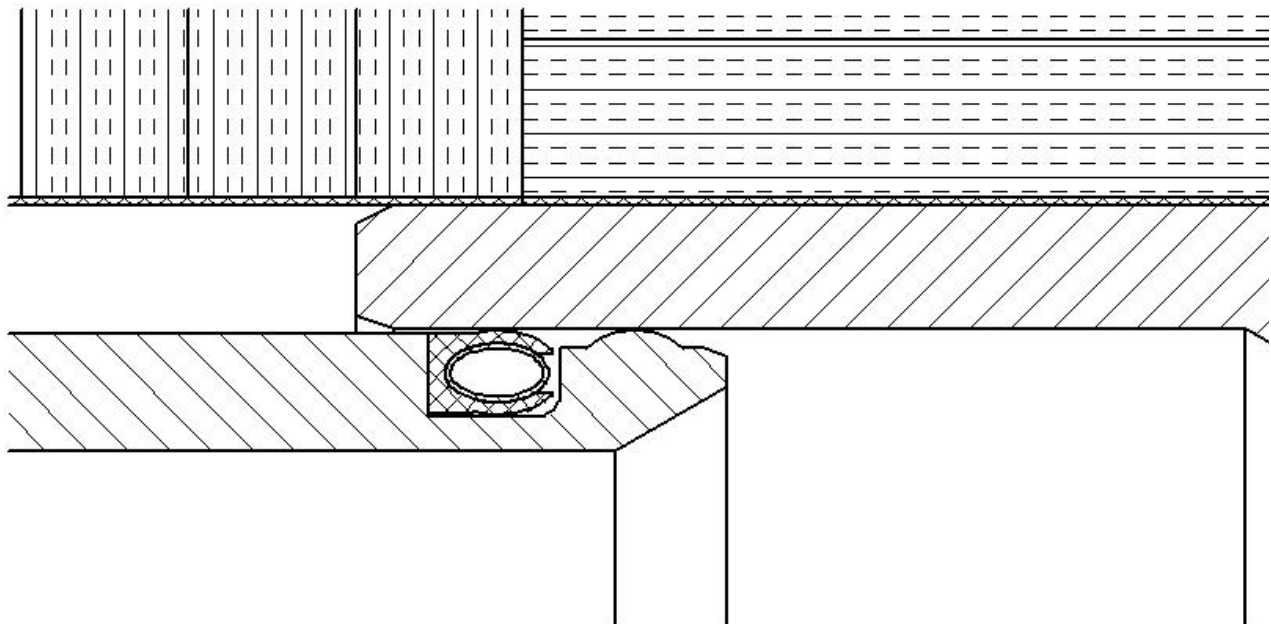


Figure 5.1.4: seals in preliminary layout 2

5.2 Selection of a preliminary layout for definitive design

Layout 2 was selected for the development of the definitive layout, because it allowed easier sliding of the outer connection part in the insulation and no additional part was required.

6 Definitive Design

The definitive layout was created in an iterative process. Changes in design affected thermal as well as structural properties. Therefore, finding a design meeting all requirements took several loops of iteration.

One detail was changed compared to preliminary design. A conical shape was chosen for the spot faces of the screen wire mesh insulation. Hence, the fluid liner was still properly supported by the surrounding insulation in the state of its maximum thermal expansion.

6.1 Insulation of the Connection

The minimum thickness of the Spaceloft™ insulation was calculated based on the requirement of a maximum overall thermal conductivity of 0.08 W/m-K. This value was related to the wall-thickness of the IICP. The only thermal resistances considered in this calculation were those of the silicone sealant and the Spaceloft™ because of $k_{\text{steel}} \gg k_{\text{Spaceloft}}$. The state of maximum thermal expansion of the fluid liners meant the worst case concerning heat loss, because the air-filled expansion gaps were almost filled then. Under these circumstances, the insulation material is compressed the most due to the shrinkage of the connection cavity. That is why a safety factor of 1.2 for the thermal conductivity of the Spaceloft™ insulation was introduced. From Figure 4.3.4 the following values were read for minimum temperature of the structural pipe and the fluid liner's maximum temperature:

$$k(T=3^{\circ}\text{C})=13.2 \text{ mW/m-K}$$

$$k(T=162^{\circ}\text{C})=20.1 \text{ mW/m-K}$$

Assuming that the arithmetic mean of these two values represents the average thermal conductivity and introducing a safety factor of 1.2, the following average conductivity was obtained:

$$k_{\text{Spaceloft}}=0.01998 \text{ W/m-K}$$

For the pipe measurements after assembly:

$$d_{o,liner}=4.517'' (=114.719\text{mm})$$

$$d_{i,liner}=4.267'' (=108.382\text{mm})$$

$$d_{o,st.pipe}=6.625'' (=168.275\text{mm})$$

$$d_{i,st.pipe}=5.625'' (=142.875\text{mm})$$

And the required maximum thermal conductivity 0.08 W/m-K the minimum insulation layer-thickness was determined by iteration. Applying the formulas:

$$R_{th} = \frac{\ln\left(\frac{r_2}{r_1}\right)}{2\pi * k * L} \quad (6.2.1)$$

$$\frac{1}{R_{tot}} = \frac{1}{R_1} + \frac{1}{R_2} \quad (6.2.2)$$

Where: k=thermal conductivity
 r_1 =larger radius
 r_2 =smaller radius
 L=length of the part in axial direction

For the following connection measurements:

$$d_{c,o}=122\text{mm} \quad (\text{outer radius of the female connection part})$$

$$L_{sp}=77.89\text{mm} \quad (\text{minimum axial length of Spaceloft™ applied in the connection})$$

$$L_{si}=6\text{mm} \quad (\text{overall axial length of the applied silicone sealant})$$

The overall thermal conductivity (relative to the IICP wall-thickness) was obtained:

$$k_{tot}= 0.07891\text{W/m-K}$$

For detailed calculations see Appendix B.

6.2 Design Iteration with FEM

The first design was created based on the preliminary layout 2. Using the formula for stress in thin-walled pipes, approximate values for the required wall-thicknesses were determined. A value for the maximum outer diameter of the female connection part was obtained from the conductivity calculations in 7.1. Values for the lengths of the connector parts were obtained from the minimum required axial expansion allowance calculations in 3.2. The utilized hydraulic seal size was not listed in the product data sheet, but it can be supplied by Busak+Shamban [25].

No information was available concerning the minimum required initial surface pressure in metal-to-metal sliding seals. For solid metal gaskets, the range 70-200 MPa was given in [26]. From this range, the value 100 MPa was chosen arbitrarily.

For the Finite Element Analysis, the program CosmosWorks was used. It is embedded in SolidWorks, which was utilized to make the 3D models and the drafts. The analyses were conducted using meshes of 2nd order tetrahedron elements with 10 nodes. The utilized element size was approx. 6mm, which led to approx. 7,000 elements for the male part and 17,000 for the female part. Due to the tight schedule of the project, the analyses did not include contact simulation. Instead the contact was represented by a constant surface pressure of 140 MPa (arbitrarily chosen), that was applied on the area of the metal-to-metal seal. The maximum displacement of the seal, in a direction normal to the axis of symmetry, was read from the displacement plot. This value gave the radial displacement due to a pre-tension of the seal of 140 MPa. The position of the metal-to-metal seal in the female connection part varied depending on the thermal axial expansion of the fluid liners. Therefore 3 positions of the seal in this part were simulated. Considering the 3 load cases described in 6.1, overall 9 simulations made up one iteration loop. The fluid pressure was represented by applying 6,250 psi (=43.5 MPa) to the surfaces that were assumed to be affected. Thus, the required safety factor of 1.25 for 5,000 psi was included. In order to simulate friction of the MTM-Seal, a shear force of 28 MPa (i.e. a friction coefficient of 0.2) was applied on its surface. Concerning the MTM-Seal, two cases were considered: it is faultless and its failure. In the latter case, the groove containing the PTFE hydraulic seal also was pressurized. The obtained radial displacements of the metal-to-metal seal were

read from the displacement plots the same way it was done for the seal pre-tension. The obtained displacements of the male and the female connection part were added up for each position. This value represented the required oversize of the metal-to-metal sliding seal's male part in order to obtain 140 MPa surface pressure in the seal. However, this was an average value over the axial length of the seal. The support of the fluid liner by the screen wire mesh insulation was represented by an increased wall thickness in the FEM model. Examples for stress and y-displacement plots are given in Figures 6.2.1 and 6.2.2.

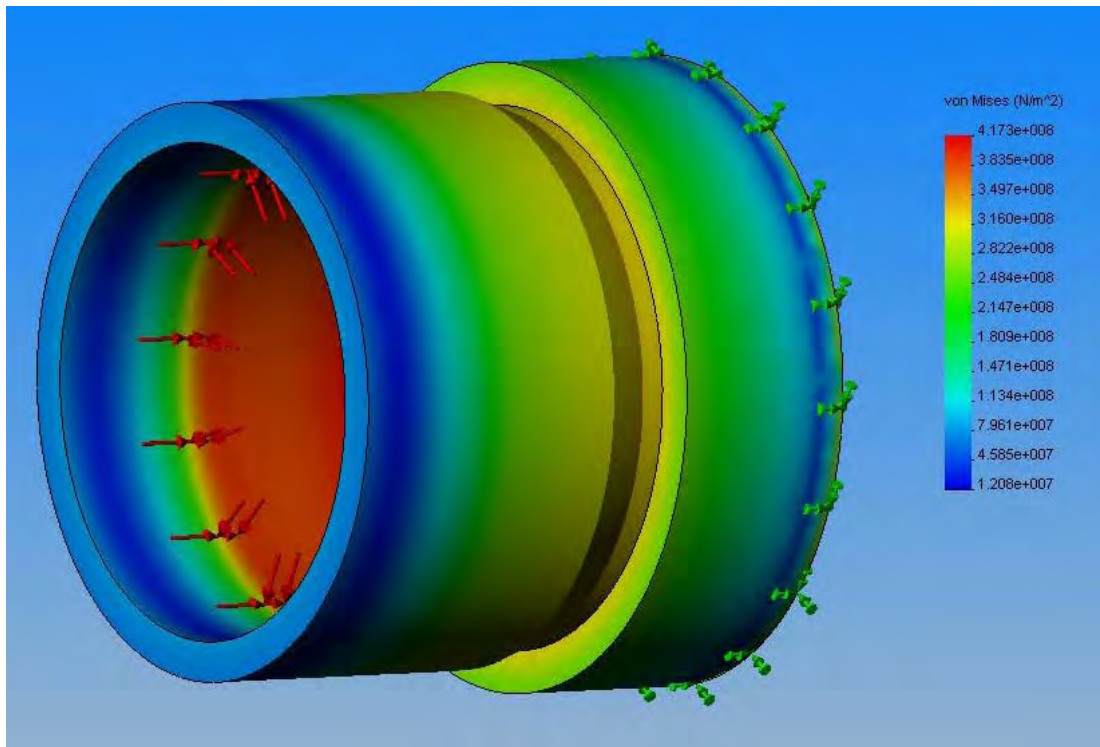


Figure 6.2.1: Von Mises stress plot for the female connection part

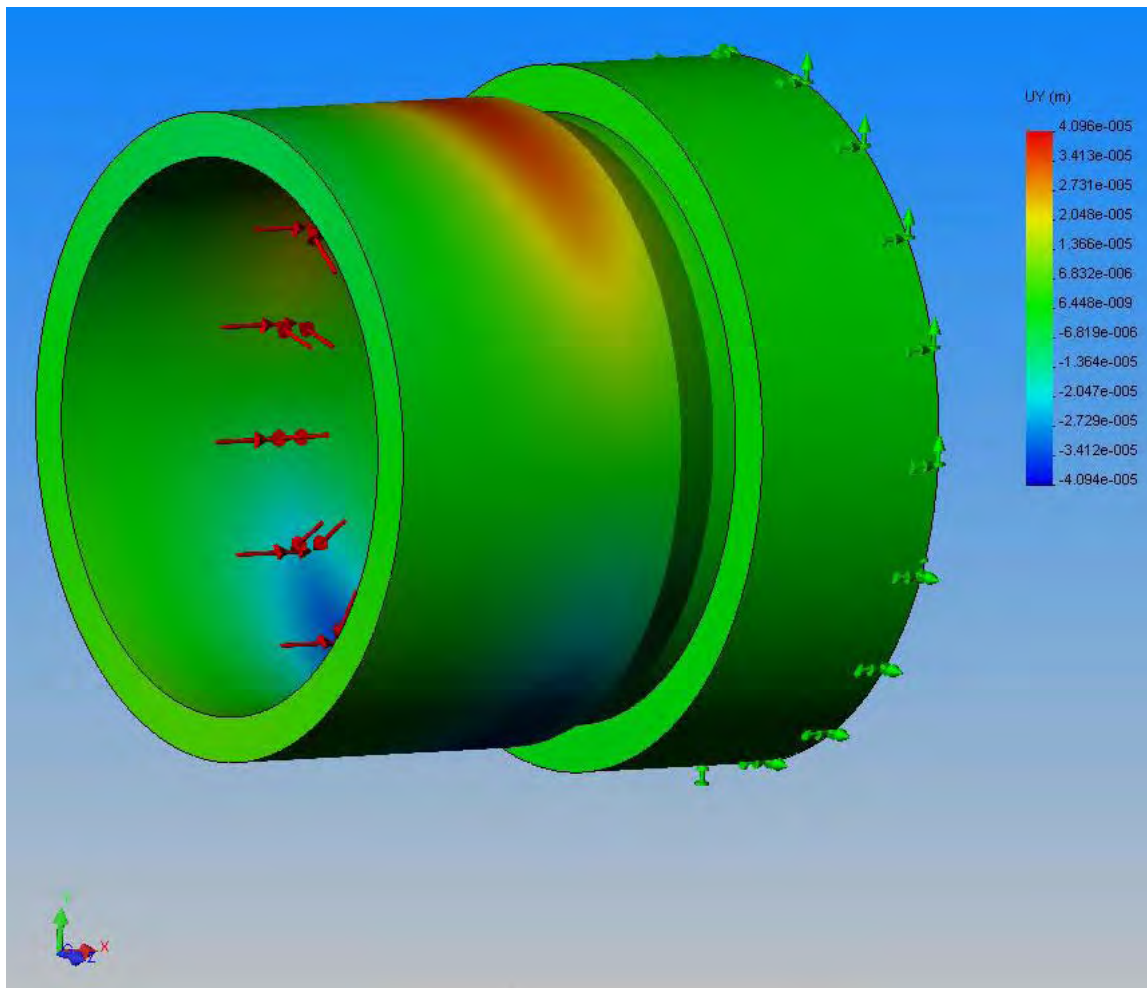


Figure 6.2.2: y-displacement plot for spring constant determination

Since steel is an isotropic material and it deforms according to Hooke's law for stresses below the yield point, a 'spring constant' could be derived. It describes the linear elastic radial displacement due to applied contact pressure in the metal-to-metal seal. The utilized formula was:

$$k_{position} = \frac{surface.pressure_{position}}{\sum radial.displacement_{position}} = \frac{140MPa}{\Delta r_{position}} \quad (6.2.1)$$

With this constant, estimated contact pressures at a given oversize were determined.

$$p = 140\text{MPa} + k_{\text{position}} * (\Delta r_{\text{oversize}} - \Delta r_{\text{position,load.case}}) \quad (6.2.2)$$

Yielded the estimated contact pressure for the considered load case and position of the male connection part in the female one.

The FEA also gave values for the maximum Von Mises stresses in the parts. For constellations with estimated surface pressures < 140 MPa, no additional stress computations were necessary, since their mechanical strength had already been proven for an even higher pressure in the seal. Otherwise another stress analysis was necessary. The yield strength of X80 is 551 MPa. The computed displacements are given in Table 6.2.1. Stresses are given in Table 6.2.2.

Loads	Radial Displacements [μm]			Required Oversize [μm]			
	Axial Expansion [mm]			Liner	Axial Expansion [mm]		
	0	15	30		0	15	30
surface pressure MTM Seal: 140 MPa							
Fluid Pressure: 43.5 MPa							
MTM Seal	41	41	41	-67	108	108	108
MTM Seal and Fluid Pressure	72	71	74	-17	89	88	91
MTM Seal Failure	90	91	99	-40	130	131	139
k_{position} [MPa/ μm]	1,2963	1,2963	1,2963				
oversize[μm] (radius)	110	110	110				
estimated pressure [MPa]	142,59	142,59	142,59				
	167,22	168,52	164,63				
	114,07	112,78	102,41				

Table 6.2.1: radial displacements, spring constants and estimated contact pressures in the mtm-seal

Loads	Von Mises stresses [MPa]				MTM-Seal pressure [MPa]			
	Axial Expansion [mm]			Liner	Axial Expansion [mm]			Liner
	0	15	30		0	15	30	
surface pressure MTM Seal: variable								
Fluid Pressure: 43.5 MPa								
MTM Seal	332	327	358	495	170	170	170	180
MTM Seal and Fluid Pressure	461	452	493	466	170	170	170	180
MTM Seal Failure	484	485	494	361	140	140	140	140

Table 6.2.2: resulting Von Mises stresses from mtm-seal pressure for friction coefficient 0.2

Figure 6.2.3 shows the connection parts developed with FEM. The edges on the inside of the female part come from small variations (0.01mm) of the wall-thickness. These were necessary to separate areas for load application.

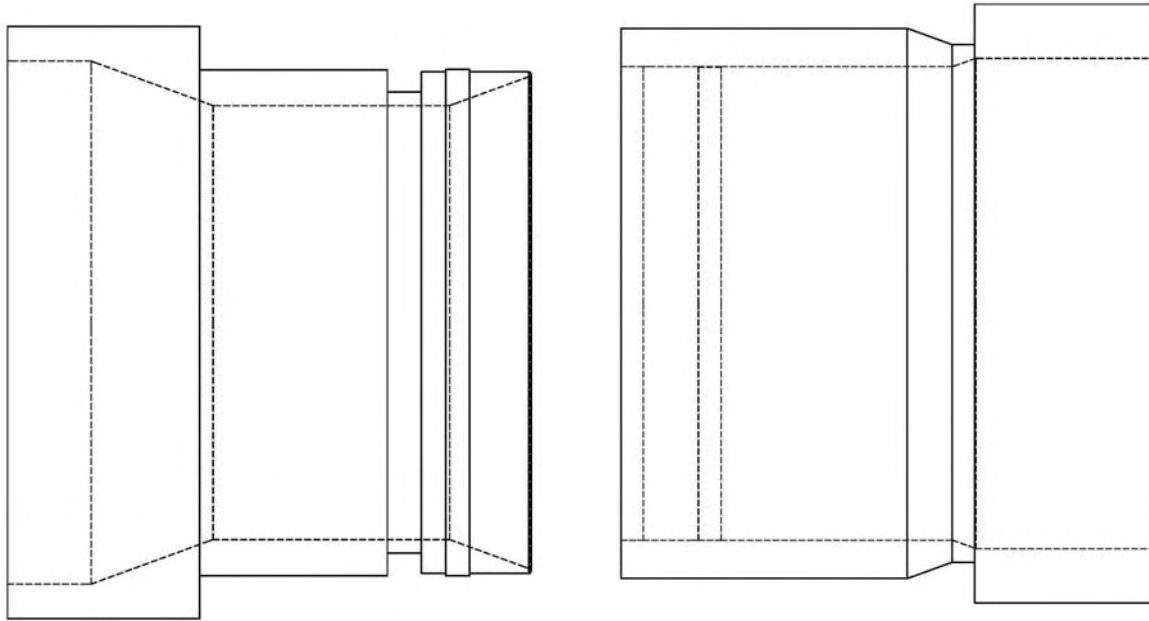


Figure 6.2.3: parts used for the FEM models: male part (left) female part (right)

6.3 Final Design

In final design, based on the connection parts designed using FEM, the rest of the connection was created. Figures 6.3.1 and 6.3.2 show the definitive design (for larger figures see Appendix C).

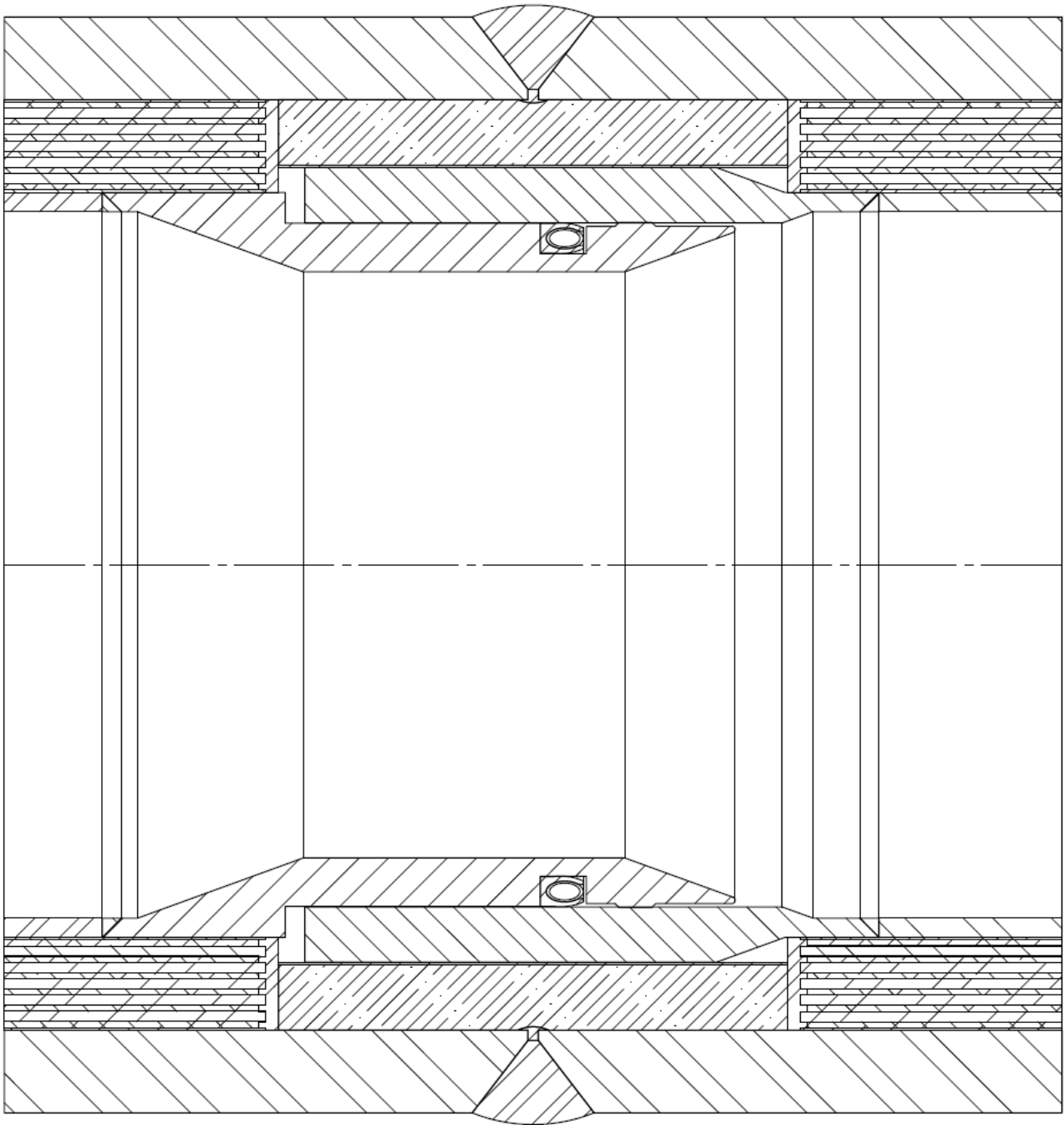


Figure 6.3.1: assembled final design for maximal temperature difference

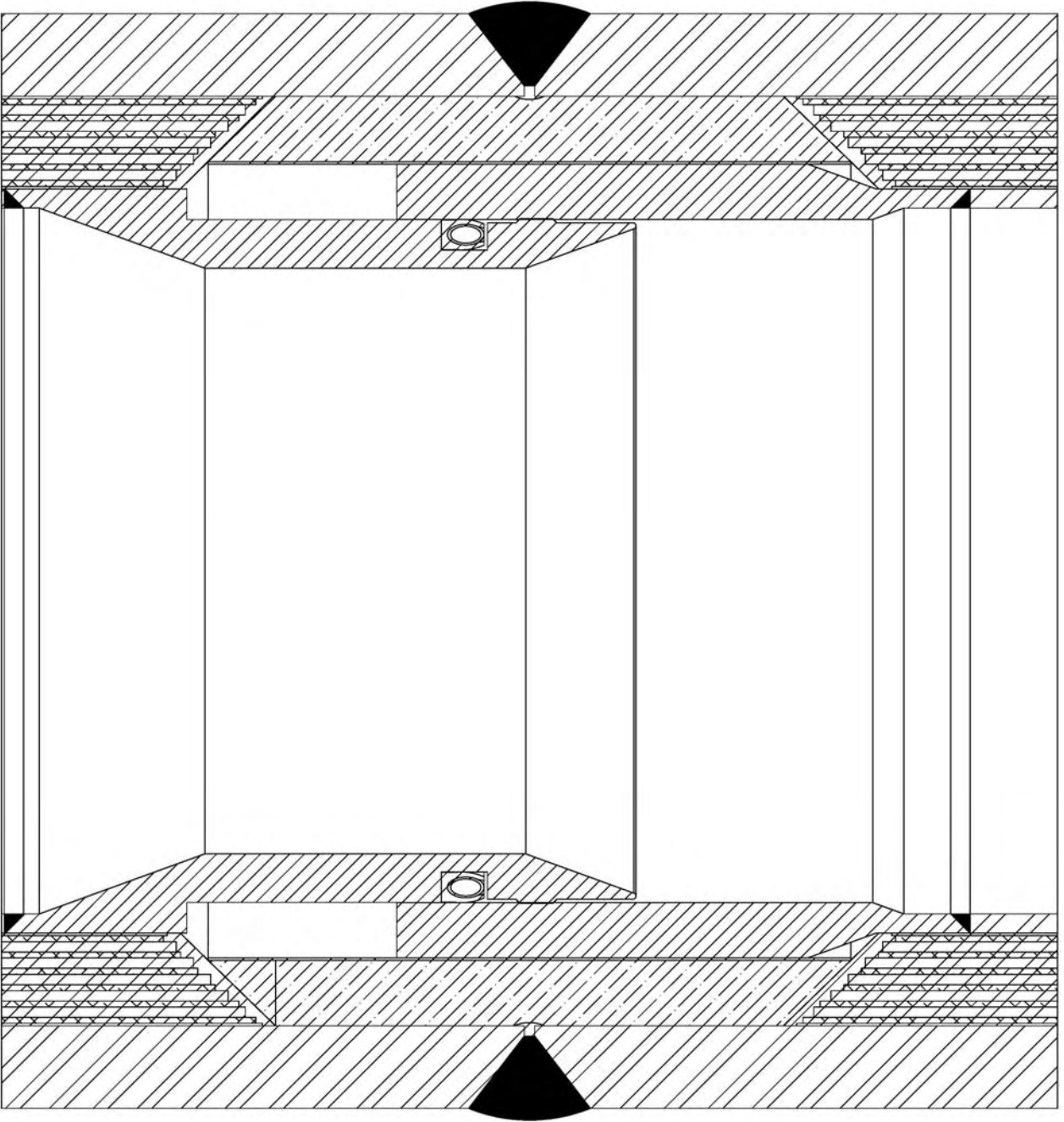


Figure 6.3.2: assembled final design for no temperature difference

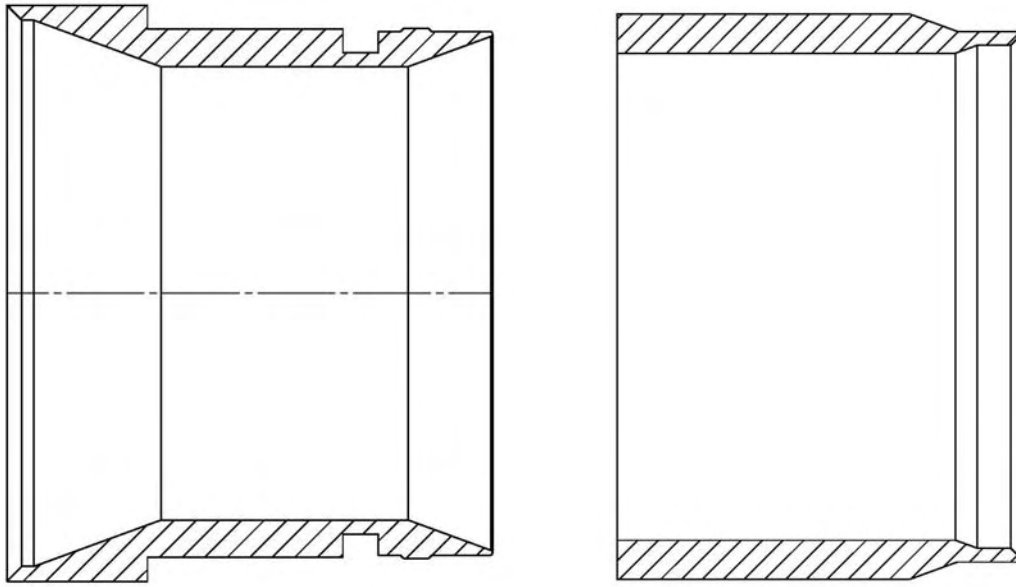


Figure 6.3.3: final designs of the male (left) and the right connection part (right)

For drafts with measurements see Appendix C.

7. Discussion

Although a definitive design of the connection with exact measurements was created, it was based on several assumptions and simplifications. These contribute to the inaccuracy of the calculations. They were necessary since for some topics, an exact mathematical description of the problem would have been too time-consuming. In other cases, no detailed information was available or the topics themselves required further research. However, it was not too early to start this project because finding working principles and concepts did not require absolute accuracy of the calculated measurements. The obtained measurements of the parts give insight to the possibilities and limitations for further layouts. The main sources of inaccuracy are listed in the following paragraphs.

Creating the pipe model, the major problem was the uncertainty about the deformation behavior of the screen wire mesh and its interaction with the intermediate liners under compression. A minor error came from the assumption of a uniform Poisson's ratio for elastic and plastic strain of 0.3.

Finite Element Analyses always introduce an error, since the shape of the part and the material behaviour are approximated, i.e. the obtained solutions are not exact. In this particular analysis, the element size was relatively large compared to the parts' measurements. An additional error came from representing the contact of the mating parts by a constant surface pressure. In reality, the distribution will be non-uniform, depending on the loads and the shape of the parts.

The effect of compression on the thermal conductivity of Spaceloft™ is unknown. For that reason, a safety factor of 1.2 was introduced in the calculations. However, the real material behavior is unknown.

8. Future Work

8.1 Pipe Model

In order to eliminate inaccuracy from assumptions and simplifications in the pipe model, the behavior of the utilized materials and their interaction requires further research. Knowledge about the deformation behavior of screen wire mesh under compression and tension would allow creating a pipe model with FEM.

The impact of high compression loads on the thermal conductivity of the screen wire mesh insulation needs to be studied. Experiments have only been carried out for pressures that are very low, compared to those necessary for plastic deformation of several layers of intermediate liners and mesh.

An existing pipe with multi-layer insulation and known measurements and thermal properties would mean a large reduction of uncertainty concerning the requirements in future connection design projects.

8.2 Finite Element Analysis

Concerning the Finite Element Analysis, the accuracy can be increased by reducing the element size and by including contact simulation. In order to allow a more accurate simulation of the support of the fluid liners by the insulation, either their overall radial stiffness must be measured or a FEM model must be created dealing with several contact simulations.

8.3 Experiments

The influence of compression on the thermal conductivity of Spaceloft™ is not known. Even the manufacturer, Aspen Aerogels, has not finished its research on the properties of their products.

The experiment-design concerning the thermal conductivity of the connection can be derived from the earlier pipe testing in the Texas A&M heat transfer lab.

More experiments see 8.1.

8.4 Expansion Bellows

Utilization of convoluted or edge-welded expansion bellows might be an option for the connection design. They should be considered in further projects. A larger figure is given in Appendix D.

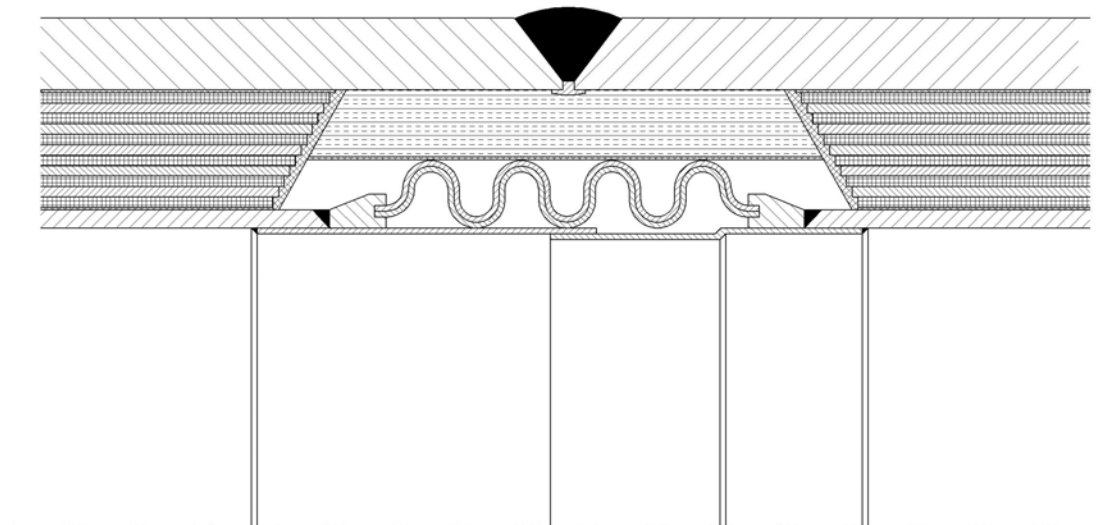


Figure 8.4.1: preliminary layout with convoluted expansion bellows

8.5 Diameter Variation

The connection designed in this project reduces the inner pipe diameter from 108.74mm to 90mm, i.e. the cross-sectional area is reduced by 31.5%. In order to maintain an equal inner diameter in the pipes and the connection, a piece of the structural pipe ends could be replaced by one with a larger diameter. Hence, the additional overall wall-thickness, which is required to accommodate the connection, would increase the outer diameter instead of decreasing the inner diameter.

References

- [1] Deutschman, A. D. *Machine Design*, Macmillan, New York, 1975, p.274.
- [2] American Petroleum Institute *Specification for Line Pipe (5L)*, 39th edition, Washington DC, 1991, p. 62.
- [3] Bruhns, O. *Aufgabensammlung Technische Mechanik 2*, Vieweg & Sohn, Braunschweig/Wiesbaden, 2000, p 13.
- [4] American Petroleum Institute *Specification for Line Pipe (5L)*, 39th edition, Washington DC, 1991, p. 17.
- [5] American Petroleum Institute, *API Bulletin on Formulas and Calculations for Casing, Tubing, Drill Pipe and Line Pipe Properties (5C3)*, Washington DC.
- [6] Pahl, G., Beitz, W. (translated by Wallace, K., Blessing, L., Bauert, F.) *Engineering Design*, Springer, London, 1996, pp. 67-68.
- [7] Ulman Dichtungstechnik GmbH, Sindelfingen-Maichingen, www.ulman.de
- [8] *Design Factors for PTFE Seals*, Machine Design, Vol. 53, No. 21, 1985, p. 215.
- [9] Brown, M. *Seals and Sealing Handbook*, 4th ed., Elsevier Advanced Technology, Oxford, 1995, pp. 223-227.
- [10] *Technical Data Sheet: Turcon® Variseal®*, Busak+Shamban, May 2006, p. 4.
- [11] *Technical Data Sheet: Turcon® Variseal®*, Busak+Shamban, May 2006, p. 9.
- [12] *Metal-To-Metal Seals Serve Critical Applications*, Petroleum Engineer International, Vol. 65, No. 12, 1993, p. 9.
- [13] Müller, H., Nau, B., *Fluid Sealing Technology*, Marcel Dekker, New York, 1998, pp. 398-399.
- [14] http://www.efunda.com/materials/polymers/properties/polymer_datasheet.cfm?MajorID=SI&MinorID=1.
- [15] Product Data Sheet, *Clear Encapsulant -- RTVS-61*, ITW Polymer Technologies.
- [16] Product Information Sheet, *FireMaster607™*, Thermal Ceramics.
- [17] *A New Way To Think About industrial Insulation*, Aspen Aerogels, p. 1.
- [18] *Cryogel™-Pyrogel® Product Brochure*, Aspen Aerogels.
- [19] Product Data Sheet, *Spaceloft™ 3251 6251 9251*, Aspen Aerogels.
- [20] *Introduction to Mylar® Polyester Films*, DuPont Teijin Films.
- [21] http://www.grafixplastics.com/mylar_apps.asp.

[22] http://www.azom.com/details.asp?ArticleID=1114#_Key_Properties.

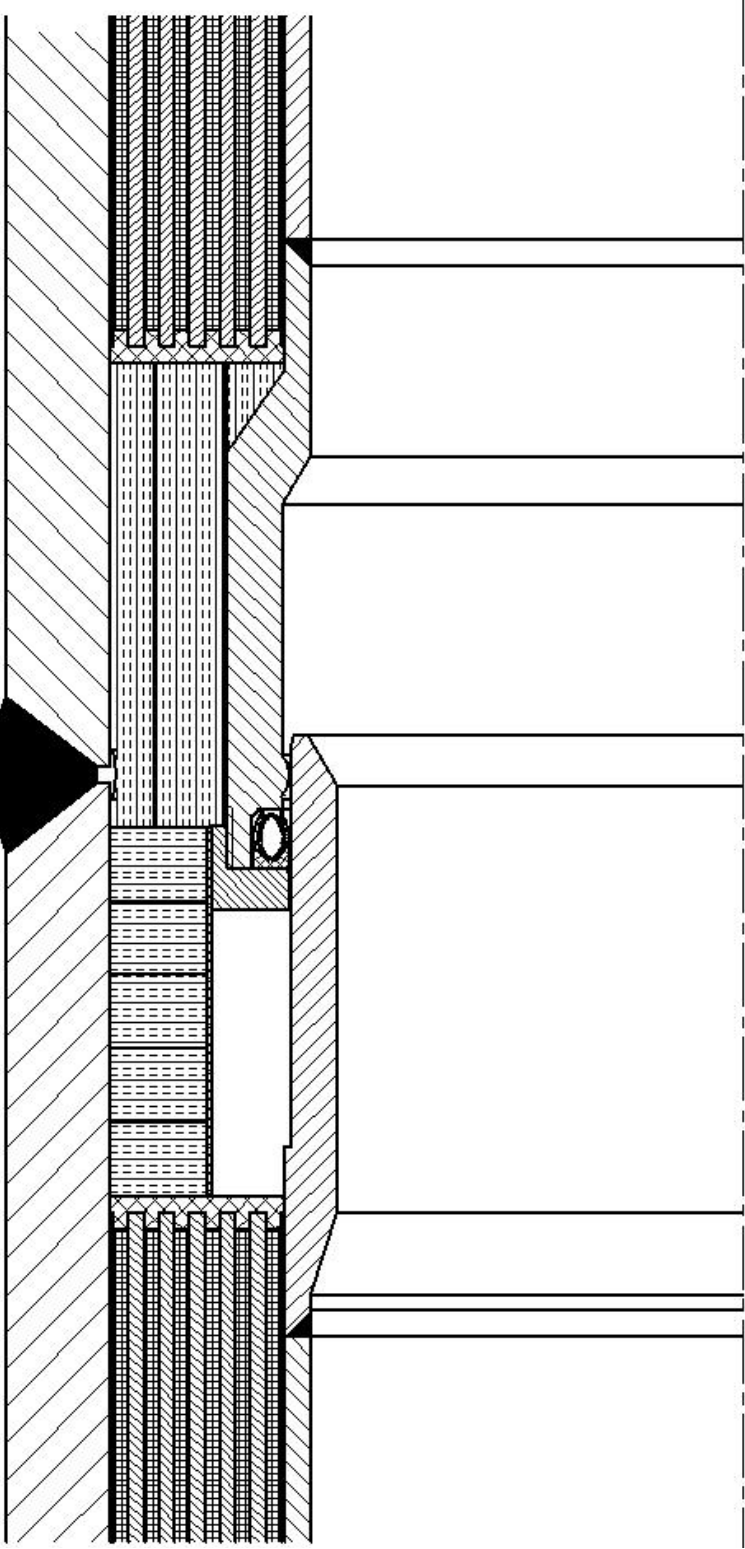
[23] http://www.engineeringtoolbox.com/thermal-conductivity-d_429.html.

[24] *Technical Data Sheet: Turcon© Variseal©*, Busak+Shamban, May 2006, p. 11.

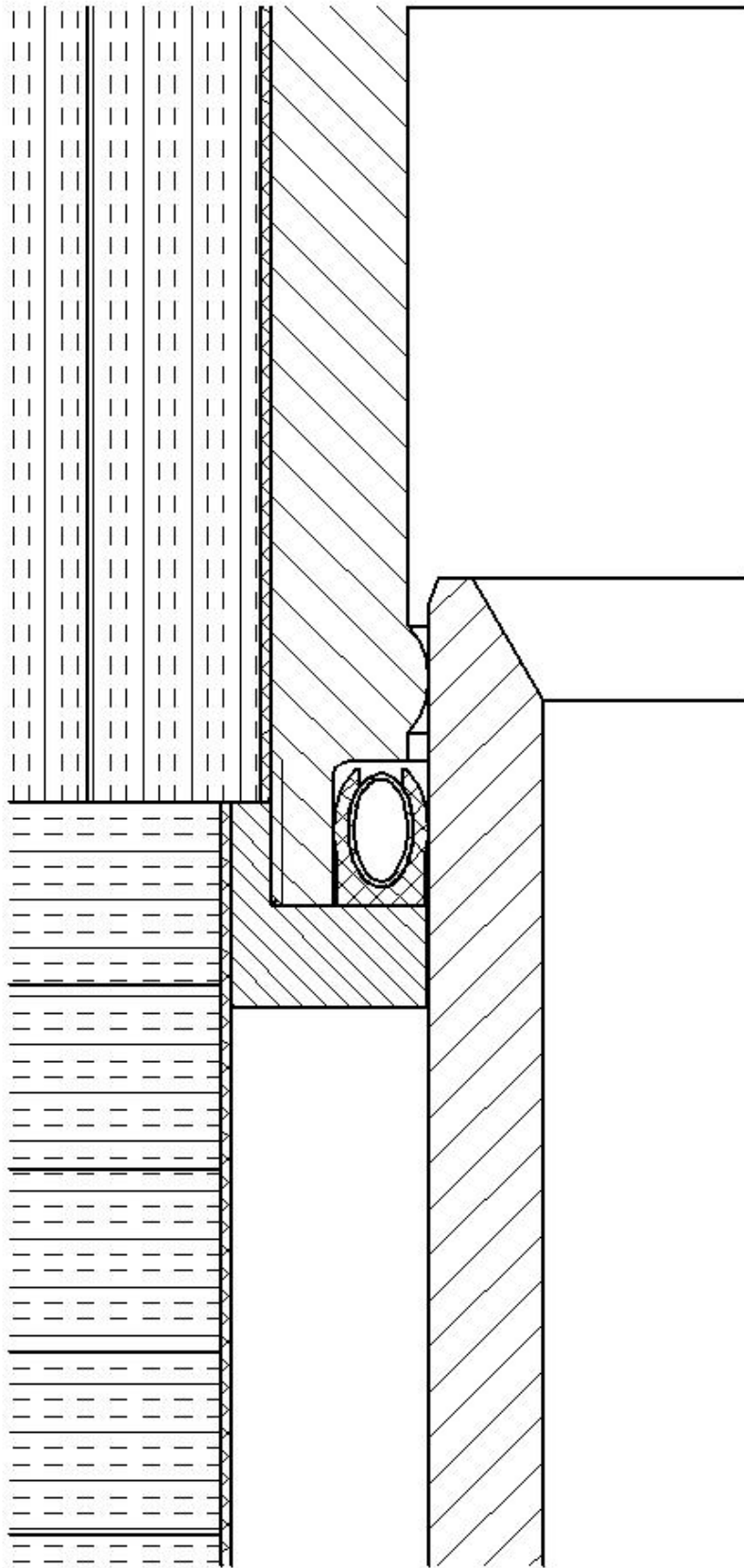
[25] *Technical Data Sheet: Turcon© Variseal©*, Busak+Shamban, May 2006, p. 22.

[26] Müller, H., Nau, B., *Fluid Sealing Technology*, Marcel Dekker, New York, 1998, p. 431.

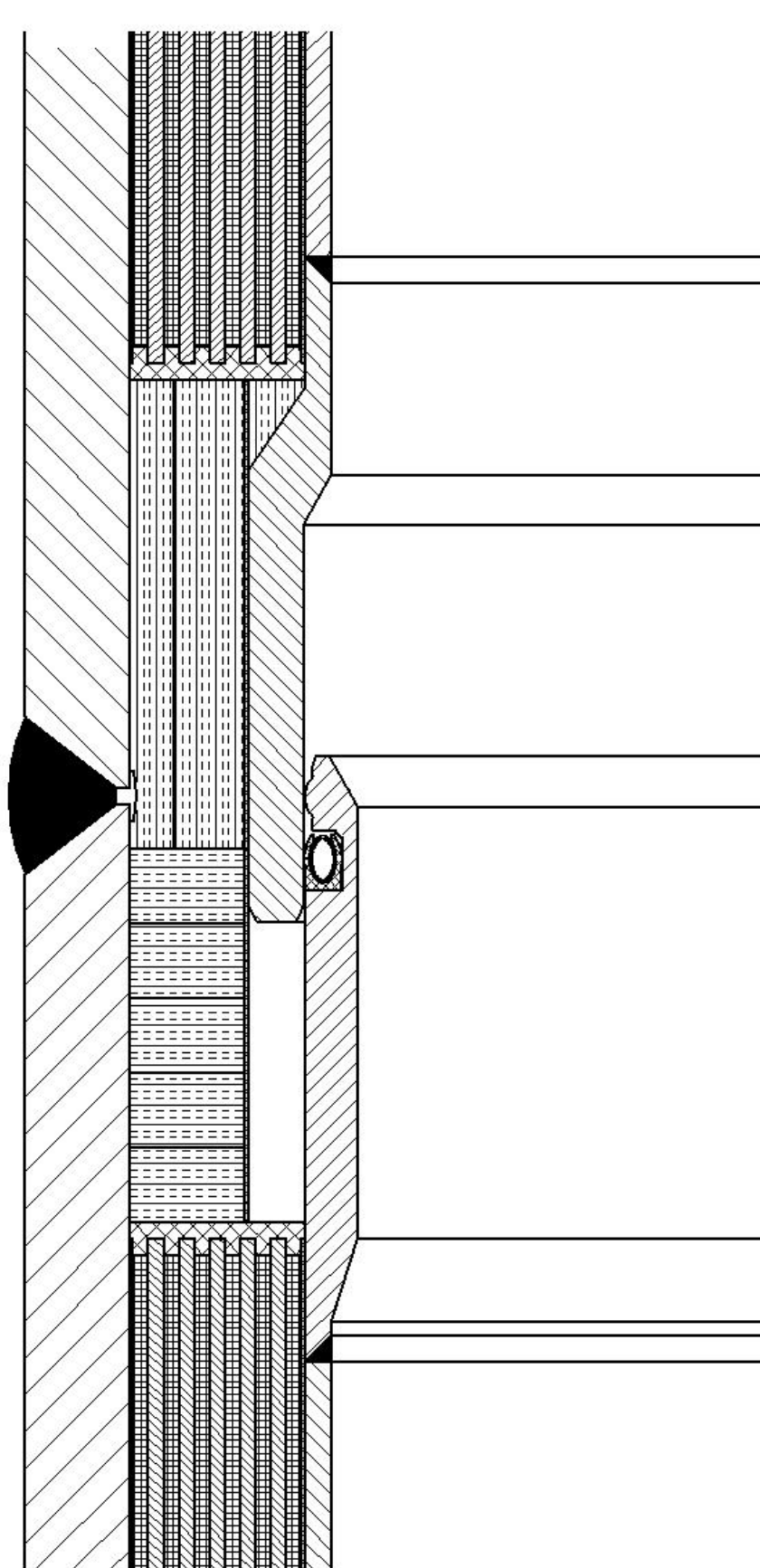
Appendix A: Preliminary Layouts 1&2



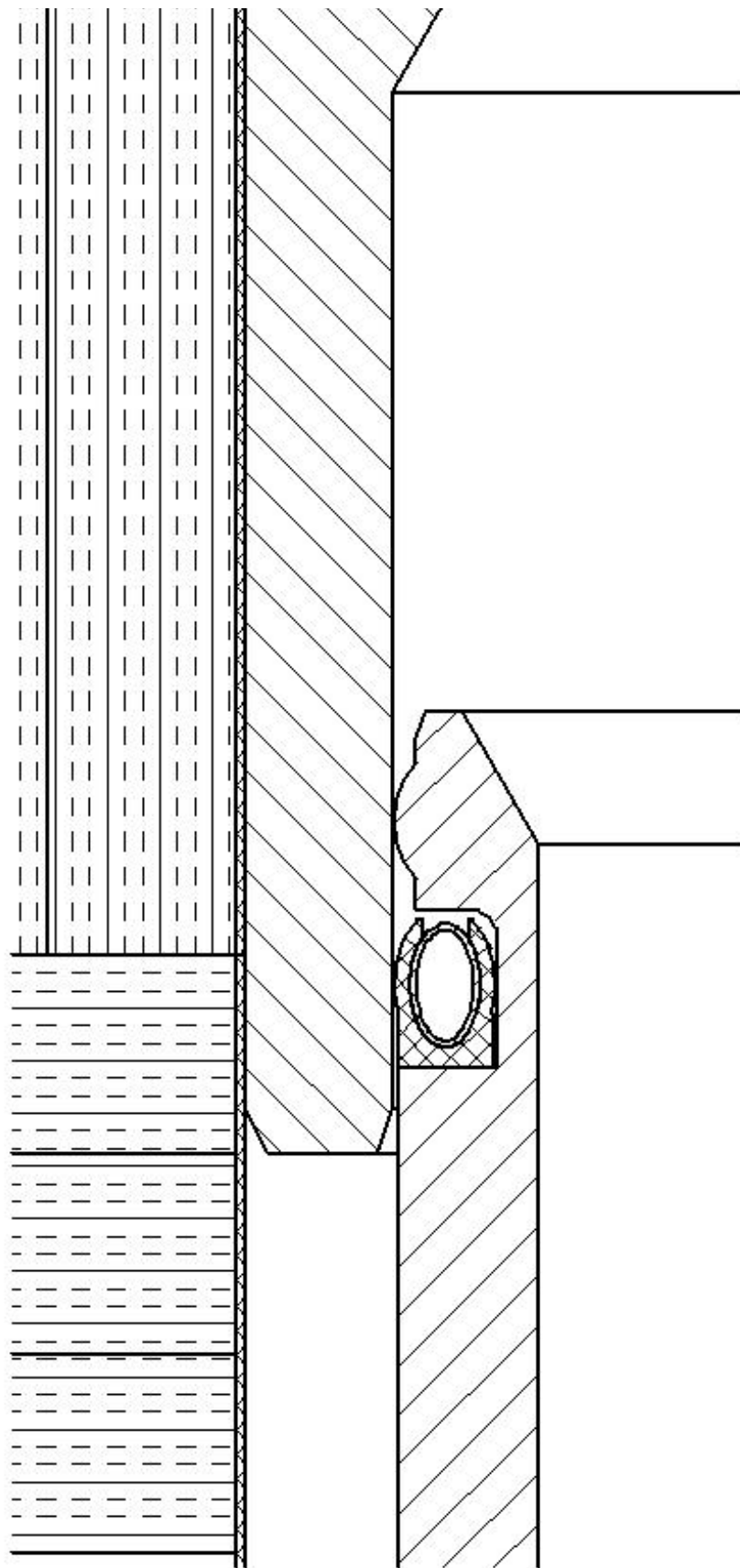
preliminary layout 1



seals in preliminary layout 1



preliminary layout 2

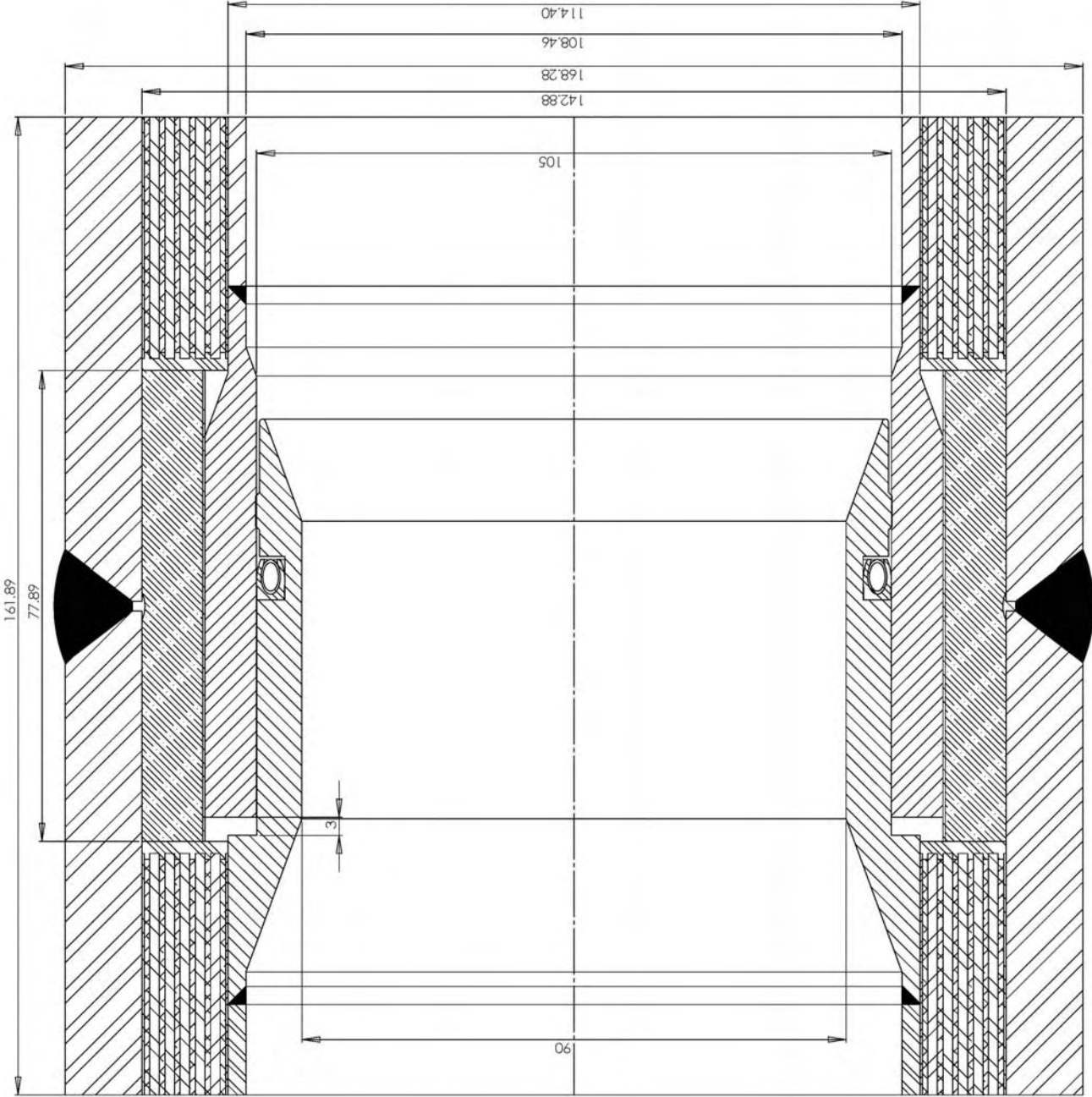


seals in preliminary design 2

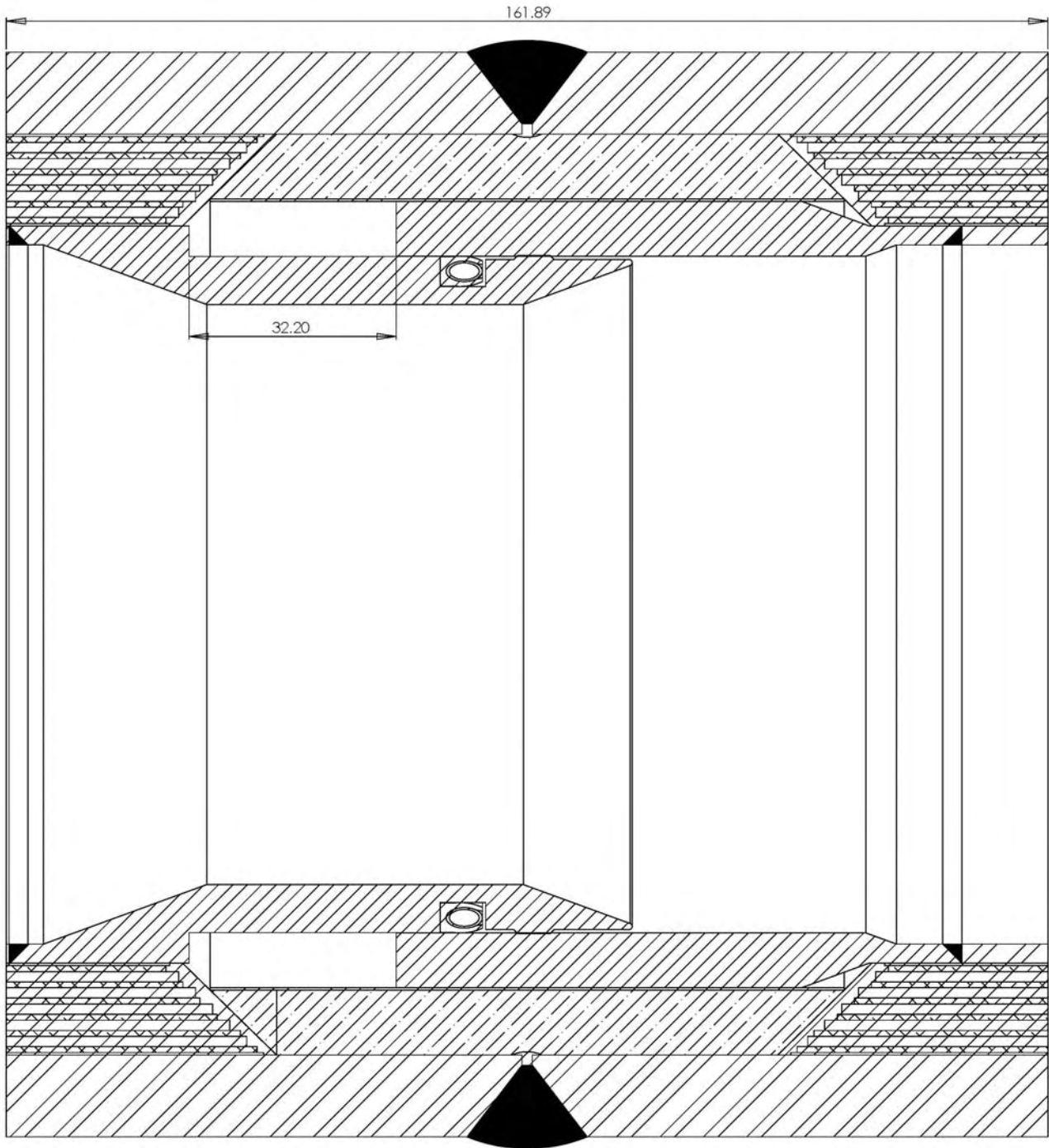
Appendix B: Thermal Conductivity

$L_{sp} =$	77,89	mm	for the state of maximum thermal expansion of the liners
$L_{si} =$	6	mm	two spot faces, 3mm applied on each
$L_{tot} =$	83,89	mm	total length of the connection
$k_{sp,3^{\circ}C} =$	0,0132	W/m-K	conductivity at 3°C
$k_{sp,162^{\circ}C} =$	0,0201	W/m-K	conductivity at 162°C
$f =$	1,2		safety factor
$k_{sp} =$	0,01998	W/m-K	obtained conductivity for Spaceloft
$k_{si} =$	0,19	W/m-K	
$d_{o,st.pipe} =$	168,275	mm	
$d_{i,st.pipe} =$	142,875	mm	
$d_{o,liner} =$	114,719	mm	
$d_{i,liner} =$	108,382	mm	
$d_{c,o} =$	122	mm	outer diameter of the female connection part
$R_{sp} =$	16,1533	K/W	thermal resistance of the Spaceloft layer
$R_{si} =$	30,6421	K/W	thermal resistance of the silicone sealant
$R_{tot} =$	10,5773	K/W	
$k_{tot} =$	0,07891	W/m-K	total thermal conductivity relative to the pipe measurements

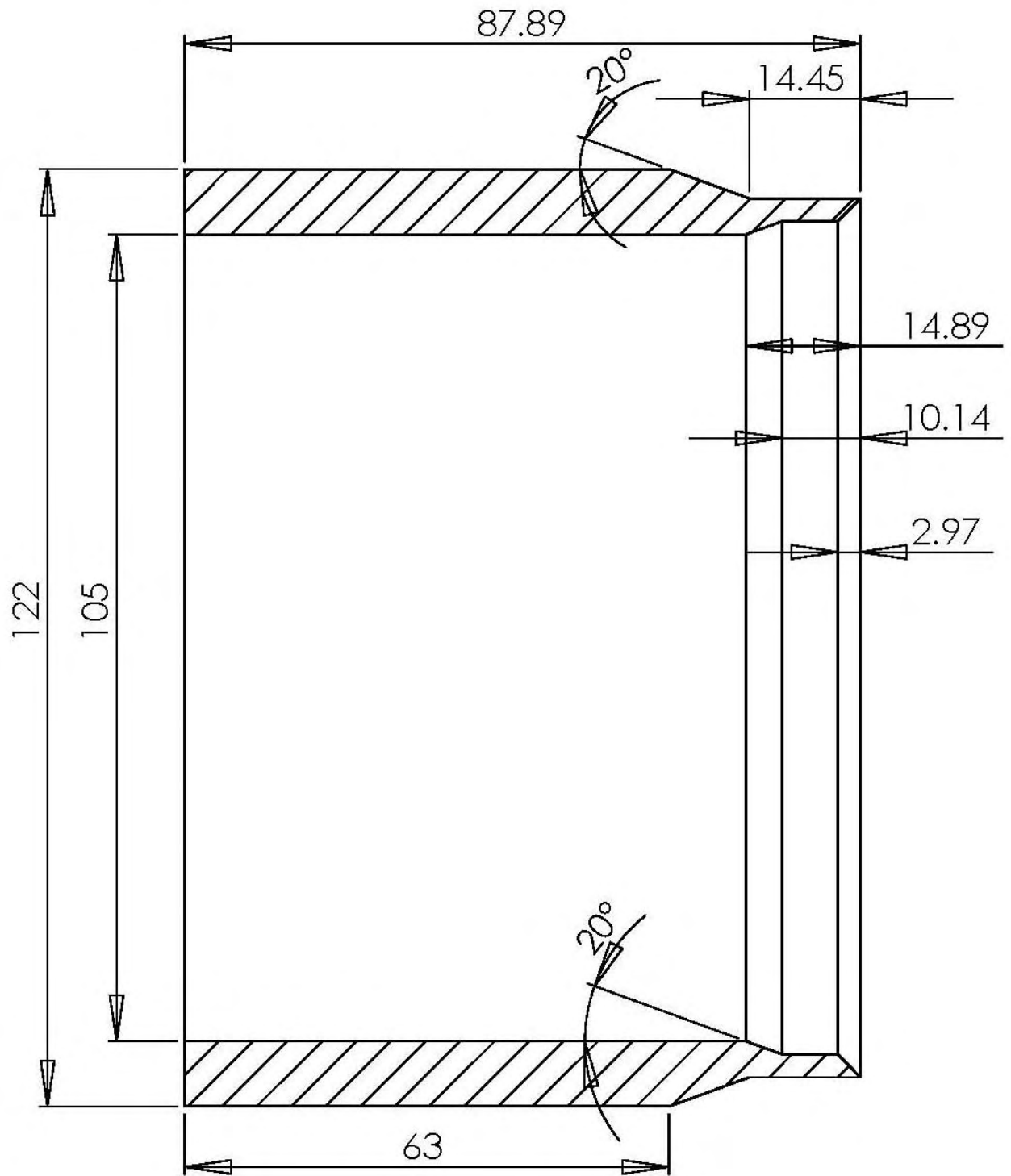
Appendix C: Final Design



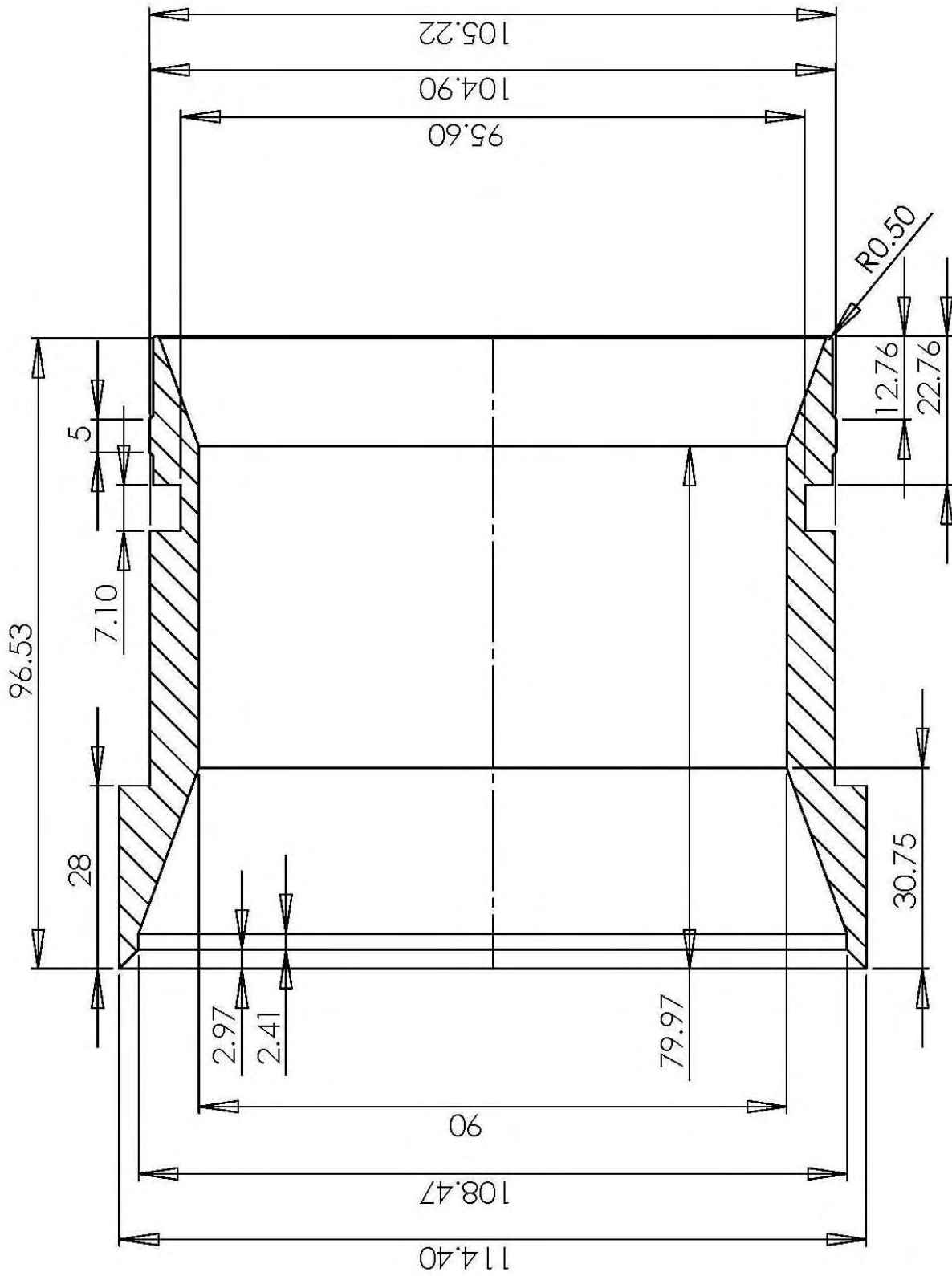
assembled final design at maximum temperature difference



assembled final design without temperature difference

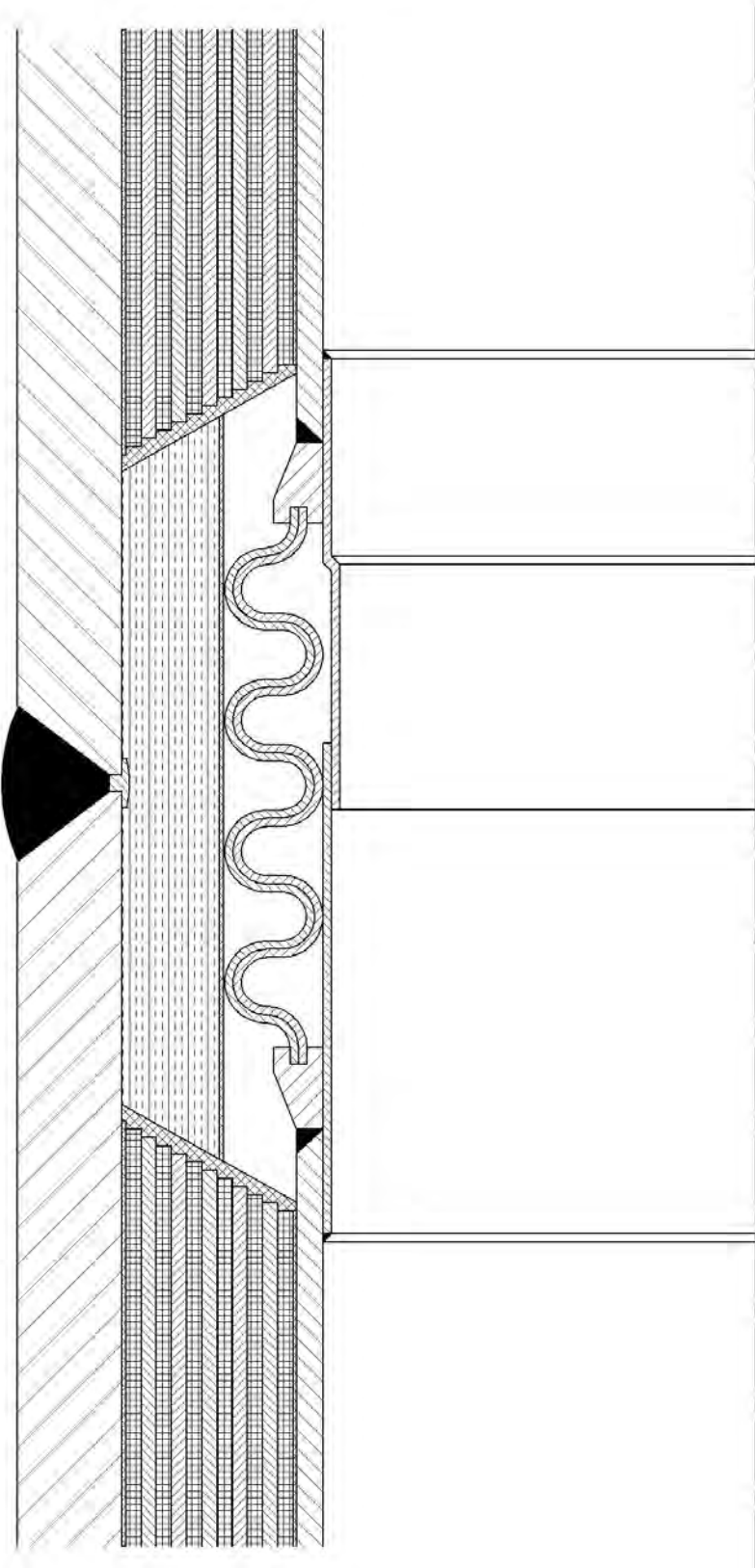


female connection part with measurements



male connection part with measurements

Appendix D: Preliminary Layout with Expansion Bellows



preliminary design with convoluted expansion bellows